HUMBOLDT-UNIVERSITÄT ZU BERLIN

Lebenswissenschaftliche Fakultät
Institut für Biologie

Bachelorarbeit

Zum Erwerb des akademischen Grades Bachelor of Science

A physiological-based pharmacokinetic/ pharmacodynamic (PBPK/PD) model of the angiotensin II receptor blocker (ARB) losartan

Ein physiologisch-basiertes pharmakokinetisches/ pharmakodynamisches (PBPK/PD) Modell des Angiotensin II Rezeptorblockers Losartan

vorgelegt von

Ennie Joana Sophie Tensil

Matrikelnummer: 623801

E-Mail: ennie@tensil.de

Geburtsdatum und -ort: 31.01.2002 in Berlin

Arbeitsgruppe: Systems Medicine of the Liver

Berlin, 2025-07-13

Erstprüfer: Dr. Matthias König
Zweitprüfer: Prof. Dr. Hanspeter Herzel

Contents

Abstract

English

Losartan is an angiotensin II receptor antagonist commonly used in the treatment of hypertension and heart failure. Its pharmacokinetics and pharmacodynamics are influenced by a range of physiological and genetic factors, which may affect therapeutic efficacy. This thesis presents a physiologically based pharmacokinetic/pharmacodynamic (PBPK/PD) model of losartan and its active metabolite E3174 to explore these influences systematically. The modular SBML-based model includes submodels for absorption, hepatic metabolism, renal excretion, and pharmacodynamic effects via the renin-angiotensin-aldosterone system (RAAS). Simulations were conducted to investigate the impact of dose, hepatic and renal impairment, as well as CYP2C9 and ABCB1 polymorphisms. The model successfully reproduced observed pharmacological trends, including a dose-dependent increase in pharmacodynamic response, likely reflecting enhanced receptor blockade at higher systemic exposures. Hepatic dysfunction blunted the pharmacodynamic response to losartan, whereas renal impairment reduced metabolite clearance and lead to modest enhancement in pharmacodynamic effect. Genetic variability in CYP2C9 significantly altered E3174 formation and downstream RAAS inhibition, whereas ABCB1 activity had only minor effects on systemic exposure. The model provides mechanistic insight into inter-individual variability in losartan therapy and supports its potential use in individualized dosing strategies.

Deutsch

Losartan ist ein Angiotensin-II-Rezeptor-Antagonist, der häufig zur Behandlung von Bluthochdruck und Herzinsuffizienz eingesetzt wird. Seine Pharmakokinetik und Pharmakodynamik werden von einer Reihe physiologischer und genetischer Faktoren beeinflusst, die die therapeutische Wirksamkeit beeinträchtigen können. In dieser Arbeit wird ein physiologisch basiertes pharmakokinetisches/pharmakodynamisches (PBPK/PD) Modell von Losartan und seinem aktiven Metaboliten E3174 vorgestellt, um diese Einflüsse systematisch zu untersuchen. Das modulare SBML-basierte Modell umfasst Teilmodelle für die Absorption, den hepatischen Metabolismus, die renale Ausscheidung und die pharmakodynamischen Effekte über das Renin-Angiotensin-Aldosteron-System (RAAS). Es wurden Simulationen durchgeführt, um die Auswirkungen der Dosis, der Leber- und Nierenschädigung sowie der CYP2C9- und ABCB1-Polymorphismen zu untersuchen. Das Modell reproduzierte erfolgreich die beobachteten pharmakologischen Trends, einschließlich eines dosisabhängigen Anstiegs der pharmakodynamischen Reaktion, der wahrscheinlich auf eine verstärkte Rezeptorblockade bei höheren systemischen Expositionen zurückzuführen ist. Leberfunktionsstörungen schwächten die pharmakodynamische Reaktion auf Losartan ab, während Nierenfunktionsstörungen die Metaboliten-Clearance verringerten und zu einer mäßigen Verstärkung der pharmakodynamischen Wirkung führten. Die genetische Variabilität von CYP2C9 veränderte die Bildung von E3174 und die nachgeschaltete RAAS-Hemmung erheblich, während die ABCB1-Aktivität nur geringe Auswirkungen auf die systemische Exposition hatte. Das Modell bietet einen mechanistischen Einblick in die interindividuelle Variabilität der Losartan-Therapie und unterstützt seine potenzielle Verwendung in individualisierten Dosierungsstrategien.

1 Introduction

1.1 Blood pressure

1.1.1 Hypertension

Hypertension, or high blood pressure (140/90 mmHg or higher), is a chronic medical condition characterized by persistently elevated pressure in the blood vessels [1]. It is a significant global health concern that affects millions of people worldwide. Hypertension is often called a "silent killer" because many people with the condition do not experience noticeable symptoms, yet it significantly increases the risk of serious health complications [1]. Risk factors for hypertension include old age, genetics, being overweight, obese or not physically active and a unhealthy diet (high-salt and too much alcohol) [1].

In 2019, an estimated 626 million women and 652 million men aged 30-79 years were living with hypertension, representing a doubling of cases since 1990 [59]. This chronic condition is a major risk factor for cardiovascular diseases, including stroke, heart disease, and renal failure, contributing to approximately 8.5 million deaths annually [59, 22]. The prevalence of hypertension varies across regions and countries, with some nations experiencing rates exceeding 50% in their adult populations [59]. Despite its widespread occurrence, hypertension remains a treatable condition, with numerous effective and relatively low-cost medications available [1]. Addressing this global health challenge requires a dual approach: implementing primary prevention strategies to reduce hypertension prevalence and enhancing treatment and control measures for those already affected [1]. The clinical need for effective hypertension management is evident, as uncontrolled high blood pressure significantly increases the risk of cardiovascular events and organ damage [22].

1.1.2 Renin-angiotensin-aldosterone system (RAAS)

The renin-angiotensin-aldosterone system (RAAS) is a critical regulatory mechanism in the human body, responsible for maintaining blood pressure, fluid balance, and electrolyte homeostasis. An overview of this system is depicted in Fig 1. RAAS is activated in response to low blood pressure (e.g. due to dehydration or blood loss), low sodium levels in the blood, or sympathetic nervous system activation during stress or exercise. These triggers stimulate the juxtaglomerular cells in the kidneys to release renin, an enzyme that initiates the RAAS cascade. Renin cleaves angiotensinogen, a plasma protein produced by the liver. This cleaving, also described as limited proteolysis, generates the peptide angiotensin I, an inactive precursor. Angiotensin I travels through the bloodstream to the lungs and kidneys, where the angiotensin-converting enzyme (ACE) converts it into angiotensin II though another limited proteolysis step [21].

Angiotensin II is a potent vasoconstrictor that exerts its effects by binding to specific types of receptors, thus increasing blood pressure and volume in several ways. Angiotensin II binding to the angiotensin II type 1 receptors (AT1 receptors), mediates most of the physiological and pathophysiological effects [3]. It influences the vascular tone by narrowing the blood vessels in systemic arterioles. It also stimulates the adrenal glands, located on top of the kidneys, to secrete aldosterone, which acts on the kidneys to increase sodium and water reabsorption and excrete potassium. Angiotensin II itself also increases sodium reabsorption through increased activity of the Na-H antiporter in the proximal convoluted tubule. Additionally it increases the sympathetic outflow from the central nervous system and stimulates the release of vasopressin (antidiuritic hormone, ADH) from the hypothalamus, which promotes water retention by the kidneys [21].

Dysregulation of the RAAS, particularly through excessive activity of angiotensin II, is implicated in the pathogenesis of hypertension, heart failure, kidney damage, and various cardiovascular diseases.

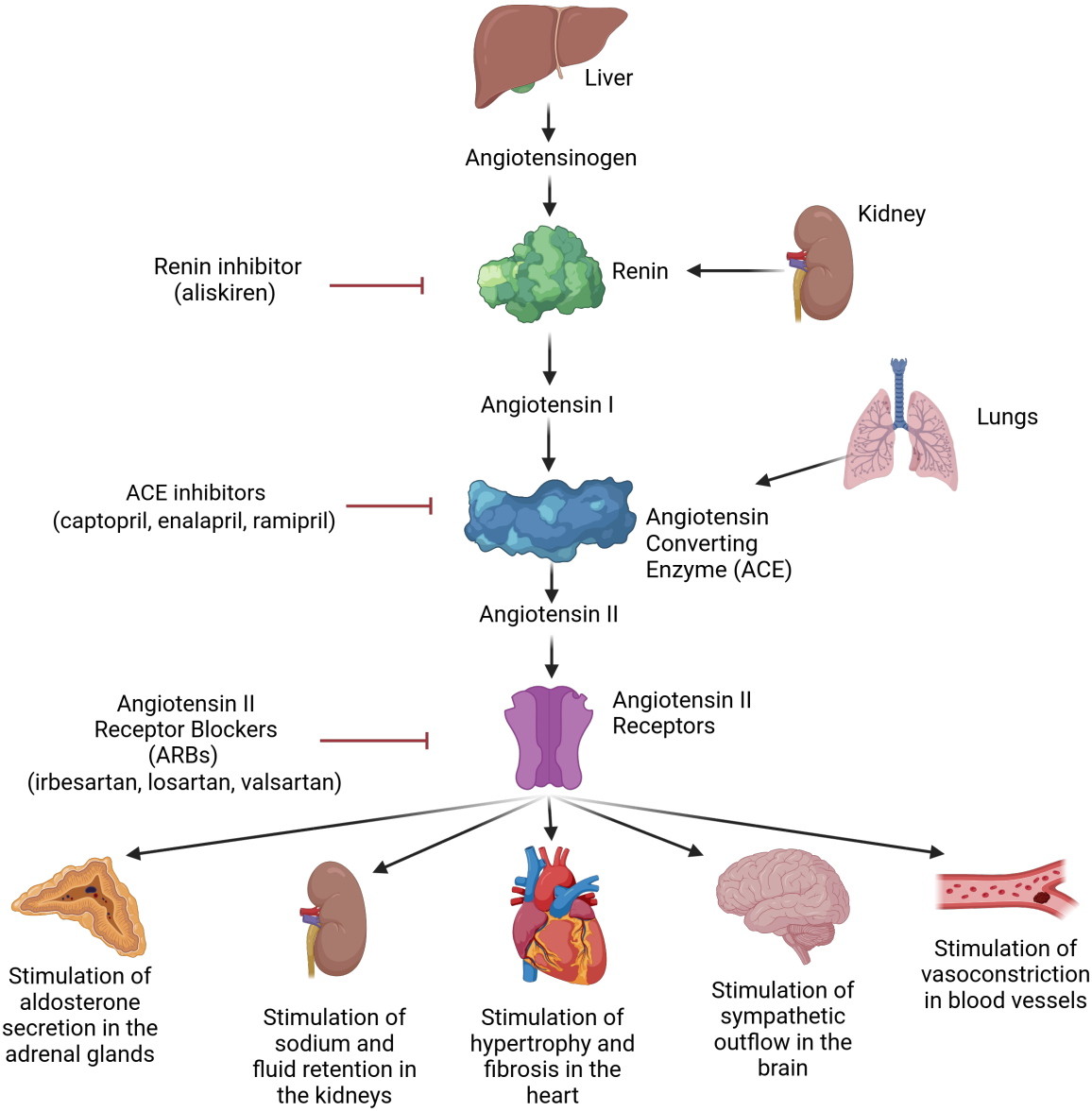

Figure 1: **Overview Renin-angiotensin-aldosterone system (RAAS).**

1.1.3 Blood pressure medication

Because hypertension is a leading risk factor that influences global morbidity and mortality, a wide range of effective antihypertensive medications were developed. A key therapeutic target in management of patients with essential hypertension is the renin-angiotensin-aldosterone system (RAAS). Routinely used RAAS inhibitors are for example renin inhibitors, angiotensin-converting enzyme (ACE) inhibitors and angiotensin receptor blockers (ARBs). Beta blockers like propranolol lower plasma renin by inhibiting sympathetic stimulation, while direct renin inhibitors like aliskiren block renin activity itself, reducing angiotensin peptide formation [3, 48]. ACE inhibitors like ramipril block the conversion of angiotensin I to II, lowering angiotensin II and aldosterone while increasing renin, but may cause side effects like dry cough and angioedema [18, 3]. Angiotensin II receptor blockers (ARBs) with a prominent player being losartan, developed in the 1990s, selectively block the AT1 receptor, preventing angiotensin II action regardless of its synthesis and offering greater specificity than ACE inhibitors [8]. Other common antihypertensives using different pharmacological mechanisms are diuretics and calcium channel blockers. Diuretics increase water and electrolyte excretion by inhibiting ion transport in the nephron, while calcium channel blockers lower blood pressure by reducing calcium influx,

leading to vasodilation and decreased cardiac activity [6, 38].

1.2 Losartan

Losartan, an orally active, non-peptide angiotensin II receptor blocker (ARB), is widely used in clinical practice to counteract the harmful effects of elevated angiotensin II levels. Losartan is primarily used to treat hypertension and protect against related complications, such as stroke, heart attack, and kidney damage, especially in individuals with diabetes [75]. By competitively inhibiting the binding of angiotensin II to the AT1 receptor, losartan effectively reduces blood pressure and mitigates the risk of adverse cardiovascular events. The active metabolite, E3174, is 10- to 40-fold more potent than the parent compound, contributing substantially to its antihypertensive effect [52]. Nevertheless, losartan remains a highly potent angiotensin II competitive antagonist on its own and, therefore, is not considered a prodrug [52].

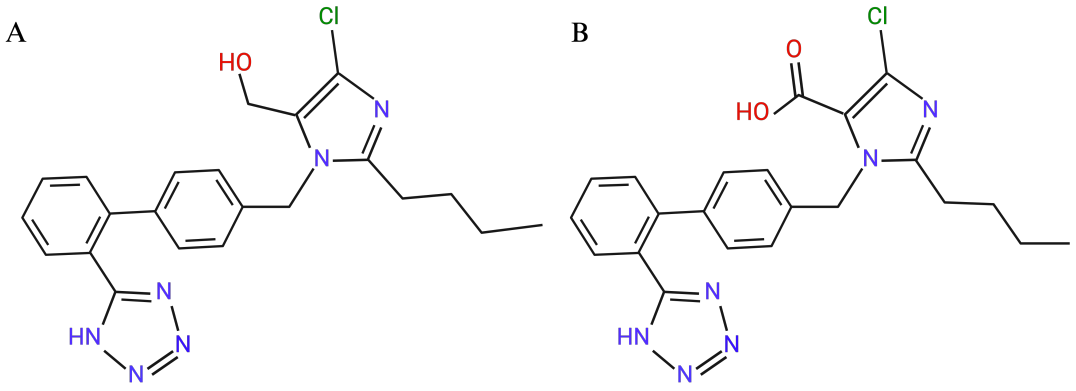

Figure 2: **Chemical structure of (A) losartan and (B) E3174.** Losartan ($C_{22}H_{23}ClN_6O$) is the parent compound, CHEBI:6541; InChIKey: PSIFNNKUMBGKDQ-UHFFFAOYSA-N. Its main active metabolite is produced through oxidation of the C5-hydroxymethyl on the imidazol ring to the 5-carboxylic acid metabolite E3174, CHEBI:74125; InChIKey: ZEUXAIYYDDCIRX-UHFFFAOYSA-N.

The drug was granted FDA approval on 14 April 1995. It is generally well-tolerated and has a favorable safety profile, with side effects such as dizziness, upper respiratory infection, nasal congestion, and back pain. It is available under various brand names, including Cozaar, and is often prescribed as part of a broader treatment plan that includes lifestyle changes such as a low-sodium diet and regular exercise [15].

Losartan is available as losartan potassium tablets as well as a combination tablet of losartan potassium and hydrochlorothiazide, which reduces blood pressure further than either drug given separately [24]. The available doses are 25, 50 and 100 mg tablet, with 50 mg being the usually recommended daily dose and 100 mg the daily maximum. Losartan should be avoided in pregnancy, as is the case with all other angiotensin-receptor antagonists [75]. With its proven efficacy and versatility, losartan has become a cornerstone in the management of cardiovascular and renal diseases, offering significant benefits to patients worldwide.

1.3 Losartan pharmacokinetics

The pharmacokinetics of a drug describe the influence of the body on a drug after administration due to absorption, distribution, metabolism and elimination (ADME). Fig. 3 depicts an illustration for the processes involved in the pharmacokinetics of losartan.

Absorption After oral administration, losartan is rapidly absorbed from the gut through enterocytes into blood plasma. Peak plasma concentrations (c_{max}) are occurring approximately 1 to 2 hours post-dose (t_{max}) while plasma concentrations of the active metabolite E3174 (losartan

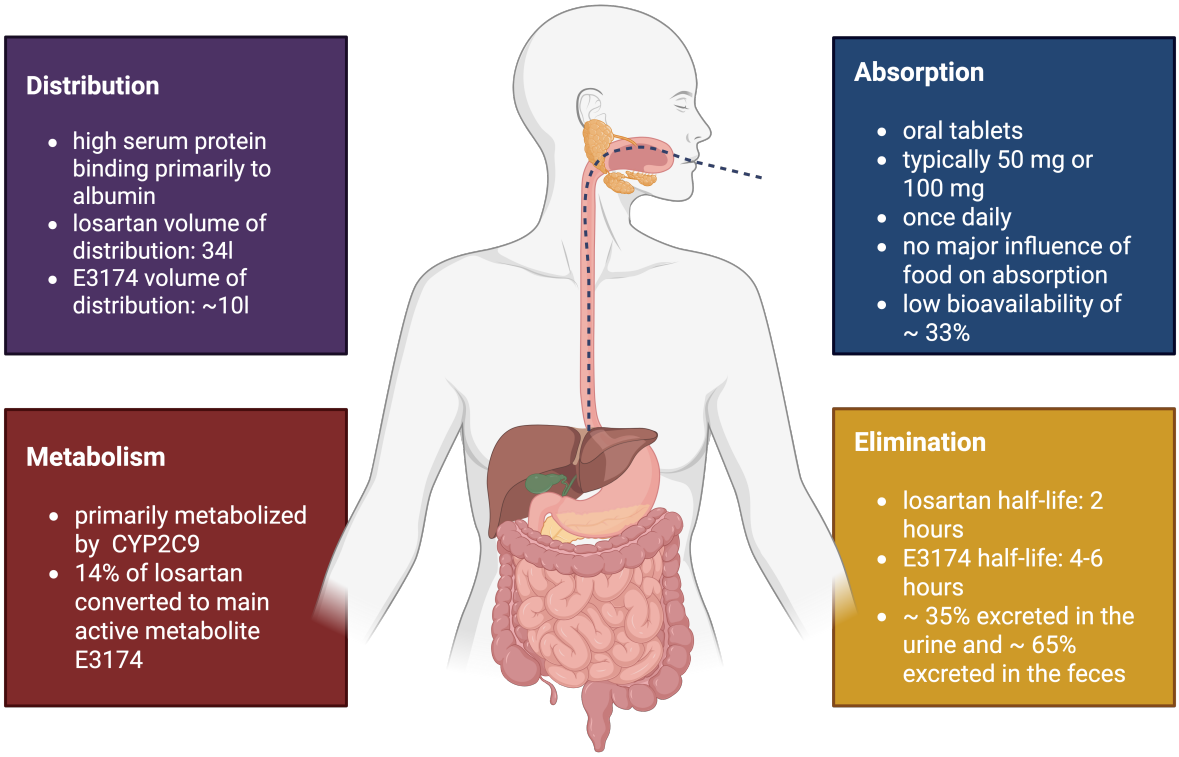

Figure 3: **Losartan pharmacokinetics** The pharmacokinetics of losartan can be described through absorption, distribution, metabolism and elimination (ADME) of the drug.

carboxylic acid) peak approximately 3 to 4 hours after administration. Losartan is a substrate of the organic anion uptake transporter OATP2B at the apical membrane of the enterocytes [20]. Its bioavailability (fraction that reaches the systemic circulation) is relatively low, around 33 %, due to first-pass metabolism in the liver [52].

The first-pass effect describes a pharmacological phenomenon in which certain drugs undergo metabolism at a specific location in the body. Due to this, only a fraction of the dose administered orally appears in the systemic blood circulation or at its site of action, compared to intravenous administration. For most drugs, the liver is the main site responsible for this effect, but the lungs, vasculature, and gastrointestinal tract can also be the cause. The extent of the first-pass effect can differ between patients [32].

The area under the plasma concentration-time curve (AUC) for E3174 is about 4 to 8-fold greater than for losartan potassium [52, 62]. If administered with meals, the rate of absorption and the area under the plasma concentration-time curve (AUC) of losartan and its metabolite are decreased slightly by approximately 10% [77, 74].

Distribution and metabolism The volume of distribution V_d for losartan and E3174 are 34 l and 10 l, respectively [52, 11, 8]. These low values correspond to the substances' high serum protein binding of 98.6 – 98.8% and 99.7%, respectively, primarily to albumin [11, 62, 57].

Losartan undergoes extensive hepatic metabolism, primarily through the cytochrome P450 isoenzymes CYP2C9 and CYP3A4, resulting in the formation of an active carboxylic acid metabolite, E3174, and several other inactive metabolites. Among these enzymes, the CYP2C9 is the dominant metabolic pathway of losartan. The isoenzyme CYP3A4 is only involved in losartan clearance at supraphysiological concentrations [89]. Losartan is converted in human liver microsomes in a two-step oxidation involving a slow first step (oxidation to aldehyde intermediate E3179) and then a rapid second step (oxidation to carboxylic acid E3174) [94, 80,

79]. After oral administration, approximately 14% of a losartan dose is converted to E3174 [52]. Depending on the CYP2C9 genotype, the enzyme for metabolism can be deficient (Sec. 1.6).

A minor losartan metabolite sometimes referred to as L158 [14] has been identified in human plasma and urine, though its biosynthetic origin remains unclear. Evidence suggests it may arise from glucuronidation of E3174 (or possibly losartan itself) via UDP-glucuronosyltransferases (UGTs) [2]. Although the specific structure and kinetics of L158 remain to be fully characterized, its presence underscores the role of UGT-mediated metabolism in losartan clearance.

Elimination The pharmacokinetic profile of losartan is characterized by a biphasic elimination process, with a terminal half-life ($t_{1/2}$) of about 2 hours for losartan and 4 to 6 hours for E3174 [52, 62]. Both losartan and its metabolite are excreted through urine and feces, with the renal route accounting for approximately 35% - 44% and the fecal route for approximately 65% of the elimination [14, 15]. Less than 5% of a losartan potassium dose is excreted unchanged renally in patients with normal renal function [74]. Renal clearance is 4.3 to 5.6 L/h for losartan potassium 50 mg and about 1.5 L/h for its metabolite [14, 15].

1.4 Losartan pharmacodynamics

Pharmacodynamics refer to the biochemical and physiological effects of a drug on the body, including the mechanisms underlying these effects. Losartan exerts its pharmacodynamic effects mainly through modulation of the renin–angiotensin–aldosterone system (RAAS). Losartan's primary mechanism of action involves the selective blocking of the angiotensin II type 1 (AT1) receptor. The activation of AT1 receptors on various tissues leads to vasoconstriction, aldosterone secretion, sodium and water retention and sympathetic nervous system stimulation. By blocking this receptor, losartan prevents angiotensin II from exerting its effects, leading to vasodilation, reduced systemic vascular resistance, reduced blood pressure, and decreased aldosterone levels. This action reduces sodium and water retention, contributing to further decreases in blood pressure.

As mentioned above, suppression of aldosterone secretion is an important pharmacodynamic consequence of AT1 receptor blockade. In the adrenal cortex's glomerulosa zone, aldosterone is synthesized from cholesterol through enzymatic steps, with aldosterone synthase converting corticosterone to aldosterone in the final stage [87]. Normally, angiotensin II binding to AT1 receptors stimulates the expression of CYP11B2, the aldosterone synthase coding gene [70]. Angiotensin II is thought to influence this synthesis through multiple pathways, like modulation of intracelluar calcium concentration [70] and activation of NAPDH oxidase activity in the mitochondria [66]. Losartan is supressing these effects, leading to reduced aldosterone levels and thus decreased sodium reabsorption and water retention in the distal nephron.

Blockade of AT1 receptors also disrupts the negative feedback loop that normally inhibits renin secretion. Though there is no evidence for a direct negative feedback function of angiotensin II on renin production [60], findings still demonstrate a strong negative effect [39]. Current studies theorise a baroreceptor mechanism responsible for this phenomenon [58]. Losartan administration is associated with increased plasma renin activity and consequently elevated concentrations of both angiotensin I and angiotensin II. Since losartan does not inhibit ACE, the conversion of angiotensin I to angiotensin II proceeds unimpeded, but the biological effects of angiotensin II are largely neutralized at the AT1 receptor level. The AT1 receptor selectivity is a key aspect of losartan's pharmacodynamics, distinguishing it from other antihypertensive agents that affect the RAAS more broadly, such as angiotensin-converting enzyme (ACE) inhibitors.

Losartan also indirectly enhances the effects of angiotensin II on the unblocked AT2 receptors, which are thought to mediate vasodilatory effects [**Gigante1998**].

1.5 Hepatic and renal impairment

Hepatic impairment Hepatic impairment refers to the reduced functional capacity of the liver due to acute or chronic liver diseases, such as cirrhosis, an advanced stage of liver disease. The liver plays a critical role in drug metabolism and detoxification, and its dysfunction can significantly alter the pharmacokinetics of many drugs by affecting their pharmacokinetics. To assess the severity of liver dysfunction, clinicians commonly use the Child-Pugh-Turcotte (CPT) scoring system. This system classifies hepatic impairment into three categories based on the five clinical and laboratory parameters. The three categories are: Class A (5–6 points) mild hepatic impairment, class B (7–9 points) moderate hepatic impairment and class C (10–15 points) severe hepatic impairment (as shown in Fig. 4).

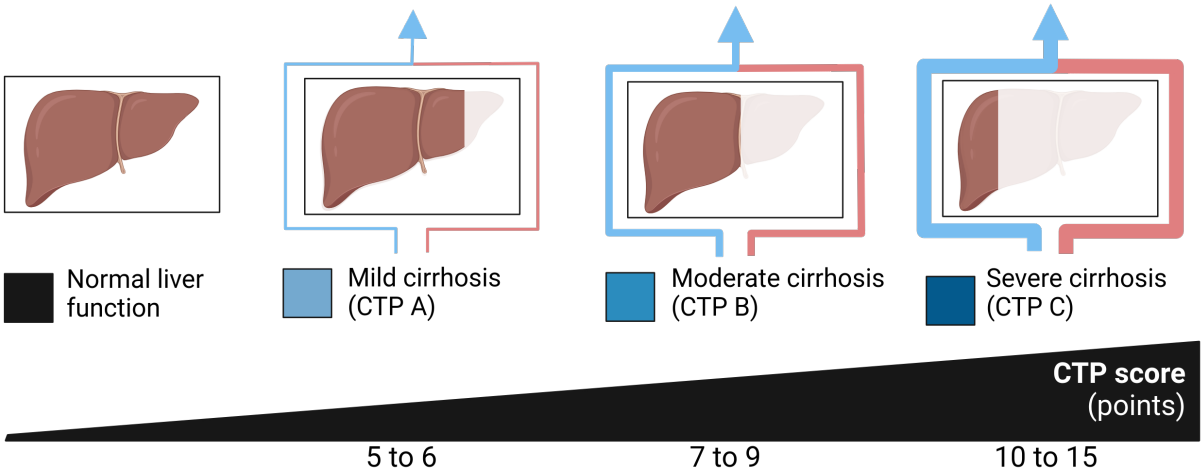

Figure 4: **Impairment strength in liver dysfunction.** Hepatic impairment can significantly affect drug metabolism and excretion. Hepatic impairment is commonly assessed using the Child-Turcotte-Pugh (CTP) score, which classifies liver function based on clinical and laboratory markers.

Losartan is primarily metabolized in the liver by CYP2C9 into its active metabolite, E3174. In patients with stable alcoholic cirrhosis, the total plasma clearance of losartan is reduced by approximately 50%, leading to a 4- to 5-fold increase in plasma concentrations compared to healthy individuals [55, 75]. Additionally, the oral bioavailability of losartan is nearly doubled [75]. Despite these changes, the conversion of losartan to its active metabolite (E3174) after intravenous administration remains similar between cirrhotic patients (7.6% – 16.8%) and healthy subjects (8.2% – 17.7%) [55]. The pharmacokinetics of E3174 are slightly altered in cirrhotic patients, resulting in a 1.5- to 2-fold increase in its plasma concentration. These findings indicate that hepatic impairment, particularly cirrhosis, leads to elevated plasma concentrations of losartan, justifying lower starting doses in affected patients. This dose adjustment is especially important in heart failure, where liver dysfunction often coexists and sensitivity to RAAS inhibition is increased [88, 37].

Renal impairment Renal impairment refers to a reduction in kidney function, which can range from mild dysfunction to complete renal failure. This condition impairs the kidneys' ability to filter waste products, regulate fluid and electrolyte balance, and eliminate drugs and their metabolites. Renal impairment is commonly evaluated through clinical measures such as glomerular filtration rate (GFR), serum creatinine levels, and creatinine clearance (CrCl). It can be categorized into stages based on severity, from mild (Stage 1–2) to end-stage renal disease (Stage 5).

In patients with renal impairment, the renal clearance of losartan and its active metabolite is reduced, yet E3174 plasma levels generally remain unchanged [74]. In acute renal failure, losartan clearance may decrease further, possibly due to inhibited hepatic metabolism from ac-

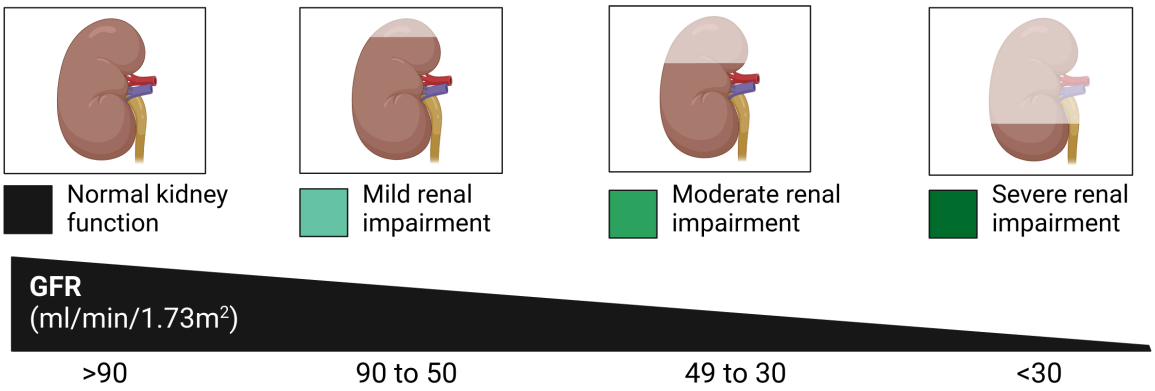

Figure 5: **Impairment strength in kidney dysfunction.** Renal impairment can significantly affect drug metabolism and excretion. Renal impairment is assessed using the glomerular filtration rate (GFR), with reduced GFR indicating reduced renal function and drug clearance.

cumulated uremic toxins [93]. In chronic renal failure (CRF), key pharmacokinetic parameters like C_{max}, T_{max}, and AUC_{0-24} for losartan and E3174 remain similar to those in healthy individuals [75]. Although about 35-44% of E3174 is renally cleared, its AUC does not increase in CRF, suggesting compensatory changes in absorption, conversion, or hepatic clearance [74, 63, 73]. In dialysis patients, losartan levels rise but E3174 does not, as neither compound is dialyzable, so post-dialysis supplementation is unnecessary [63, 73]. While no strict dose adjustment is required based on renal function alone, caution is advised in moderate to severe renal dysfunction, considering diet, co-medications, and diuretic use [55].

1.6 Genotypes and genetic variants

ABCB1 The ATP Binding Cassette Subfamily B Member 1 (ABCB1) gene encodes the P-glycoprotein (P-gp) efflux transporter, also known as multidrug resistance protein 1 (MDR1), which plays a crucial role in drug disposition and pharmacokinetics [25, 33]. This transporter is involved in the efflux of various drugs, including losartan [25]. P-gp is expressed in a polarized manner (apical) in the plasma membrane of cells in barrier and elimination organs e.g. intestinal epithelium, proximal renal tubular system and blood brain barrier, where it has protective and excretory functions [7].

Genetic polymorphisms in the ABCB1 gene have been associated with variations in losartan pharmacokinetics. The 2677G>T and 3435C>T polymorphisms, in particular, have been shown to affect expression and function of the MDR1 [72] and could therefore affect the hypotensive response to losartan. Patients with the CT or TT genotype at the 3435C>T locus demonstrated a significantly higher mean decrease in systolic blood pressure compared to those with the CC genotype [25]. Some studies suggest that the ABCB1 c.2677G>T/c.3435C>T diplotype may increase the early-phase absorption of losartan, although it does not appear to affect the total absorption [72]. However, the influence of ABCB1 polymorphisms on losartan disposition remains controversial, with some research indicating that the 3435C>T polymorphism does not significantly impact losartan pharmacokinetics [31, 91].

Cytochrome P450 2C9 (CYP2C9) The most important drug-metabolizing enzymes belong to the cytochrome P450 superfamily, including the three families CYP1, CYP2 and CYP3, which are the major contributors to the oxidative metabolism of many drugs [95]. Nonsynonymous single-nucleotide polymorphisms (SNPs) are the most common genetic mutation in human CYP genes, as they cause amino acid changes in the coding region of the corresponding CYP [95]. The genetic variants occur at different frequencies and are phenotypically ethnicity depended [10].

Tab. 1 and Fig. 6 contain information and frequencies for genetic variants reported to influence losartan pharmacokinetics.

Table 1: Information about CYP2C9 genetic variants. Data from PharmGKB [23].

Category	**∗1**	**∗2**	**∗3**	**∗13**
Nucleotide change (PharmVar)	Wild type	3608C>T	42614A>C	3276T>C
Effect on protein (NP_000762.2)	Wild type	p.R144C (Arg144Cys)	p.I359L (Ile359Leu)	p.L90P (Leu90Pro)
Position at NC_000010.11 (GRCh38.p2)	Reference	g.94942290C>T	g.94981296A>C	g.94941958T>C
Position at NG_008385.2 (RefSeqGene)	Reference	g.9133C>T	g.48139A>C	g.8801T>C
rsID	Reference	rs1799853	rs1057910	rs72558187
CYP2C9 allele nucleotide	Reference	T	C	C
Function impact	Normal function	Decreased function	No function	No function

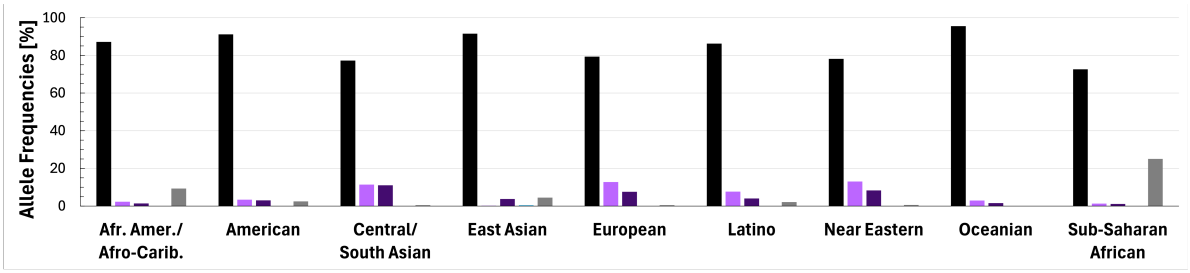

■ *1	87.1	91.2	77.2	91.5	79.3	86.3	78.2	95.5	72.6
■ *2	2.2	3.3	11.4	0.2	12.7	7.6	13.0	2.9	1.3
■ *3	1.4	3.0	11.0	3.8	7.6	4.0	8.3	1.6	1.1
■ *13	0.0	-	-	0.3	-	-	0.0	-	-
■ Other	9.3	2.5	0.4	4.2	0.4	2.1	0.6	0.0	25.0

Figure 6: **CYP2C9 allele frequencies across different biogeographical populations.** Data were obtained from PharmGKB CYP2C9 information Tab. [23].

Losartan is metabolised through the CYP system in the liver, mainly by CYP2C9 but also CYP3A4 (only at very high losartan concentrations). The CYP2C9 gene is located on the long arm of chromosome 10 and encodes a protein of 490 amino acids [69]. CYP2C9 makes up about 20% of hepatic CYP content and metabolizes over 100 clinical drugs [56]. More than 33 alleles have been identified [95]. The wild type allele is depicted as *1 and the most studied alleles are *2 and *3. The allele *2 is produced by an missense mutation of 3608C>T causing the substitution of R144C (Arg to Cys transversion) [67]. The allele *3 is a missense mutation of 42614A>C on exon 7 that leads to an I359L substitution (Ile to Leu). The allele *13, a 3276T>C mutation causing a L90P substitution (Leu to Pro) was also reported in the context of losartan metabolism [51]. In Europeans, the reported prevalence of the CYP2C9 *1, *2, and *3 alleles are 79%, 12.7%, and 7.5%, respectively [56]. There is no data on *13 prevalence in European subjects. Although combinations of the wild-type allele with the respective polymorphisms are most common, homozygous combinations of *2 or *3, as well as the heterozygous combination of *2 and *3, are observed at frequencies below 2% [83].

Due to these polymorphisms, the activity of CYP2C9 varies up to 10-fold in humans [74]. The oxidation rate of losartan was found to be reduced in liver microsomes from individuals who were heterozygous or homozygous for the CYP2C9 *3 allele, as well as in those homozygous for the CYP2C9*2 allele [90]. A significantly higher plasma $AUC_{losartan}/AUC_{E3174}$ ratio was observed in individuals homozygous for the CYP2C9*2 or *3 alleles compared to those with the CYP2C9*1 allele, with approximately 4-fold and 30-fold increases, respectively [52]. Similarly elevated ratios were also reported in individuals with CYP2C9*1/*3 and *2/*3 genotypes following a single oral dose of losartan. Carriers of the CYP2C9*3 allele exhibited markedly reduced levels of E3174, with homozygotes converting less than 1% of the administered dose into E3174 [92]. Moreover, individuals homozygous or heterozygous for the CYP2C9*3 allele

had a substantially lower E3174 AUC (7–50%) compared to those with the wild-type genotype. The *1/*3 genotype has been linked to a diminished response to losartan treatment, indicated by higher blood pressure levels [71]. Individuals with the CYP2C9*1/*3 genotype exhibited a 1.6-fold increase in losartan AUC compared to those with the wild-type allele [71]. Similarly, subjects with the CYP2C9*1/*2 genotype showed a 3.0-fold higher losartan AUC than the wild type [19].

1.7 Physiologically-based pharmacokinetic/ pharmacodynamic (PBPK/PD) model

A physiologically-based pharmacokinetic/ pharmacodynamic (PBPK/PD) model allows to simulate and predict the pharmacokinetics of a substance and the respective pharmacodynamic response in the human body. These models are constructed using a system of coupled ordinary differential equations (ODEs) to describe the absorption, distribution, metabolism, and elimination (ADME) of a drug. By integrating physiological, pharmacokinetic, and biochemical parameters, PBPK models enable detailed descriptions of the compartments within the body and the transport of substances through the systemic circulation. In combination with a pharmacodynamic model (PD), the effect profile and optimal dosage of a drug can be predicted in order to achieve the desired exposure.

The defined compartments in a PBPK/PD model represent various organs or tissues that include parameters for metabolites, tissue volumes, reactions, and flow rates. Physiological processes are incorporated, allowing for precise predictions of ADME.

These models serve as useful tools for studying medical questions, testing hypotheses *in silico*, and predicting the pharmacokinetics of both established and novel drugs. PBPK/PD modeling has applications in exploring the impact of physiological changes or disease conditions — such as varying degrees of drug dosing, cirrhosis or renal failure — on drug behavior. It can also be used for metabolic phenotyping with test compounds, assessing how minor changes, such as variations in enzyme genotypes, affect an entire system.

1.8 Question, scope and hypotheses

Within this project the effects of different dosing, genetic variants (genotypes) of key proteins involved in losartan metabolism and hepatic and renal impairment on losartan pharmacokinetics and pharmacodynamics were studied utilizing computational modelling. Specifically, a physiological-based pharmacokinetic/ pharmacodynamic (PBPK/PD) model of losartan was developed to systematically analyse the following questions:

- What are the effects of different administered doses of losartan on its pharmacokinetics and pharmacodynamics?
- What are the effects of genetic variants of CYP2C9 or ABCB1 genotypes on losartan pharmacokinetics and pharmacodynamics?
- What are the effects of renal or hepatic impairment on losartan pharmacokinetics and pharmacodynamics?

The objective is to improve our understanding of the underlying causes of inter-individual variability in blood pressure regulation through ARBs such as losartan, which could be used further to optimize treatment strategies and improve patient outcomes.

2 Methods

Within this work the following methods were used: systematic literature search for losartan (Sec. 2.1), data curation of clinical studies (Sec. 2.2), parameter optimisation of model parameters using clinical data (Sec. 2.4), and calculation of pharmacokinetic parameters (Sec. 2.5).

2.1 Systematic literature research

A systematic literature search was conducted to select studies that included data on the pharmacokinetics of losartan. PubMed was searched using the keywords `losartan AND pharmacokinetics` and PKPDAI [28], a website for searching pharmacokinetic literature, using `losartan` on 2024-08-27. Based on the search an initial literature corpus on the pharmacokinetics of losartan was generated. Available PDFs were retrieved for the literature. Articles on clinical trials of losartan with sufficient PK/PD data were selected based on pre-specified inclusion criteria. In addition to healthy subjects, trials in patients with renal and hepatic impairment were included, as well as studies including CYP2C9 data. Studies in animals, paediatric or other unsuitable patients (e.g. severely impaired or single subject), as well as reviews and computational models were excluded. Furthermore, studies containing only PD data, cocktail or combination drug application were ruled out. Due to the abundance of studies reporting similar pharmacokinetic data, redundant information was omitted to keep the project within a manageable timeframe. In addition, the literature was searched for *in vitro* studies to determine kinetic parameters and enzyme kinetic information.

2.2 Data curation

Data from the selected literature were curated and uploaded to the open pharmacokinetics database PK-DB [29]. The articles were screened for patient information such as age, sex, specific diseases and drugs, losartan dosing protocol and losartan pharmacokinetic or pharmacodynamic profiles. These data were then curated using standard protocols for pharmacokinetic information [29]. Data from figures were digitised using WebPlotDigitizer [68]. Data from tables and textual descriptions were also curated in a specific format as described in [29].

Data were systematically curated according to the following structure: (i) Groups: Patient groups were entered into the database with relevant group characteristics such as age, height, weight, sex and ethnicity. Information on CYP2C9 genotype, renal or hepatic impairment and other diseases was coded. (ii) Individuals: For some trials, individual patient characteristics were reported. Information on individual subject characteristics was recorded in the same way as for the groups. (iii) Interventions: In each trial, losartan was given to patients either as an oral dose in the form of a tablet or capsule, or as an intravenous dose in the form of a solution. Information on dose, time of administration (if multiple doses were administered), and route of administration were recorded. (iv) Time course data: In each study, the authors reported a number of different parameters. The main data of interest were the time courses of concentrations and amounts of losartan or its metabolite losartan carboxylic acid in plasma and urine. (v) Pharmacokinetic/pharmacodynamic data: In addition, many studies reported pharmacokinetic parameters such as C_{max}, T_{max} and $T_{1/2}$ and pharmacodynamic parameters such as renin, aldosterone, and angiotensin I / II concentrations, systolic and diastolic blood pressure, and heart rate.

The extensive heterogeneous data set provided the database for model development and validation. All data are available in PK-DB (`https://pk-db.com`) [29] with an overview of the curated studies in Tab. 2.

2.3 Computational model

The PBPK and tissue models were developed in the Systems Biology Markup Language (SBML) [36, 40]. The libraries sbmlutils [46] and cy3sbml [47] were used for the programmatic manipulation and visualisation of the models. The models are ordinary differential equation (ODE) models solved numerically using sbmlsim [45] based on the high performance SBML simulator libroadrunner [78, 86]. The model is made available in SBML under a CC-BY 4.0 licence with all model equations from `https://github.com/matthiaskoenig/losartan-model`. The version of the model used in this thesis is 0.7.0 [84].

The developed PBPK/PD model consists of a whole-body model linking sub-models for the intestine, kidney, liver and RAAS via the systemic circulation (Fig. 8).

Hepatic functional impairment Liver impairment was modelled as a gradual increase in cirrhosis by scaling liver function with the parameter `f_cirrhosis` from 0.0 (no cirrhosis) to 0.95 (critical cirrhosis). The cirrhosis implementation is based on a recent indocyanine green model of cirrhosis [43, 44] with parameters for mild (0.40), moderate (0.70) and severe cirrhosis (0.81) corresponding to the Child-Pugh-Turette classes CPT A, CPT B and CPT C respectively. The original system given by Child and Turcotte had five criteria to categorise patients: serum bilirubin, serum albumin, ascites, neurological disorder and clinical nutritional status [9]. It was later modified by Pugh, who replaced clinical nutritional status with prothrombin time [64]. Cirrhosis is modelled as a combination of a reduction in functional liver volume and shunting of blood around the liver, both of which lead to a reduction in liver function.

Renal functional impairment Renal impairment was modelled as a progressive decline in renal function by scaling all renal processes with the factor `f_renal_function`, where 1.0 represents normal function and ¡1.0: reduced renal function. The cut-offs for the different stages of renal impairment were based on the international KDIGO guidelines [81] with mild renal impairment (0.69), moderate renal impairment (0.32) and severe renal impairment (0.19) [54].

CYP2C9 The genetic variability in CYP2C9 allele activity was modeled using allele-specific scaling factors obtained from in vitro data [53, 49, 85]. The activities of the *2, *3 and *13 alleles were scaled relative to the wild-type allele (*1) with values of 0.6, 0.17 and 0.05, respectively. Genotype-specific activities were calculated as the average of the two alleles, producing scaling factors of 1 (*1/*1), 0.8 (*1/*2), 0.585 (*1/*3), 0.525 (*1/*13), 0.6 (*2/*2), 0.385 (*2/*3) and 0.17 (*3/*3).

ABCB1 The Genetic variability in ABCB1 allele activity in exon 21 (c.2677 G or c.2677 T) and exon 26 (c.3435 C or c.3435 T) was modeled using allele-specific scaling factors obtained from in vitro data [34, 76]. The activities of the c.2677 G, c.2677 T, c.3435 C, c.3435 T alleles were scaled relative to the wild-type allele (c.2677 G and c.3435 C) with values of 1.0, 0.122, 1.0 and 0.49 respectively. Genotype-specific activities were calculated as the average of the two alleles of both exons, producing scaling factors of 1.0 (GG/CC), 0.653 (GT/CT) and 0.306 (TT/TT).

2.4 Parameter optimization

Parameter fitting was used to minimise the distance between experimental data and model predictions by optimising a subset of twelfth parameters of the model. For this purpose, a subset of curated time curves from healthy subjects, as well as subjects with hepatic or renal impairment after single or multiple dose application was used, as listed in Tab. 2. Parameters were optimised in a multistep process. First, model parameters affecting losartan pharmacokinetics were optimised. Next, parameters for the pharmacodynamics of losartan were optimised. This strategy

allowed to first optimize the pharmacokinetic model and subsequently the pharmacodynamic model.

The cost function, which depends on the parameter $\vec{p}$, minimised the sum of the quadratic weighted residuals $r_{i,k}$ for all time courses k and data points i. Time courses were weighted by the number of participants in each study n_k and individual time points with the standard deviation $\sigma_{i,k}$ associated with the measurement, resulting in weights $w_{i,k} = n_k/\sigma_{i,k}$.

$$F(\vec{p}) = 0.5 \sum_{i,k} (w_{i,k} \cdot r_{i,k}(\vec{p}))^2$$

Multiple optimisation runs (n=100) were performed with different initial parameters based on a local optimiser, with the optimal parameters used in the final model. The fitted parameters are shown in Tab. For validation, all data after multiple applications, disease states, CES1 activity other than wild-type were used.

2.5 Pharmacokinetic/ pharmacodynamic parameters

Pharmacokinetic parameters of losartan, E3174 and L158 were calculated from plasma concentration time curves, urinary and fecal excretion using standard non-compartmental methods. The elimination rate k_{el}[1/min] was calculated by linear regression in logarithmic space in the decay phase. The area under the curve AUC [mmole·min/L] was calculated using the trapezoidal rule and extrapolated to infinity by linear interpolation. Apparent clearance Cl [ml/min] was calculated as $Cl/F = k_{\mathrm{el}} \cdot V_{\mathrm{d}}$ with apparent volume of distribution $V_{\mathrm{d}}/F = D/(AUC_{\infty} \cdot k_{el})$. D is the applied dose of losartan.

For the pharmacodynamic readouts of the RAAS system the respective maximal and minimal values were calculated.

3 Results

3.1 Losartan data

Clinical studies on the pharmacokinetics of losartan were identified through systematic literature research. Searches conducted on PKPDAI and PubMed resulted in 191 and 681 studies, respectively. Additionally, 68 studies were identified through manual literature searches. After removing duplicates, a total of 745 studies were identified, as illustrated in Fig. 7. Among these, 561 studies had a full-text availability.

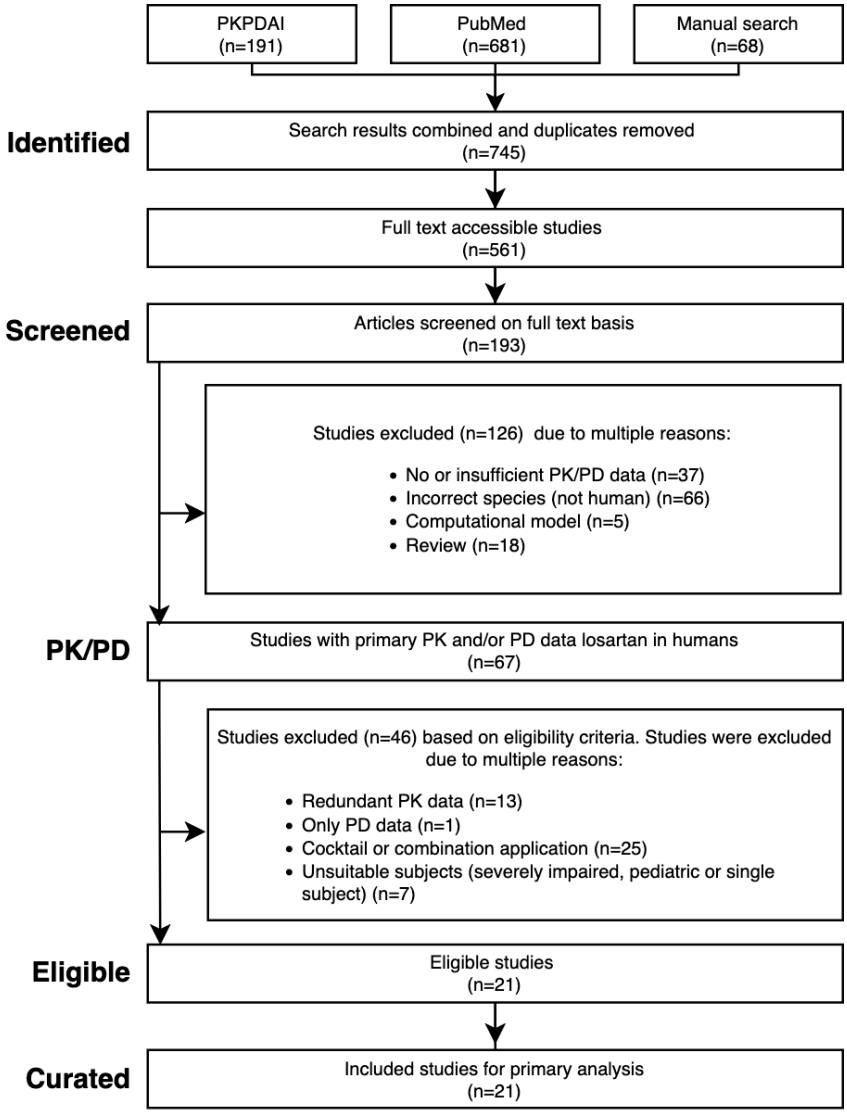

Figure 7: **PRISMA flow diagram** Overview of data selection for the pharmacokinetics/ pharmacodynamics dataset of losartan established in this work. PubMed, PKPDAI, and manual searches were used for the literature search on the pharmacokinetics of losartan. Application of the eligibility criteria resulted in 21 studies, which were curated for this work.

In order to meet the project's time limitations, only articles explicitly mentioning losartan pharmacokinetic data — preferably related to CYP2C9 and/or ABCB1 genotypes or renal/hepatic impairment — in their titles were selected for screening, leading to the exclusion of 368 articles. Subsequently, 193 articles were assessed in full text, and 67 of these studies contained primary pharmacokinetic and/or pharmacodynamic data from human subjects. Additional exclusions were made based on predefined eligibility criteria, such as the absence of time-course data, unsuitable subjects (e.g. severely impaired or single subject), cocktail or combination drug

application or repetitive study designs involving a single oral dose of 50 or 100 mg of losartan. The latter were classified as "redundant PK data" in Fig. 7, and mainly cut out due to time constraints. Ultimately, 21 studies meeting all criteria were selected and curated for PBPK model development.

Table 2: **Summary of studies for modeling.** Overview of study identifiers, PK-DB IDs, administred substance and administration route, dosing regimens, doses [mg], and subject characteristics, including health status, renal functional impairment (*RFI*), hepatic functional impairment (*HFI*), and the studied genotypes (*CYP2C9*, *ABCB1*).

Study	PK-DB	Substance	Route	Dosing	Dose [mg]	Healthy	RFI	HFI	CYP2C9	ABCB1
Bae2011 [5]	PKDB00895	losartan potassium	po	single	50	✓			✓	
Donzelli2014 [13]	PKDB00953	losartan	po	single	12.5	✓			✓	
FDA1995S60 [16]	PKDB00965	C14 losartan, e3174	po/iv, iv	single	100/30, 20	✓				
FDA1995S67 [17]	PKDB00966	losartan, e3174	po/iv, iv	single	50/10, 10			✓		
Fischer2002 [19]	PKDB00894	losartan	po	multi	50	✓			✓	
Han2009a [30]	PKDB00909	losartan potassium	po	single	50	✓			✓	
Huang2021 [35]	PKDB00919	losartan potassium	po	single	50	✓			✓	
Kim2016 [41]	PKDB00896	losartan	po	single	50	✓				
Kobayashi2008 [42]	PKDB00920	losartan potassium	po	single	25	✓				
Lee2003b [50]	PKDB00899	losartan potassium	po	single	50	✓			✓	
Li2009 [51]	PKDB00912	losartan	po	single	50	✓			✓	
Lo1995 [52]	PKDB00922	losartan potassium, e3174	po/iv	single	50, 100/20, 30	✓				
Munafo1992 [57]	PKDB00921	losartan	po	single	40, 80, 120	✓				
Oh2012 [61]	PKDB00054	losartan	po	single	2	✓				
Ohtawa1993 [62]	PKDB00911	losartan	po	single, multi	25, 50, 100, 200	✓				
Puris2019 [65]	PKDB00642	losartan potassium	po	single	12.5					
Sekino2003 [71]	PKDB00961	losartan	po	single	25	✓			✓	
Shin2020 [72]	PKDB00898	losartan potassium	po	single	50	✓				✓
Sica1995 [74]	PKDB00910	losartan	po	multi	100		✓			
Tanaka2014 [82]	PKDB00136	losartan	po	single	50	✓				
Yasar2002a [92]	PKDB00897	losartan	po	single	50	✓			✓	

3.2 Computational model

3.2.1 Model overview

A PBPK/PD model was developed based on curated study data to simulate the pharmacokinetics and pharmacodynamics of losartan. The whole-body framework integrates systemic circulation with submodels of key organs involved in losartan metabolism, including the gastrointestinal tract, liver, and kidneys, along with a RAAS model, as illustrated in Fig. 8.

By combining these components, the model enables simulations that capture both local processes and their interactions within the broader circulatory system. It supports the calculation of pharmacokinetic and pharmacodynamic parameters and provides time-course simulations of losartan, its active metabolite E3174, and relevant RAAS biomarkers — such as renin, angiotensin I, and aldosterone — in compartments like plasma, urine, and feces, as well as the resulting blood pressure response.

This comprehensive model also allows for simulation under various physiological and patho-

logical conditions. The following sections describe the individual PBPK/PD submodels in detail.

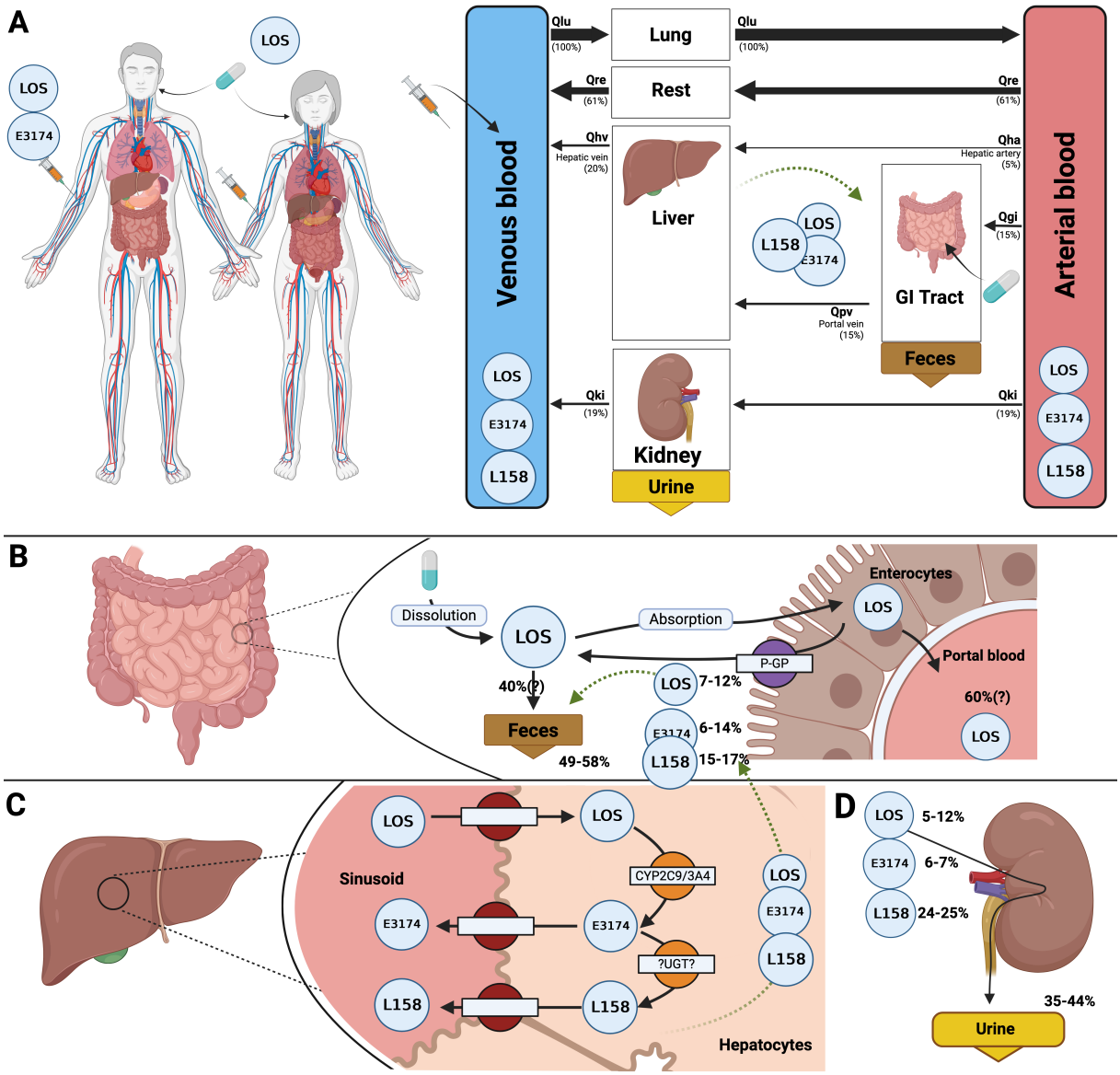

Figure 8: **Overview of the physiologically-based model of Losartan. A)** Whole body model showing circulation via the arterial and venous blood, with organs (liver, GI tract, kidney) influencing the pharmacokinetics of losartan (LOS). **B)** Intestine model illustrating the dissolution and absorption of LOS by enterocytes and the P-glycoprotein mediated efflux back into the intestine. Approximately 49-58 % of the dose is excreted as losartan or metabolites (E3174 and L158) **C)** Hepatic model depicting the uptake of losartan by hepatocytes and its conversion by cytochrome p450 2C9 and 3A4 (CYP2C9, CYP3A4) to losartan carboxylic acid E3174 (14 % of losartan dose) and the following conversion by UDP-glucuronosyltransferase (UGT) to L158. Losartan and its metabolites can also re-enter the intestinal model via enterohepatic circulation (biliary export). **D)** Renal model showing excretion of losartan, E3174 and L158 via urine, approximately 5-12 %, 6-7 % and 24-25 %, respectively.

3.2.2 Intestine model

The computational model of the intestine describes the dissolution, absorption, and transport of losartan, as well as the excretion of its metabolites, E3174 and L158, within the gastrointestinal tract. As shown in Fig. 9, the model is structured into five compartments: the stomach, intestinal lumen, enterocytes, blood plasma and feces. Losartan dissolves in the stomach and is subsequently absorbed into the plasma via enterocytes. However, it can also undergo efflux back into the intestinal lumen via P-glycoprotein, which contributes to fecal excretion. Additionally,

enterohepatic circulation facilitates the re-entry of losartan metabolites, E3174 and L158, into the intestinal lumen, where they can be excreted through the feces.

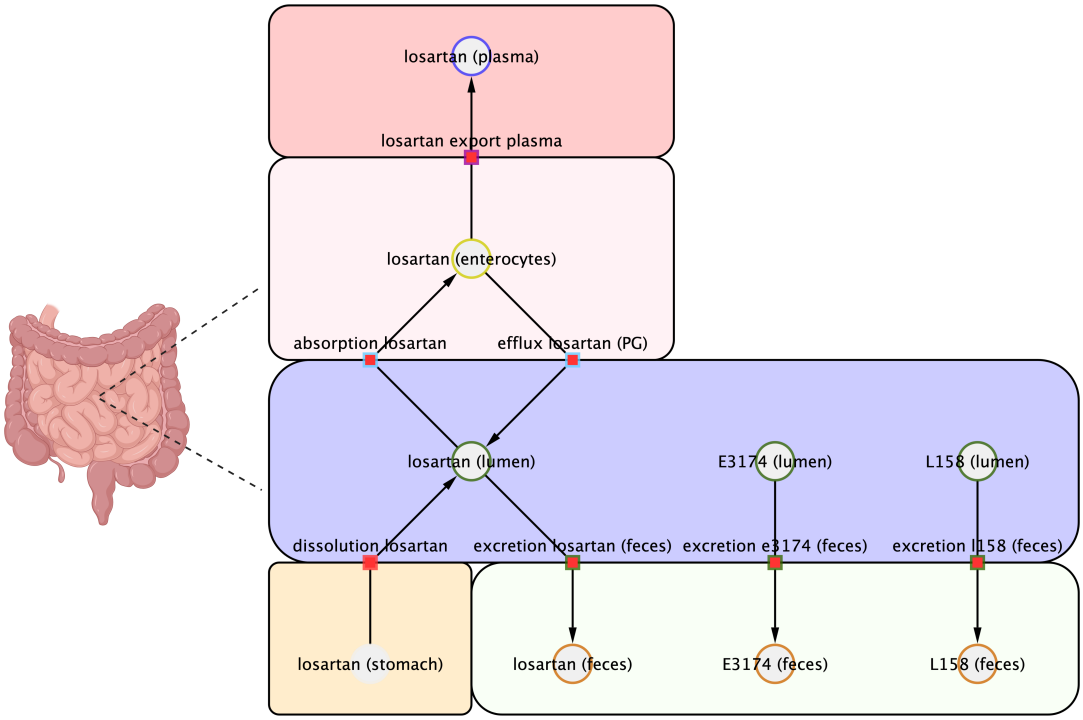

Figure 9: **Pharmacokinetic model of losartan in the small intestine** Losartan dissolves in the stomach and enters the intestinal lumen after oral administration, where it can be absorbed into the enterocytes and exported into the blood plasma. P-glycoprotein causes an efflux back into the intestinal lumen and fecal excretion of losartan. Metabolites E3174 and L158 undergo reabsorption into the intestinal lumen thought the enterohepatic circulation and are excreted into feces. Red squares indicate transport processes, and arrows show the direction of flow.

Dissolution Losartan is most often administered orally as a tablet (PODOSE los, in mg), which dissolves in the stomach. The dissolution rate $\text{dissolution}_{\text{los}}$ [mmol/min] is determined by the following equation:

$$\text{dissolution}_{los} = \frac{Ka_{dis\_los}}{60} \cdot \frac{\text{PODOSE}_{los}}{\text{Mr}_{los}}$$

$\text{Ka}_{\text{dis\_los}}$ [hr^{-1}] is the absorption rate constant for losartan, $\text{PODOSE}_{\text{los}}$ the oral dose of losartan [mg], and Mr_{los} is the molecular weight of losartan [g/mol]. The ordinary differential equation is:

$$\frac{d\,\text{PODOSE}_{los}}{dt} = -\text{dissolution}_{los} \cdot \text{Mr}_{los}$$

Absorption The dissolved losartan in the intestinal lumen is absorbed irreversibly via the organic anion uptake transporter OATP2B1 at the apical membrane of the enterocytes, via the following transport reaction:

$$\text{LOSABS} = f_{OATP2B1} \cdot f_{los\_abs} \cdot \text{LOSABS}_k \cdot \text{V}_{gu} \cdot \text{los}_{lumen}$$

The parameter $\text{f}_{\text{OATP2B1}}$ controls the OATP2B1 activity (1: reference activity, <1 reduced activity, >1 increased activity). $\text{F}_{\text{los\_abs}}$ [-] is the fraction of the losartan in the intestinal lumen that is absorbed. Since $\text{1-F}_{\text{los\_abs}}$ corresponds to the unabsorbed fraction, this parameter also

governs the proportion excreted in feces. LOSABS_k [min^{-1}] describes the absorption rate, Vgu [L] the volume of the intestine and los_lumen [mmolL] the losartan concentration in the lumen.

Efflux A fraction of absorbed losartan can be exported back into the intestinal lumen via the P-glycoprotein and excreted, as described via:

$$\text{LOSEFL} = f_{abcb1} \cdot f_{LOSEFL\_k} \cdot \text{LOSABS}_k \cdot \text{V}_{gu} \cdot \text{los}$$

The parameter f_abcb1 controls the P-glycoprotein activity (1: reference activity, <1 reduced activity, >1 increased activity), $\text{f}_\text{LOSEFL\_k}$ is the rate for losartan efflux (PG) relative to absorption and LOSABS_k is the rate of losartan absorption [min^{-1}]. The concentration of losartan in the enterocytes [mmol/L] is represented by the variable los. The change of losartan in the lumen is described via:

$$\frac{d\,\text{los}_{lumen}}{dt} = \left(-\frac{\text{LOSABS}}{\text{V}_{lumen}} + \frac{\text{LOSEFL}}{\text{V}_{lumen}} - \frac{\text{LOSEXC}}{\text{V}_{lumen}}\right) + \frac{\text{dissolution}_{los}}{\text{V}_{lumen}}$$

The ODE corresponding to the change in losartan concentration in enterocytes is:

$$\frac{d\,\text{los}}{dt} = \frac{\text{LOSABS}}{\text{V}_{entero}} - \frac{\text{LOSEFL}}{\text{V}_{entero}} - \frac{\text{LOSEX}}{\text{V}_{entero}}$$

Export into plasma The remaining losartan in the enterocytes is exported into the blood plasma. This process is described by reaction equation:

$$\text{LOSEX} = \text{LOSABS}_k \cdot \text{V}_{gu} \cdot \text{los}$$

LOSEX (mmol/min) is calculated using the rate of losartan absorption LOSABS_k [min^{-1}], the intestinal volume V_gu and the amount of losartan in the enterocytes 'los' [mmol/L]. The following ODE describes the change in losartan plasma concentration:

$$\frac{d\,\text{los}_{ext}}{dt} = \frac{\text{LOSEX}}{\text{V}_{ext}}$$

Excretion of losartan and metabolites The fraction of losartan that is initially not absorbed or transported back into the intestine via P-glycoprotein is excreted in the feces, as described in:

$$\text{LOSEXC} = (1 - F_{los\_abs}) \cdot \text{LOSABS}_k \cdot \text{V}_{gu} \cdot \text{los}_{lumen}$$

As described earlier, $\text{1-F}_\text{los\_abs}$ represents the unabsorbed fraction of losartan that is excreted in feces [-]. LOSABS_k [mmol/min] describes the absorption rate, V_gu [L] the volume of the intestine and los_lumen [mmolL] the lumen losartan concentration. The metabolites of losartan, E3174 and L158, are also partially excreted in feces due to the enterohepatic circulation from the liver into the bile and thus the intestine. The excretion of the major active metabolite E3174 is described in:

$$\text{E3174EXC} = \text{METEXC}_k \cdot \text{V}_{gu} \cdot \text{e3174}_{lumen}$$

The kinetic constant METEXC_k describes the rate of metabolite feces excretion [min^{-1}], V_gu the intestinal volume and $\text{e3174}_\text{lumen}$ the luminal concentration of E3174. Similarly, the excretion of L158 is described by:

$$\text{L158EXC} = \text{METEXC}_k \cdot \text{V}_{gu} \cdot \text{l158}_{lumen}$$

The change of the metabolites in the lumen is described via:

$$\frac{d\,\mathrm{e3174}_{lumen}}{dt} = -\frac{\mathrm{E3174EXC}}{\mathrm{V}_{lumen}}$$

$$\frac{d\,\mathrm{l158}_{lumen}}{dt} = -\frac{\mathrm{L158EXC}}{\mathrm{V}_{lumen}}$$

The accumulation of losartan and its metabolites in feces is described by the following ODEs:

$$\frac{d\,\mathrm{los}_{feces}}{dt} = \mathrm{LOSEXC}$$

$$\frac{d\,\mathrm{e3174}_{feces}}{dt} = \mathrm{E3174EXC}$$

$$\frac{d\,\mathrm{l158}_{feces}}{dt} = \mathrm{L158EXC}$$

3.2.3 Kidney model

The computational kidney model simulates the renal excretion of losartan, as well as the excretion of its metabolites E3174 and L158 from the blood plasma. As shown in Fig. 10, the model is structured into two compartments: the blood plasma and urine Renal clearance is modeled as unidirectional flow from plasma to urine.

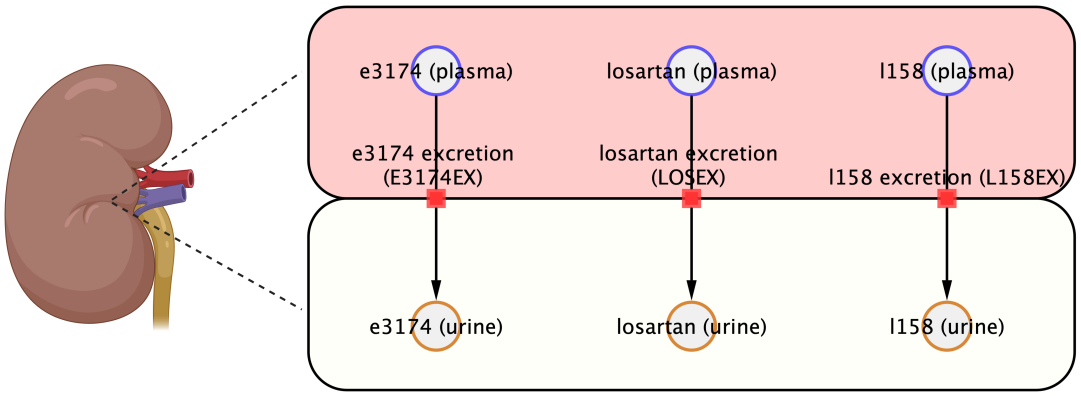

Figure 10: **Pharmacokinetic model of losartan in the kidneys** Losartan and its metabolites E3174 and L158 undergo renal clearance from plasma (upper box) into urine (lower box).

Excretion The model assumes passive, unidirectional excretion with no tubular reabsorption. Renal impairment reduces the excretion rate proportionally. The urinary excretion also referred to as renal clearance of all three compounds - losartan, E3174 and L158 - is described by the following equations.

$$\mathrm{LOSEX} = f_{renal\_function} \cdot \mathrm{LOSEX}_k \cdot \mathrm{V}_{ki} \cdot \mathrm{los}_{ext}$$

$$\mathrm{E3174EX} = f_{renal\_function} \cdot \mathrm{E3174EX}_k \cdot \mathrm{V}_{ki} \cdot \mathrm{e3174}_{ext}$$

$$\mathrm{L158EX} = f_{renal\_function} \cdot \mathrm{L158EX}_k \cdot \mathrm{V}_{ki} \cdot \mathrm{l158}_{ext}$$

The parameter $f_{renal\_function}$ is a scaling factor for renal function (1: normal renal function; <1 impaired renal function; >1 increased renal function) and Vki [L] corresponds to the kidney volume. $LOSEX_k$, $E3174EX_k$ and $L158EX_k$ represent the urinary excretion rate constants (min^{-1}) and los_{ext}, $e3174_{ext}$ and $l158_{ext}$ are the plasma concentration [mmol/L] of losartan, E3174 and L158, respectively. The net change in plasma concentration of losartan and its metabolites is described by the following ODEs:

$$\frac{d\,\mathrm{los}_{ext}}{dt} = -\frac{\mathrm{LOSEX}}{\mathrm{V}_{ext}}$$

$$\frac{d\,\mathrm{e3174}_{ext}}{dt} = -\frac{\mathrm{E3174EX}}{\mathrm{V}_{ext}}$$

$$\frac{d\,\mathrm{l158}_{ext}}{dt} = -\frac{\mathrm{L158EX}}{\mathrm{V}_{ext}}$$

where V_{ext} is the plasma volume [L]. The ODEs for urinary changes equal the excretion for losartan and its metabolite are defined as follows:

$$\frac{d\,\mathrm{los}_{urine}}{dt} = \mathrm{LOSEX}$$

$$\frac{d\,\mathrm{e3174}_{urine}}{dt} = \mathrm{E3174EX}$$

$$\frac{d\,\mathrm{l158}_{urine}}{dt} = \mathrm{L158EX}$$

3.2.4 Liver model

The computational liver model simulates the hepatic uptake of losartan, its enzymatic conversion into metabolites, and the subsequent export of these metabolites back into the plasma. Furthermore, losartan, E3174 and L158 undergo biliary export from the liver and enter the intestinal lumen due to enterohepatic circulation. As illustrated in Fig. 10, the model is structured into four compartments: the blood plasma, the liver, the bile and the intestinal lumen.

Import The uptake of losartan into hepatocytes from the blood plasma of the portal vein is simulated using:

$$\mathrm{LOSIM} = \mathrm{LOSIM}_k \cdot \mathrm{V}_{li} \cdot (\mathrm{los}_{ext} - \mathrm{los})$$

LOSIM is defined by the rate of losartan import $LOSIM_k$ [min^{-1}], the liver volume V_{li} [L] and the losartan concentrations los_{ext} and los in plasma and liver, respectively [mmol/L].

Biotransformation into metabolites In the hepatocytes, a fraction of losartan is converted into its main active metabolite E3174. The enzyme CYP2C9 catalyzes this biotransformation, which is modeled using Michaelis-Menten kinetics:

$$\mathrm{LOS2E3174} = f_{cyp2c9} \cdot \mathrm{LOS2E3174}_{Vmax} \cdot \mathrm{V}_{li} \cdot \frac{\mathrm{los}}{\mathrm{los} + \mathrm{LOS2E3174}_{Km\_los}}$$

The relative activity of the enzyme CYP2C9 is represented by the parameter f_{cyp2c9} (1: normal activity (wildtype); <1 reduced activity; >1.0 increased activity). The influence of CYP3A4 activity is neglected here, since its influence on metabolite formation is much less significant. $LOS2E3174_{Vmax}$ [mmol/min/l] and $LOS2E3174_{Km\_los}$ [mmol/L] describe the maximal velocity of losartan conversion to E3174 and the Michaelis constant for this conversion, respectively. The

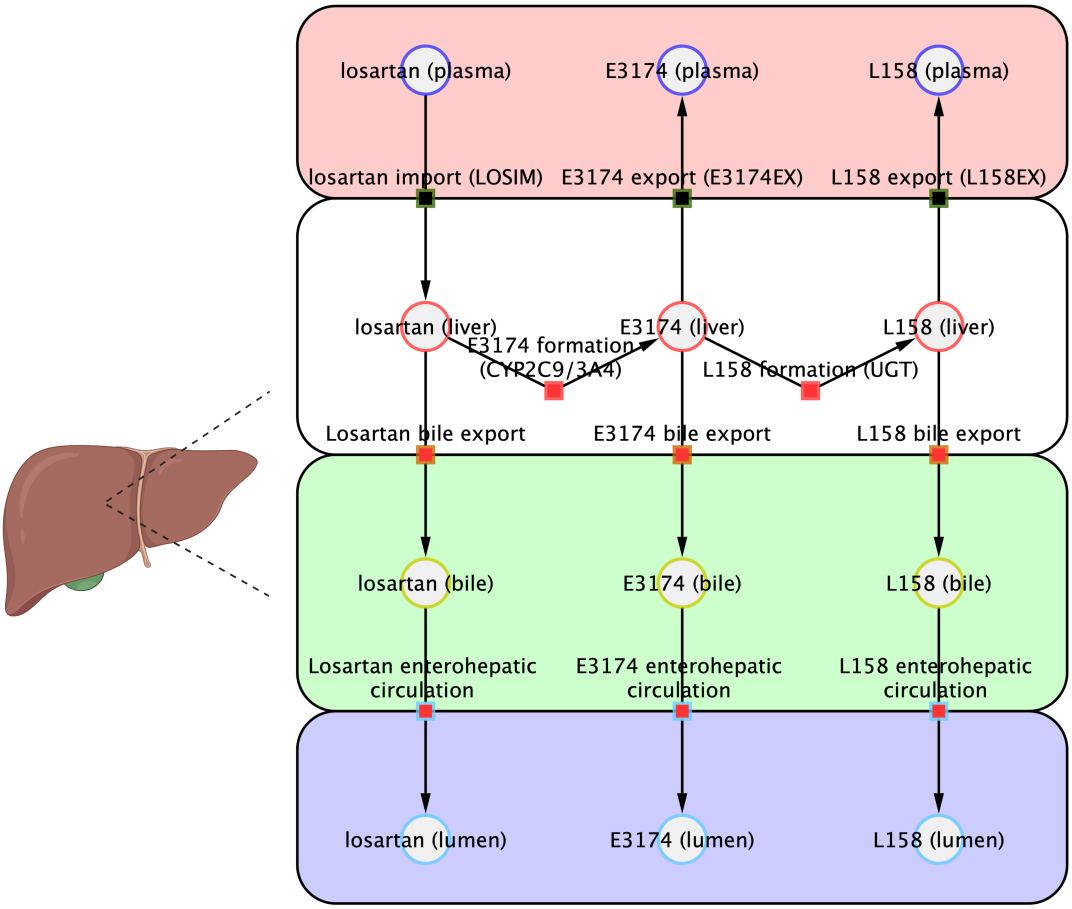

Figure 11: **Pharmacokinetic model of losartan in the liver** Losartan is transported from the portal blood plasma (upper red box) into the hepatocytes (white box), where it undergoes enzymatic biotransformation to form its metabolites, E3174 and L158. These metabolites can be exported back into the plasma or excreted into the bile (lower green box). Through enterohepatic circulation, both the parent compound and its metabolites re-enter the intestinal lumen (lower blue box).

second metabolite L158 is also formed by biotransformation in the hepatocytes, likely via UGT enzymes. This reaction is described in:

$$\mathrm{E3174L158} = \mathrm{E3174L158}_k \cdot \mathrm{V}_{li} \cdot \mathrm{e3174}$$

The conversion of E3174 to L158 via E3174L158 is modeled via mass action kinetics. $\mathrm{E3174L158_k}$ [$\mathrm{min^{-1}}$] describes the rate of E3174 conversion to L158 in the liver and e3174 represents the liver concentration of E3174 [mmol/L]. The time-dependent changes in compound concentrations within the liver are governed by the following ordinary differential equations (ODEs):

$$\frac{d\,\mathrm{los}}{dt} = \frac{\mathrm{LOSIM}}{\mathrm{V}_{li}} - \frac{\mathrm{LOS2E3174}}{\mathrm{V}_{li}} - \frac{\mathrm{LOSBIEX}}{\mathrm{V}_{li}}$$

$$\frac{d\,\mathrm{e3174}}{dt} = \frac{\mathrm{LOS2E3174}}{\mathrm{V}_{li}} - \frac{\mathrm{E3174L158}}{\mathrm{V}_{li}} - \frac{\mathrm{E3174EX}}{\mathrm{V}_{li}} - \frac{\mathrm{E3174BIEX}}{\mathrm{V}_{li}}$$

$$\frac{d\,\mathrm{l158}}{dt} = \frac{\mathrm{E3174L158}}{\mathrm{V}_{li}} - \frac{\mathrm{L158EX}}{\mathrm{V}_{li}} - \frac{\mathrm{L158BIEX}}{\mathrm{V}_{li}}$$

Metabolite export After biotransformation, the metabolites can reenter blood plasma, as described by:

$$\text{E3174EX} = \text{E3174EX}_k \cdot \text{V}_{li} \cdot (\text{e3174} - \text{e3174}_{ext})$$

$$\text{L158EX} = \text{L158EX}_k \cdot \text{V}_{li} \cdot (\text{l158} - \text{l158}_{ext})$$

In both equations, metabolite export is defined by rate constants E3174EX_k and L158EX_k [min^{-1}], liver volume V_li [L] and the difference between liver and plasma [mmol/L]. The net change in plasma concentration of metabolites is:

$$\frac{d\,\text{los}_{ext}}{dt} = -\frac{\text{LOSIM}}{\text{V}_{ext}}$$

$$\frac{d\,\text{e3174}_{ext}}{dt} = \frac{\text{E3174EX}}{\text{V}_{ext}}$$

$$\frac{d\,\text{l158}_{ext}}{dt} = \frac{\text{L158EX}}{\text{V}_{ext}}$$

V_ext represents the plasma volume [L].

Biliary export and enterohepatic circulation The enterohepatic circulation of losartan, E3174 and L158 was modeled as mass-action kinetics following equations:

$$\text{LOSBIEX} = \text{MBIEX}_k \cdot \text{V}_{li} \cdot \text{los}$$

$$\text{E3174BIEX} = \text{MBIEX}_k \cdot \text{V}_{li} \cdot \text{e3174}$$

$$\text{L158BIEX} = \text{MBIEX}_k \cdot \text{V}_{li} \cdot \text{l158}$$

$$\text{LOSEHC} = \text{LOSBIEX}$$

$$\text{E3174EHC} = \text{E3174BIEX}$$

$$\text{L158EHC} = \text{L158BIEX}$$

The biliary export depends on the rate of metabolite export in the bile MBIEX_k [min^{-1}], the liver volume Vli [L] and the concentration of each substance in the liver [mmol/L]. As no volume change occurs during enterohepatic recirculation, the rate of re-entry into the intestinal lumen equals the rate of biliary export. The corresponding changes in bile concentrations are defined by:

$$\frac{d\,\text{los}_{bi}}{dt} = \text{LOSBIEX} - \text{LOSEHC}$$

$$\frac{d\,\text{e3174}_{bi}}{dt} = \text{E3174BIEX} - \text{E3174EHC}$$

$$\frac{d\,\text{l158}_{bi}}{dt} = \text{L158BIEX} - \text{L158EHC}$$

And luminal concentration changes were defined by:

$$\frac{d\,\text{los}_{lumen}}{dt} = \frac{\text{LOSEHC}}{\text{V}_{lumen}}$$

$$\frac{d\,\mathrm{e3174}_{lumen}}{dt} = \frac{\mathrm{E3174EHC}}{\mathrm{V}_{lumen}}$$

$$\frac{d\,\mathrm{l158}_{lumen}}{dt} = \frac{\mathrm{L158EHC}}{\mathrm{V}_{lumen}}$$

$\mathrm{V}_{\mathrm{lumen}}$ represents the luminal volume [L].

3.2.5 RAAS model

In order to implement the pharmacodynamic effects of losartan, a model for RAAS and E3174 pharmacodynamic effects was developd. Losartan has minimal direct pharmacodynamic activity compared to its active metabolite E3174, and is therefore not included in this model. The physiological basis of the renin angiotensin aldosterone system is provided in Sec. 1.1.2. A technical overview of the computational RAAS model is presented in Fig. 12

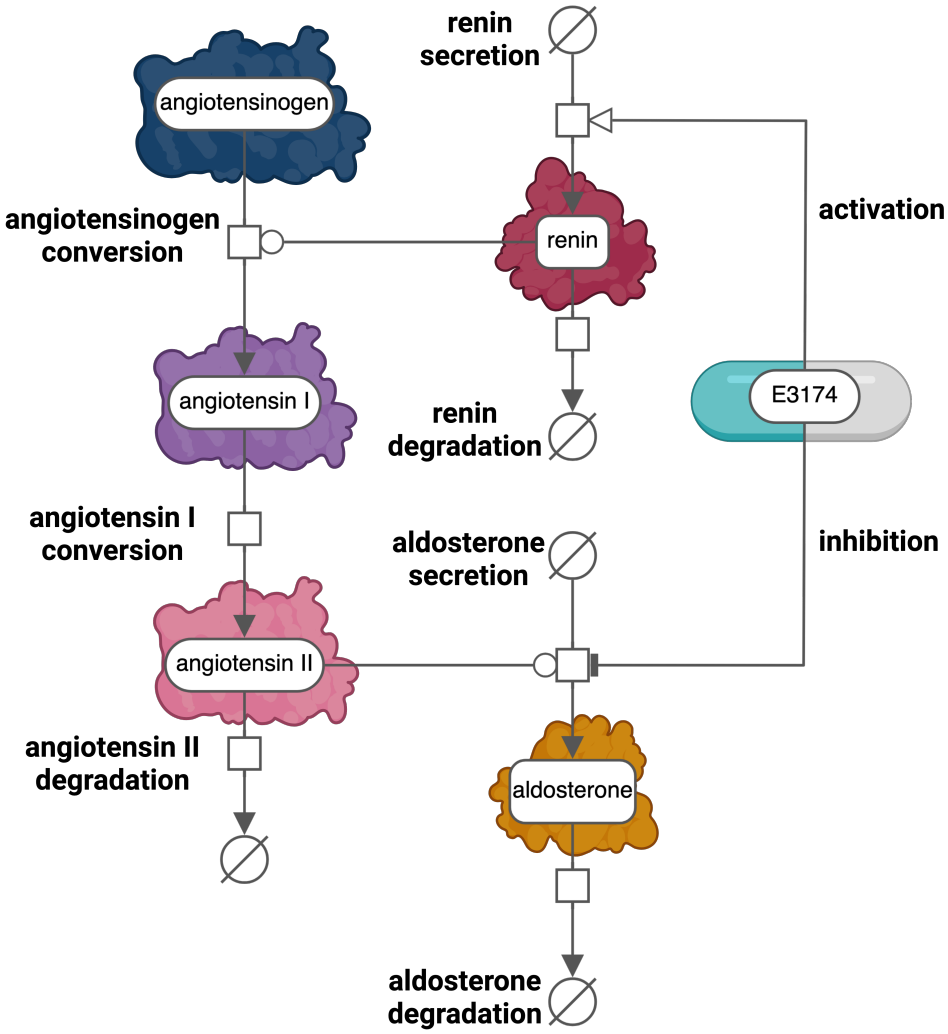

Figure 12: **Pharmacodynamic model of E3174 acting on the RAAS.** Renin is secreted (RENSEC) and catalyzes the conversion of angiotensinogen to angiotensin I (ANGGEN2ANG1), which is subsequently converted to angiotensin II (ANG1ANG2). Angiotensin II stimulates aldosterone secretion (ALDSEC). Renin, angiotensin II, and aldosterone are subject to degradation (RENDEG, ANG2DEG, ALDDEG), while angiotensinogen is maintained at a constant concentration. The active metabolite E3174 effects renin and aldosterone secretion ($\mathrm{fe}_{\mathrm{e3174}}$).

Renin Renin secretion [mmol/min] in plasma by the kidneys is stimulated by the pharmacodynamic effect of E3174, modeled using:

$$\text{RENSEC} = \text{RENSEC}_k \cdot (1 + \text{RENSEC}_{fa} \cdot fe_{\text{e3174}})$$

The secretion of renin is described by the rate of secretion RENSEC_k [mmol/min], the parameter for activation of renin secretion via E3174 RENSEC_fa [-] and the effect via E3174 represented by fe_{e3174} [-]. This effect was modeled using:

$$fe_{\text{e3174}} = \frac{\text{e3174}}{E50_{e3174} + \text{e3174}}$$

in which e3174 [mmol/L] is the plasma concentration of the active species E3174 and $\text{E50}_{\text{e3174}}$ [mmol/L] is the half-maximum effect concentration of E3174. The degradation of renin is defined as:

$$\text{RENDEG} = \text{RENDEG}_\text{k} \cdot \text{ren}$$

with ren [mmol/L] as the plasma renin concentration and RENDEG_k [l/min] being the rate of renin degradation [L/min], defined as:

$$\text{RENDEG}_\text{k} = \frac{\text{RENSEC}_\text{k}}{\text{ren}_{ref}}$$

composed of the rate of secretion RENSEC_k [mmol/min] divided by the reference concentration of renin ren_ref [mmol/L] set to 1×10^{-9} mmol/L. Thus the degradation is proportional to plasma renin. The dynamics of renin are then described as follows:

$$\frac{d\text{ren}}{dt} = \frac{\text{RENSEC} - \text{RENDEG}}{V_{\text{plasma}}}$$

Angiotensinogen conversion The conversion of angiotensinogen (ANGGEN) to angiotensin I (ANG I) is mediated by renin and described as:

$$\text{ANGGEN2ANG1} = \text{ANGGEN2ANG1}_\text{k} \cdot \text{anggen} \cdot \frac{\text{ren}}{\text{ren}_\text{ref}}$$

where $\text{ANGGEN2ANG1}_\text{k}$ [l/min] is the rate of angiotensinogen to angiotensin I conversion and anggen [mmol/L] is the angiotensinogen concentration.

Angiotensin I and II Conversion of angiotensin I to angiotensin II [mmol/min] is:

$$\text{ANG1ANG2} = \text{ANGGEN2ANG1}_\text{k} \cdot \frac{\text{anggen}_\text{ref}}{\text{ang1}_\text{ref}} \cdot \text{ang1}$$

where ang1 [mmol/L] is the plasma concentration of angiotensin I and the rate of ang1 to ang2 conversion is defined by the rate of angiotensinogen to angiotensin I conversion $\text{ANGGEN2ANG1}_\text{k}$ [l/min] and the scaling factor $\text{anggen}_\text{ref}/\text{ang1}_\text{ref}$. This leads to the following ODE:

$$\frac{d\text{ang1}}{dt} = \frac{\text{ANGGEN2ANG1} - \text{ANG1ANG2}}{V_{\text{plasma}}}$$

Angiotensin II is degraded according to:

$$\text{ANG2DEG} = \text{ANGGEN2ANG1}_\text{k} \cdot \frac{\text{anggenref}}{\text{ang2ref}} \cdot \text{ang2}$$

with ang2 [mmol/ L] being the concentration of angiotensin II in plasma. The net change in plasma concentration is:

$$\frac{d\text{ang2}}{dt} = \frac{\text{ANG1ANG2} - \text{ANG2DEG}}{V_{\text{plasma}}}$$

Aldosterone Aldosterone secretion [mmol/min] in plasma by the kidney is driven by angiotensin II and inhibited by E3174:

$$\text{ALDSEC} = \text{ALDSEC}_k \cdot (\frac{\text{ang2}}{\text{ang2}_{\text{ref}}}) \cdot (1 - \text{fe}_{e3174})$$

where ALDSEC_k [mmol/min] is the aldosterone secretion rate. Aldosterone degradation is given by:

$$\text{ALDDEG} = \text{ALDDEC}_\text{k} \cdot \text{ald}$$

where ald [mmol/L] is the aldosterone plasma concentration and the rate of aldosterone degradation ALDDEG_k [L/min] is:

$$\text{ALDDEG}_\text{k} = \frac{\text{ALDSEC}_\text{k}}{\text{ald}_{\text{ref}}}$$

The parameter ald_{ref} [mmol/L] is the reference concentration. This process yields the following differential equation:

$$\frac{d\text{ald}}{dt} = \frac{\text{ALDSEC} - \text{ALDDEG}}{V_{\text{plasma}}}$$

Blood pressure Finally, blood pressure changes in response to varying aldosterone levels. More precisely, the systolic (SBP), diastolic (DBP) and mean arterial blood pressure (MAP) [mmHg] are defined as:

$$\text{SBP} = \text{SBP}_{\text{ref}} + \text{BP}_{ald\_fe} \cdot \text{SBP}_{\text{ref}} \cdot \frac{\text{ald} - \text{ald}_{\text{ref}}}{\text{ald}_{\text{ref}}}$$

$$\text{DBP} = \text{DBP}_{\text{ref}} + \text{BP}_{ald\_fe} \cdot \text{DBP}_{\text{ref}} \cdot \frac{\text{ald} - \text{ald}_{\text{ref}}}{\text{ald}_{\text{ref}}}$$

$$\text{MAP} = \text{DBP} + \frac{\text{SBP} - \text{DBP}}{3}$$

where SBP_{ref} and DBP_{ref} are the reference blood pressure values of 120 and 80 mmHg, respectively and $\text{BP}_{\text{ald\_fe}}$ [-] is the effect of aldosterone on blood pressure. MAP is calculated via a standard formula used in physiology.

3.3 Parameter fitting

After the PBPK/PD model structure for losartan has been established, a subset of model parameters were optimized using a subset of the available data. In a first step parameters of the pharmacokinetic model were optimized (Tab. 3), subsequently parameters of the pharmacodynamic model (Tab. 4).
The results of the parameter adjustment, including the cost reduction over the optimization steps and the goodness of fit, are shown in Fig. 13a and Fig. 13b for the parameters of the pharmacokinetic model and in Fig. 14a and Fig. 14b for the parameters of the pharmacodynamic model.
Parameter optimization improved the fit of the model to the data (Fig. 13a and Fig. 14a) with most optimization runs converging to similar cost, demonstrating their effectiveness in minimizing errors. The goodness of fit plots (Fig. 14b and Fig. 14b) show that the model

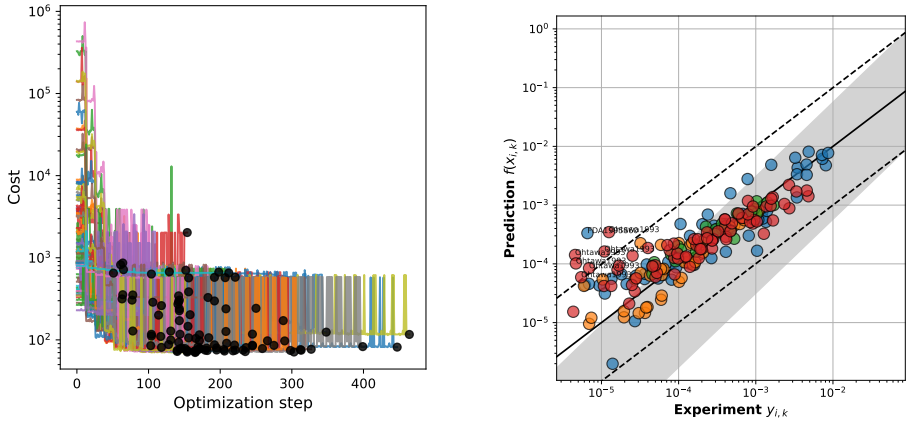

(a) Error convergence (b) Goodness-of-fit

Figure 13: **Optimization Performance.** Overview of Error convergence (cost vs. optimization step) and Godness-of-fit (predicted vs. experimental intravenous data) for the pharmacokinetic parameters.

Table 3: **Optimized parameters for the losartan pharmacokinetic model.**

Parameter name	Description	Value	Unit
`ftissue_los`	Tissue blood flow rate for DAP	0.14494	l/min
`Kp_los`	Tissue-to-plasma partition coefficient	3.26215	-
`GU__LOSABS_k`	Absorption rate of LOS in GI tract	0.03618	l/min
`GU__f_LOSEFL_k`	Efflux rate of LOS in GI tract	1.02004	-
`GU__METEXC_k`	Feces excretion rate of metabolites in GI tract	0.00003	1/min
`LI__E3174EX_k`	Hepatic export rate of E3174	0.01120	1/min
`LI__LOS2E3174_Vmax`	Hepatic Vmax of losartan conversion to E3174	0.00073	mmol/min/l
`LI__E3174L158_k`	Hepatic conversion rate of E3174 to L158	0.00113	1/min
`LI__MBIEX_k`	Biliary export rate of metabolites	0.06632	1/min
`KI__LOSEX_k`	Renal urinary excretion rate of LOS	0.07739	1/min
`KI__E3174EX_k`	Renal urinary excretion rate of E3174	0.02893	1/min
`KI__L158EX_k`	Renal urinary excretion rate of L158	0.28891	1/min

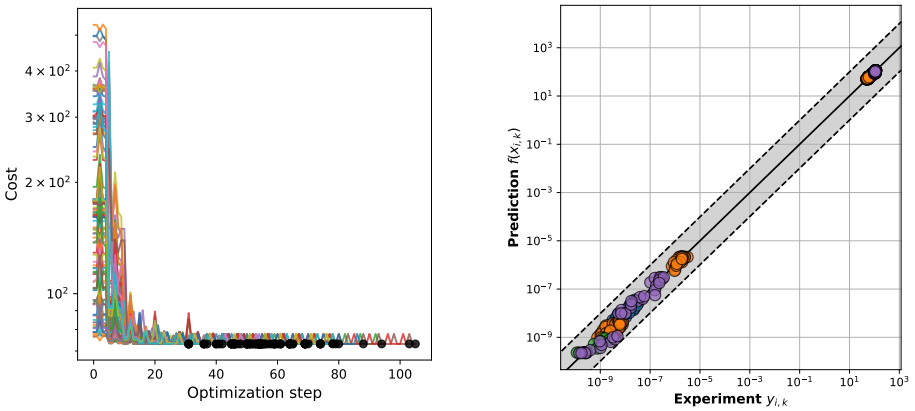

(a) Error convergence (b) Goodness-of-fit

Figure 14: **Optimization Performance.** Overview of Error convergence (cost vs. optimization step) and Godness-of-fit (predicted vs. experimental intravenous data) for the pharmacodynamic parameters.

performs well in different data sets, with many data points visually clustering closely around the identity line. Some deviations can be observed, especially in the pharmacokinetics, but overall

Table 4: **Optimized parameters for the losartan pharmacodynamic model.**

Parameter name	Description	Value	Unit
ANGGEN2ANG1_k	Conversion rate of angiotensinogen to angiotensin I	0.100300	l/min
E50_e3174	Half-maximum effect concentration of E3174	0.000291	mM
ALDSEC_k	Secretion rate of aldosterone	0.000001	mmole/min
BP_ald_fe	Effect of aldosterone on blood pressure	0.311999	-

the model is able to reproduce the data.

3.4 Model application

The developed PBPK/PD model of losartan was applied to investigate the impact of various physiological, pathological, and genetic factors on its pharmacokinetics and pharmacodynamics. Specifically, the model was used to simulate dose-dependent kinetics and dynamics (Sec. 3.4.1), as well as the effects of hepatic (Sec. 3.4.2) and renal impairment (Sec. 3.4.3) on systemic drug exposure and pharmacological response. Additionally, the influence of CYP2C9 and ABCB1 genetic polymorphisms (Sec. 3.4.5 and 3.4.4) were explored. For each simulation scenario, a set of subplots was generated to illustrate the pharmacokinetic outcomes and the downstream pharmacodynamic response of the renin-angiotensin-aldosterone system (RAAS). The pharmacokinetic profiles include plasma, urine and feces concentration-time curves for losartan, E3174, the inactive metabolite L-158 as well as the ratio of E3174 to losartan. To capture the pharmacodynamic response, the model outputs the key RAAS biomarkers renin, angiotensin I and aldosterone levels, as well as the downstream effects on blood pressure: mean arterial blood pressure, systolic and diastolic blood pressure. These results provide a comprehensive systems-level perspective on how physiological and genetic variability may affect losartan therapy.

3.4.1 Dose dependency

To evaluate dose-dependent behavior of the PBPK/PD model, simulations were performed for losartan doses ranging from 10 to 100 mg. Results are presented in Fig. 15, including time-course profiles (Panels A and C) and key pharmacokinetic/pharmacodynamic parameters (Panels B and D).

As shown in panel A, losartan and metabolite concentrations in plasma, urine, and feces increase with dose, while the E3174/losartan ratio decreases, indicating a relative saturation of metabolic conversion at higher doses. Panel B illustrates the pharmacodynamic response: higher doses lead to stronger suppression of aldosterone and blood pressure, along with compensatory increases in renin and angiotensin I. Panel C shows that AUC and Cmax increase more than proportionally with dose, especially for E3174. While losartan's elimination rate constant (kel) and half-life (t1/2) remain relatively stable, E3174 shows decreasing kel and increasing half-life with higher doses. Panel D shows that maximum renin and angiotensin I levels increase, while minimal aldosterone and systolic blood pressure decrease as dose increases.

Simulated pharmacokinetic and pharmacodynamic results match the general trends observed in curated dose-dependent clinical studies (Fig. 16).

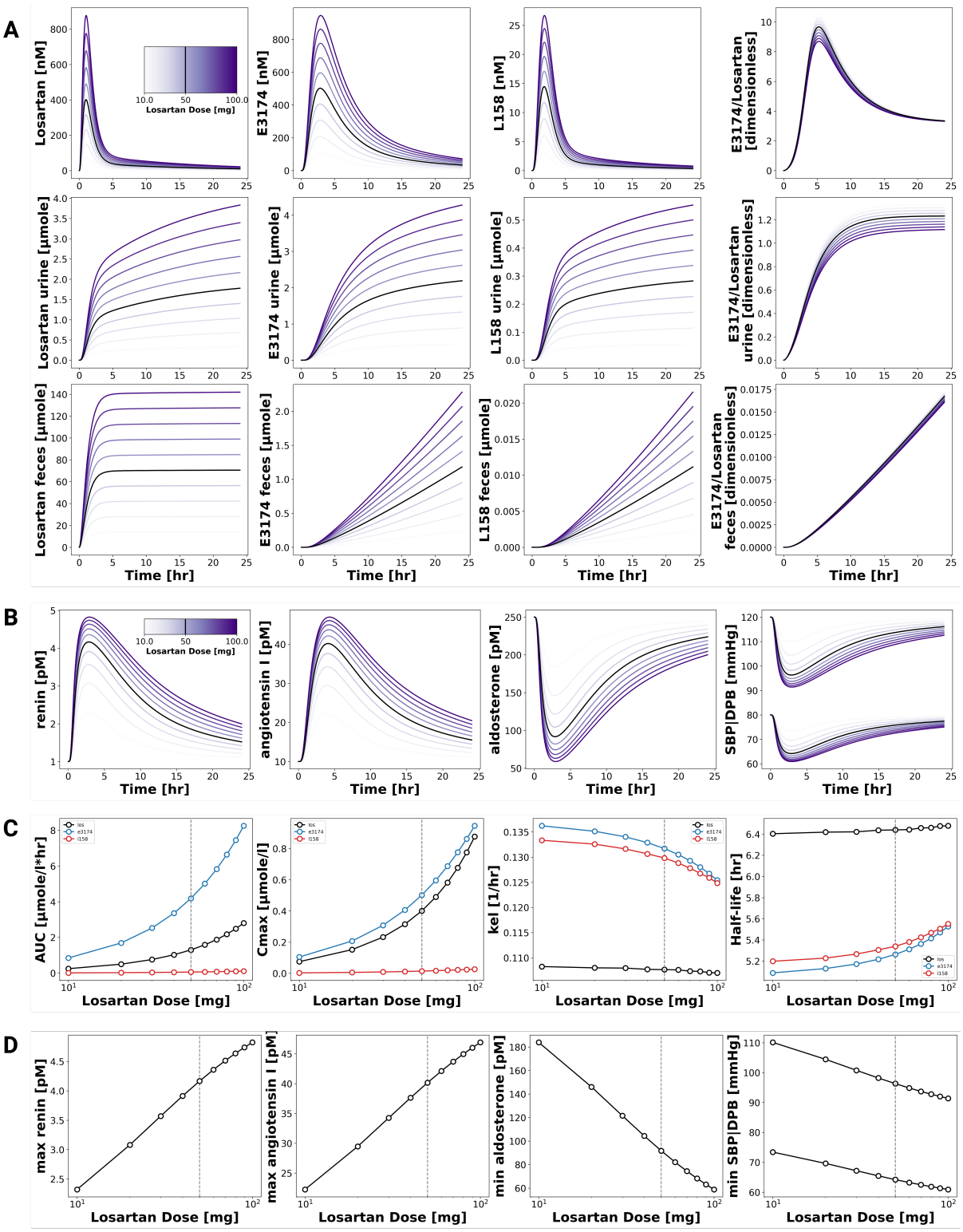

Figure 15: **Dose-dependent pharmacokinetics and pharmacodynamics of losartan and metabolites.** **(A)** Simulated plasma concentrations and excretion profiles of losartan, E3174, and L158 across doses (10–100 mg). Dose intensity is indicated by line color. The black graph marks 50 mg. **(B)** Dose–response curves for AUC, $C_{\max}$, elimination rate constant kel, and $t_{1/2}$. **(C)** Simulated RAAS biomarkers and blood pressure responses after 10–100 mg losartan. **(D)** Maximum or minimum values of selected endpoints (renin, angiotensin II, aldosterone, systolic BP).

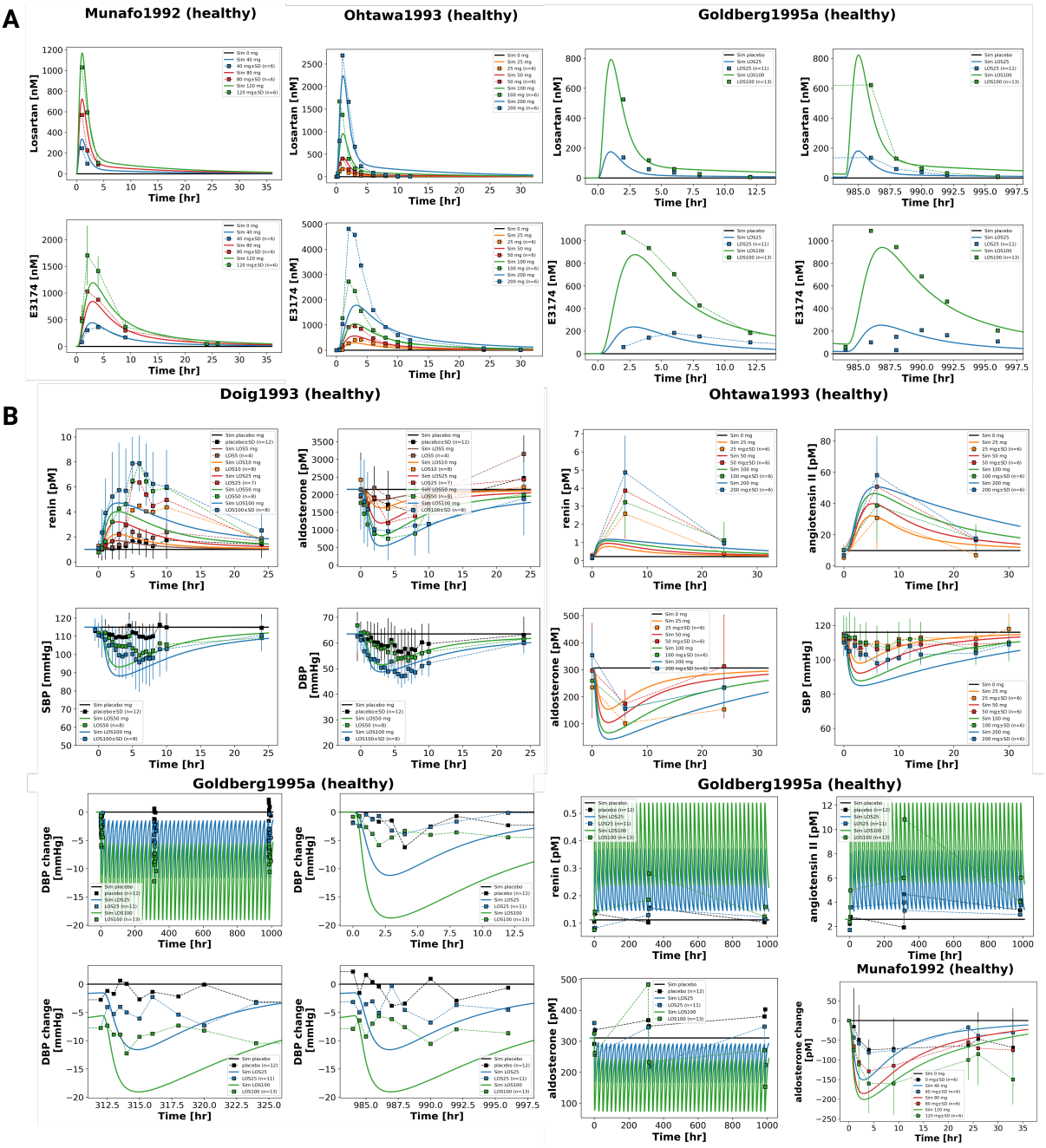

Figure 16: **Model performance of clinical data simulation across multiple dose levels. (A)** Simulated versus observed losartan pharmacokinetics. Data from [57, 62, 26] **(B)** Simulated versus observed losartan pharmacodynamics. Data from [12, 62, 26, 57]. Figures from individual studies are available in the supplements.

3.4.2 Hepatic impairment

To examine the effect of hepatic dysfunction, simulations were conducted across cirrhosis levels from 0.0 to 0.9 (Fig. 17).

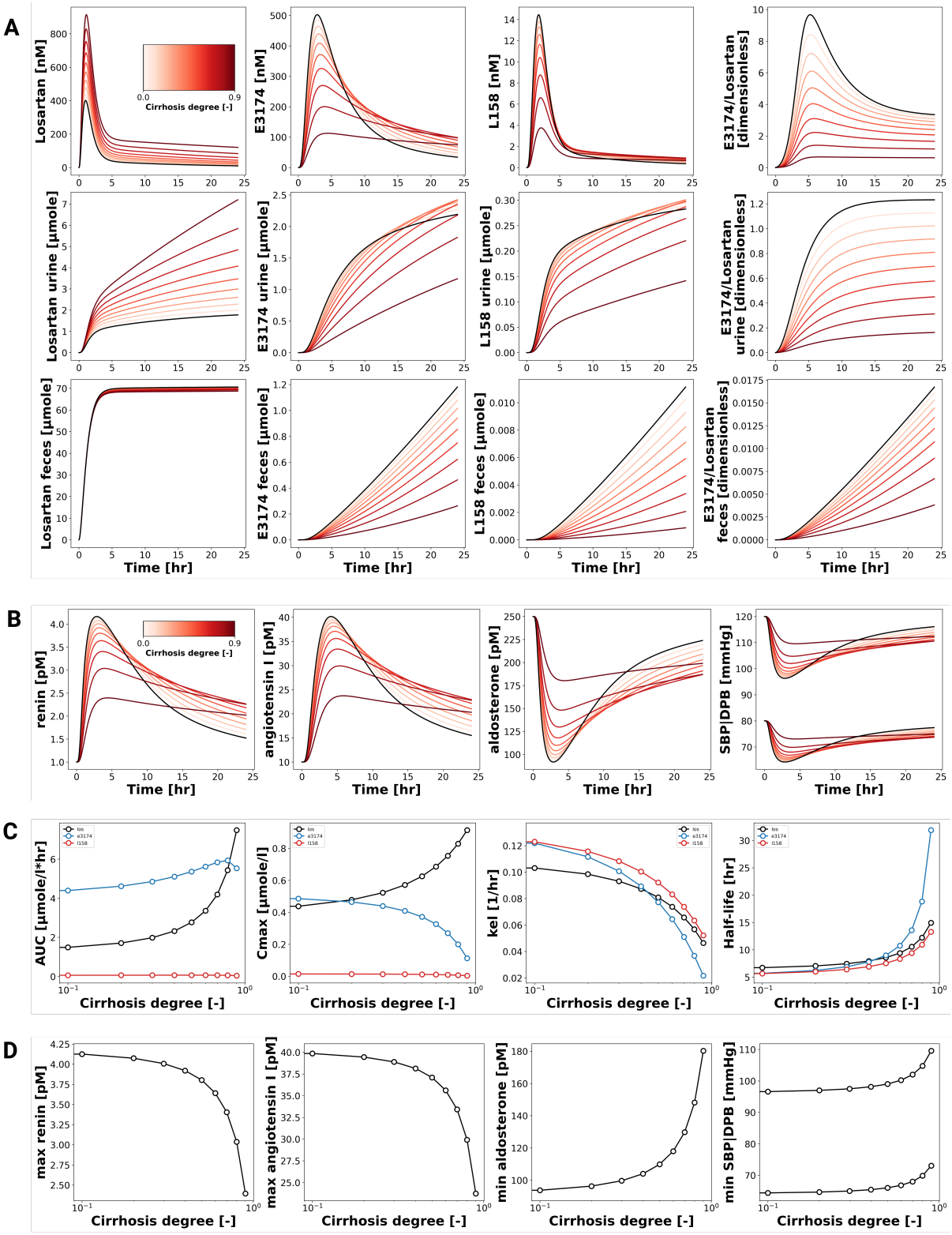

Figure 17: **Pharmacokinetics of losartan and metabolites depending on different degrees of cirrhosis.** **(A)** Simulated plasma concentrations and excretion profiles of losartan, E3174, and L158 across cirrhosis degrees. Cirrhosis degree is indicated by line color. The black line marks no cirrhosis. **(B)** Curves for AUC, $C_{\max}$, CL/F, and $t_{1/2}$ across cirrhosis degrees. **(C)** Simulated RAAS biomarkers and blood pressure responses for different stages of cirrhosis. **(D)** Maximum or minimum values of selected endpoints (renin, angiotensin II, aldosterone, systolic blood pressure SBP and diastolic blood pressure SBP) across cirrhosis degrees.

Panel A shows that with increasing cirrhosis severity, losartan levels in plasma and urine rise, while metabolite levels and the E3174/losartan ratio decline. Fecal excretion remains largely

unchanged. In the pharmacodynamic profiles (Panel B), early renin and angiotensin I levels decrease with worsening liver function, while aldosterone and blood pressure increase. In more severe cirrhosis, elevated renin and angiotensin I persist longer, and the normalization of aldosterone and blood pressure is delayed. Panel C shows increasing AUC, Cmax, and half-life for both losartan and E3174 with worsening cirrhosis, alongside decreasing kel. Panel D reveals decreasing maximum renin and angiotensin I levels, and increasing minimum aldosterone and blood pressure. Comparison with clinical data from patients with mild to moderate cirrhosis (CTP 5–9) (Fig. 18) shows that the model captures general concentration–time profiles but underestimates absolute values. The simulation captured concentration-time curve patterns of clinical data, but underestimated the concentrations.

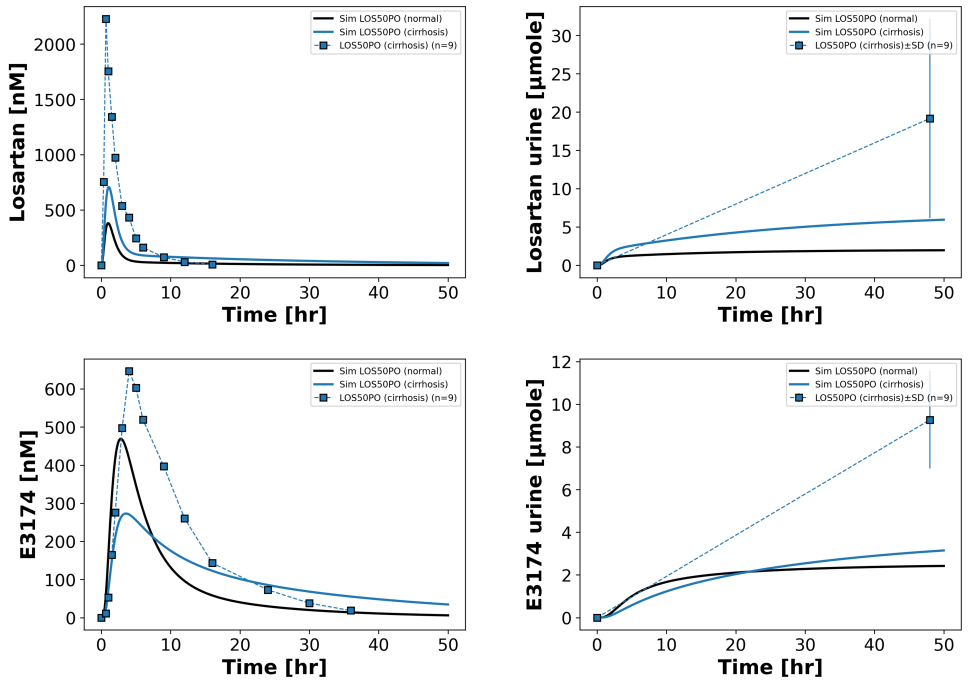

Figure 18: **Simulation FDA1995S67 [17]** Simulated versus observed losartan and E3174 plasma and urine concentrations following an 50 mg oral dose in individuals (n=9) with cirrhosis (CTP 5-9).

3.4.3 Renal impairment

To assess the influence of impaired renal function, simulations were carried out for normalized renal function levels from 0.1 to 1.0 (Fig. 19).

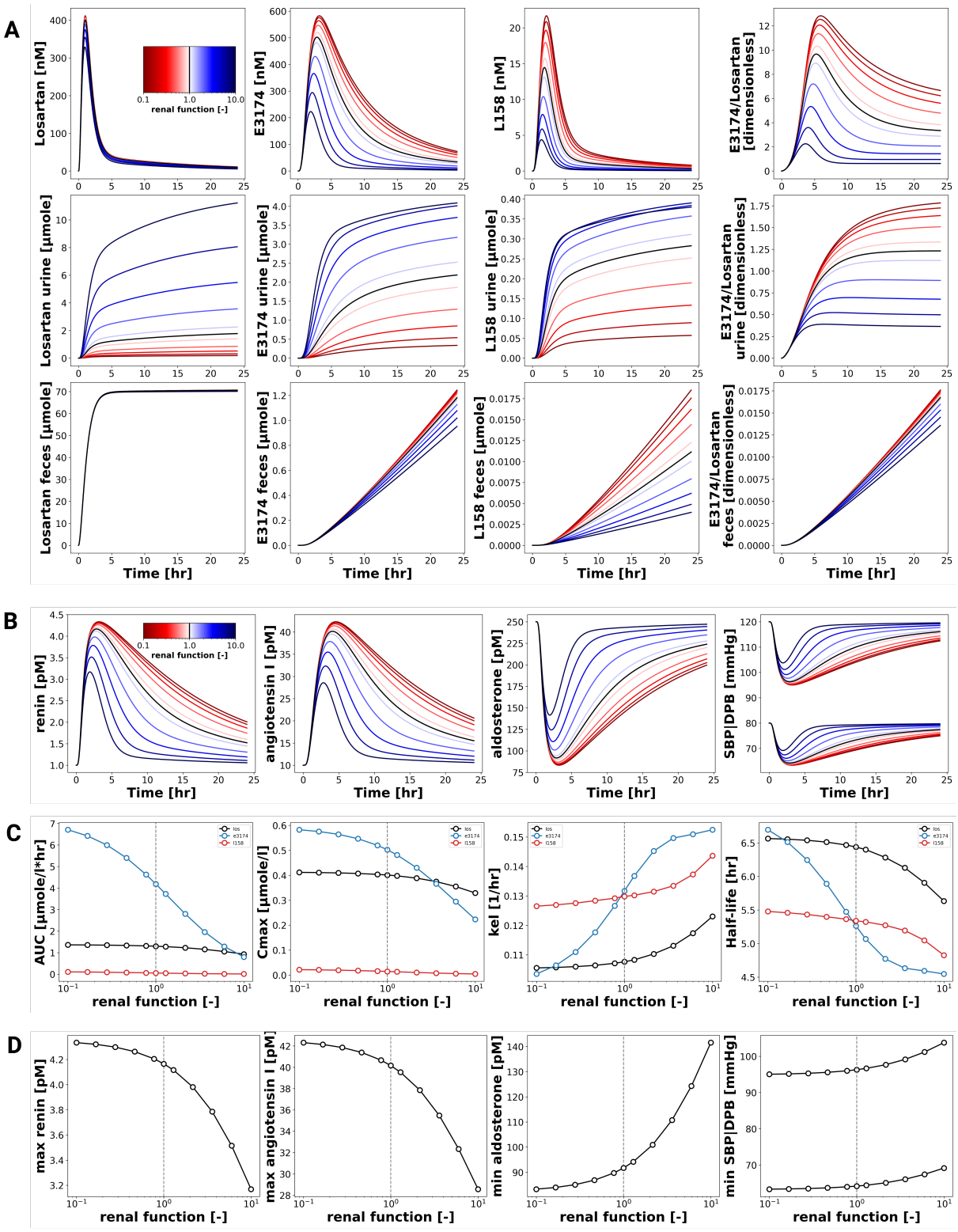

Figure 19: **Pharmacokinetics of losartan and metabolites across renal function degrees.** **(A)** Pharmacokinetic time courses for losartan, its metabolites and the metabolite to parent ratio in plasma, urine and feces different stages of renal function. **(B)** Pharmacodynamic time courses for important RAAS biomarkers different stages of renal function. **(C)** Pharmacokinetic parameters of losartan and its metabolites different stages of renal function. **(D)** Maximum or minimum values of selected endpoints (renin, angiotensin II, aldosterone, systolic BP) different stages of renal function.

As shown in Panel A, losartan plasma levels are only slightly affected by renal function. However, E3174 plasma concentrations increase with decreased function, and urinary excretion of

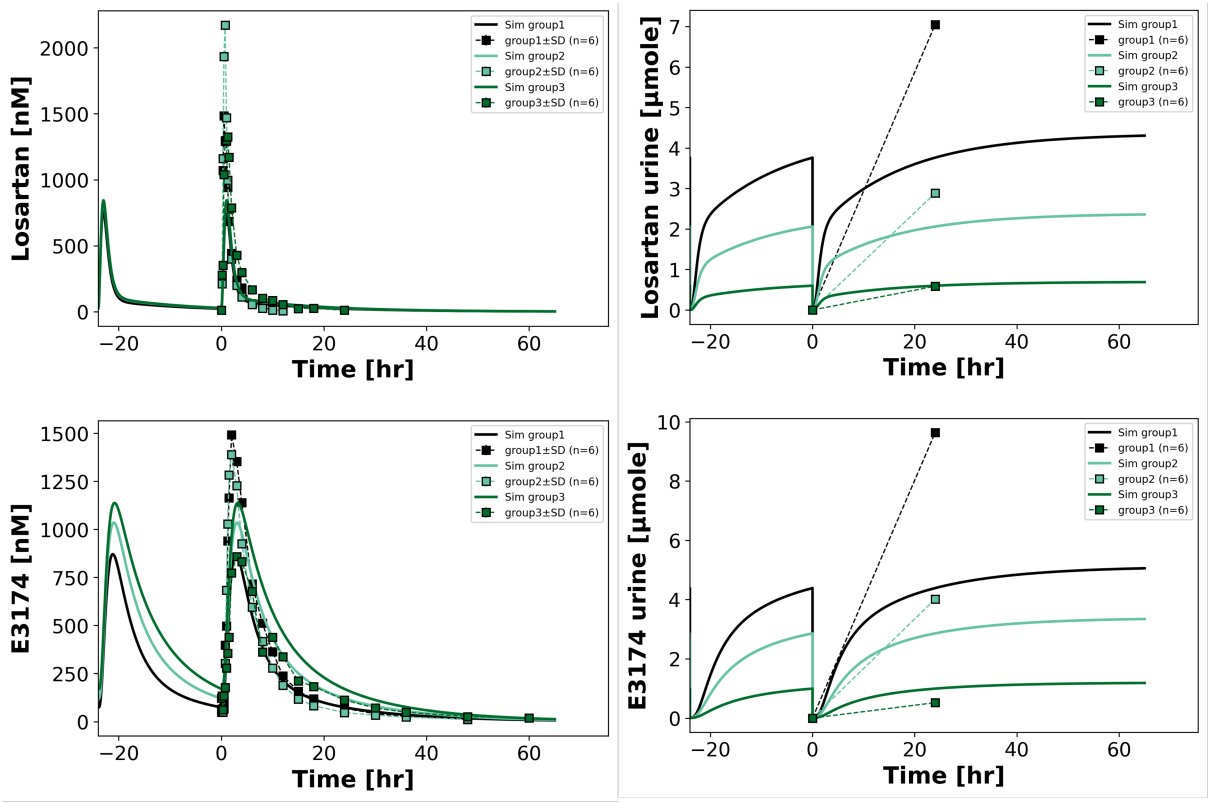

Figure 20: **Simulation Sica1995 [74].** Simulated versus observed losartan and E3174 plasma and urine concentrations following an 50 mg oral dose in individuals (each group n=6) with no to end-stage renal impairment (group 1- 3).

both losartan and metabolites declines. Fecal excretion of losartan increases slightly. The E3174/losartan ratio also increases with worsening renal function. Panel B shows stronger PD effects with reduced renal function: renin and angiotensin I levels increase, while aldosterone and blood pressure decrease. Panel C demonstrates that E3174's AUC, Cmax, and half-life rise significantly as renal function declines, while kel drops. Panel D confirms an enhanced antihypertensive effect with renal impairment. Compared to clinical data (Fig. 20), model predictions align with general trends but underestimate losartan plasma levels and slightly overestimate urinary excretion.

3.4.4 ABCB1 Genotypes

To investigate the influence of ABCB1 polymorphisms, simulations were performed for varying degrees of ABCB1 transporter activity (Fig. 21). Simulations for common diplotypes (GG/CC, GT/CT, TT/TT) are shown in the supplement. Pharmacokinetic simulations for the three common diplotypes: GG/CC (wild-type), GT/CT (heterozygous), and TT/TT (homozygous variant) can be viewed in supplementary Fig. 63.
Panel A shows that reduced ABCB1 activity leads to increased losartan and metabolite concentrations in plasma, urine, and feces. This is attributed to decreased P-glycoprotein-mediated efflux into the intestinal lumen and bile. Consequently, fecal excretion of losartan declines. As shown in panel B, reduced ABCB1 activity slightly enhances the RAAS-related pharmacodynamic effects of losartan. Panel C shows increasing AUC and Cmax for both losartan and E3174 as ABCB1 activity decreases, with little change in kel and half-life. Panel D shows moderate PD effects: renin and angiotensin I increase slightly, while aldosterone and blood pressure decrease marginally. Comparison with clinical data from a curated (Fig. 22) reveals similar trends, though the model underestimates absolute plasma and urine concentrations of losartan and E3174, as

well as the cumulative concentration of both compound in plasma and urine.

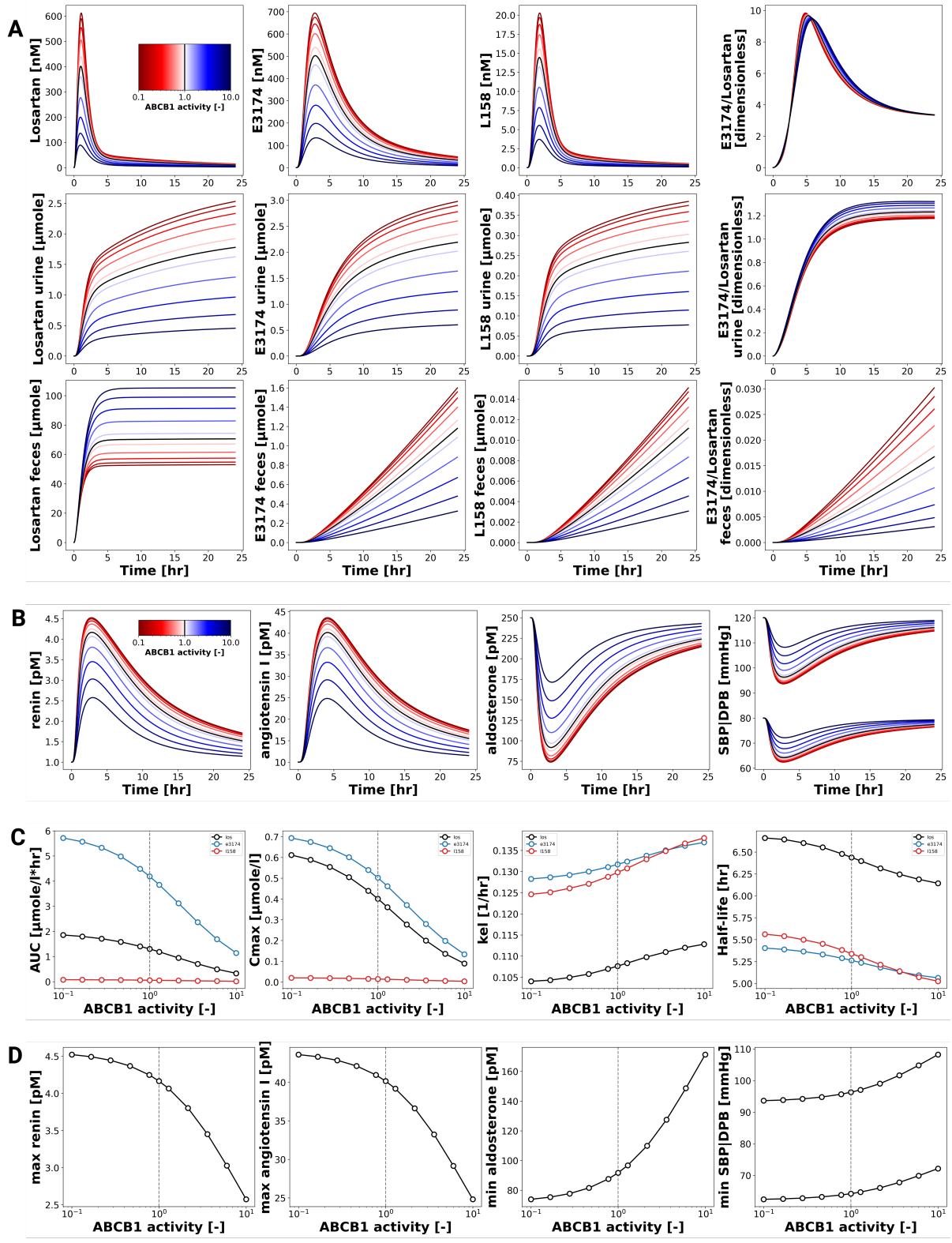

Figure 21: **Pharmacokinetics of losartan and its metabolites across varying ABCB1 activity levels** **(A)** Pharmacokinetic concentration time-courses for losartan, metabolites and metabolite to parent ratio under varying ABCB1 activity. **(B)** Pharmacodynamic concentration time-courses for key RAAS biomarkers under varying ABCB1 activity. **(C)** Pharmacokinetic parameters: AUC, Cmax, kel and half-life under varying ABCB1 activity. **(D)** Pharmacodynamic parameters: maximum renin and angiotensin I and minimum aldosterone and blood pressure (SBP, DBP) under varying ABCB1 activity.

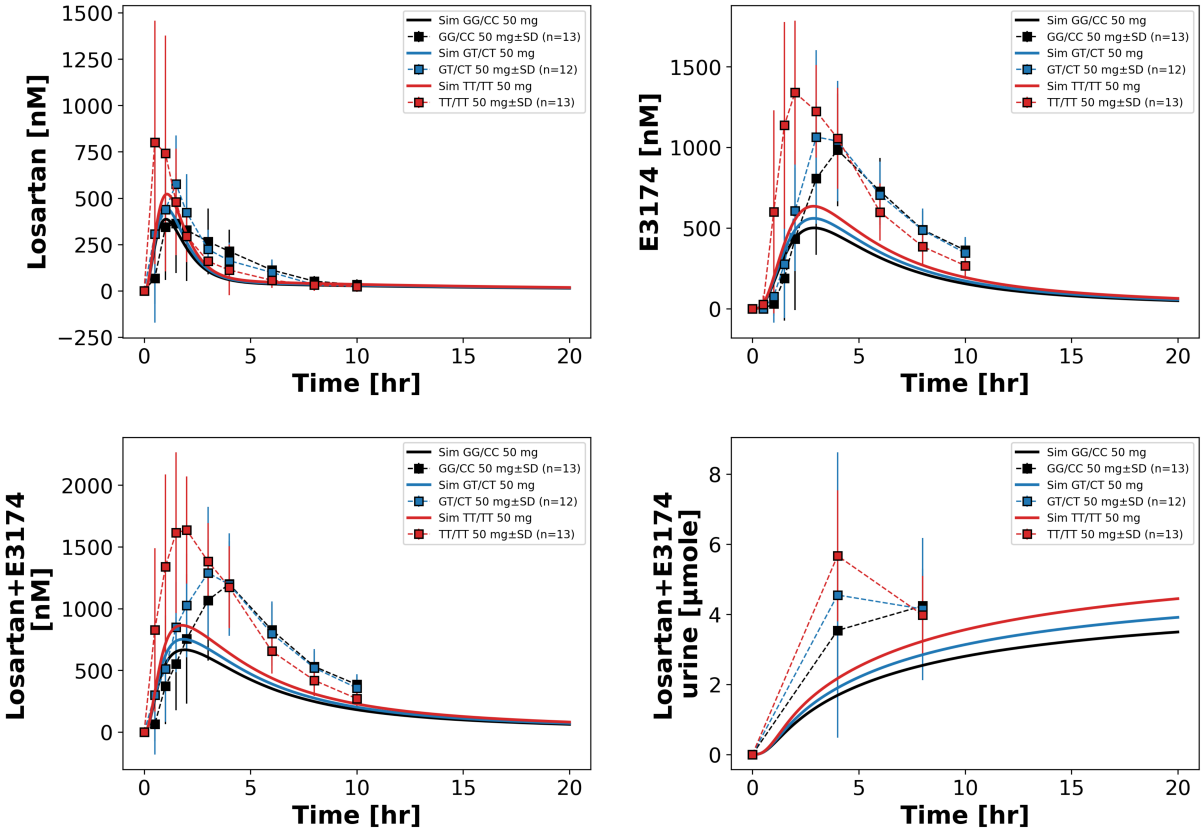

Figure 22: **Simulation Shin2020 [72]** Simulated versus observed losartan and E3174 plasma and urine concentrations following an 50 mg oral dose in individuals with genotypes GG/CC (n=13), GT/CT (n=9) and TT/TT (n=13).

3.4.5 CYP2C9 Genotypes

To evaluate the impact of CYP2C9 polymorphisms, simulations were conducted across a range of CYP2C9 activity levels (Fig. 23). Genotype-specific pharmacokinetic simulations for *1/*1 (wild type), *1/*2, *1/*3, *1/*13, *2/*2, *2/*3 and *3/*3 are included in the supplementary Fig. 64.

Panel A shows that lower CYP2C9 activity results in higher plasma, urine, and fecal levels of losartan and reduced levels of E3174, due to impaired metabolic conversion. Panel B illustrates that reduced CYP2C9 activity diminishes the pharmacodynamic response: less aldosterone and blood pressure reduction, and smaller increases in renin and angiotensin I. Panel C confirms that losartan's AUC and Cmax rise with lower activity, while E3174's values fall. Kel and half-life remain relatively constant. Panel D shows that maximum renin and angiotensin I levels decrease, while minimum aldosterone levels rise and blood pressure effects are attenuated. Compared with clinical data from seven curated studies (Fig. 24), the model successfully reproduces general genotype-dependent trends but tends to underestimate absolute exposure levels across CYP2C9 genotypes.

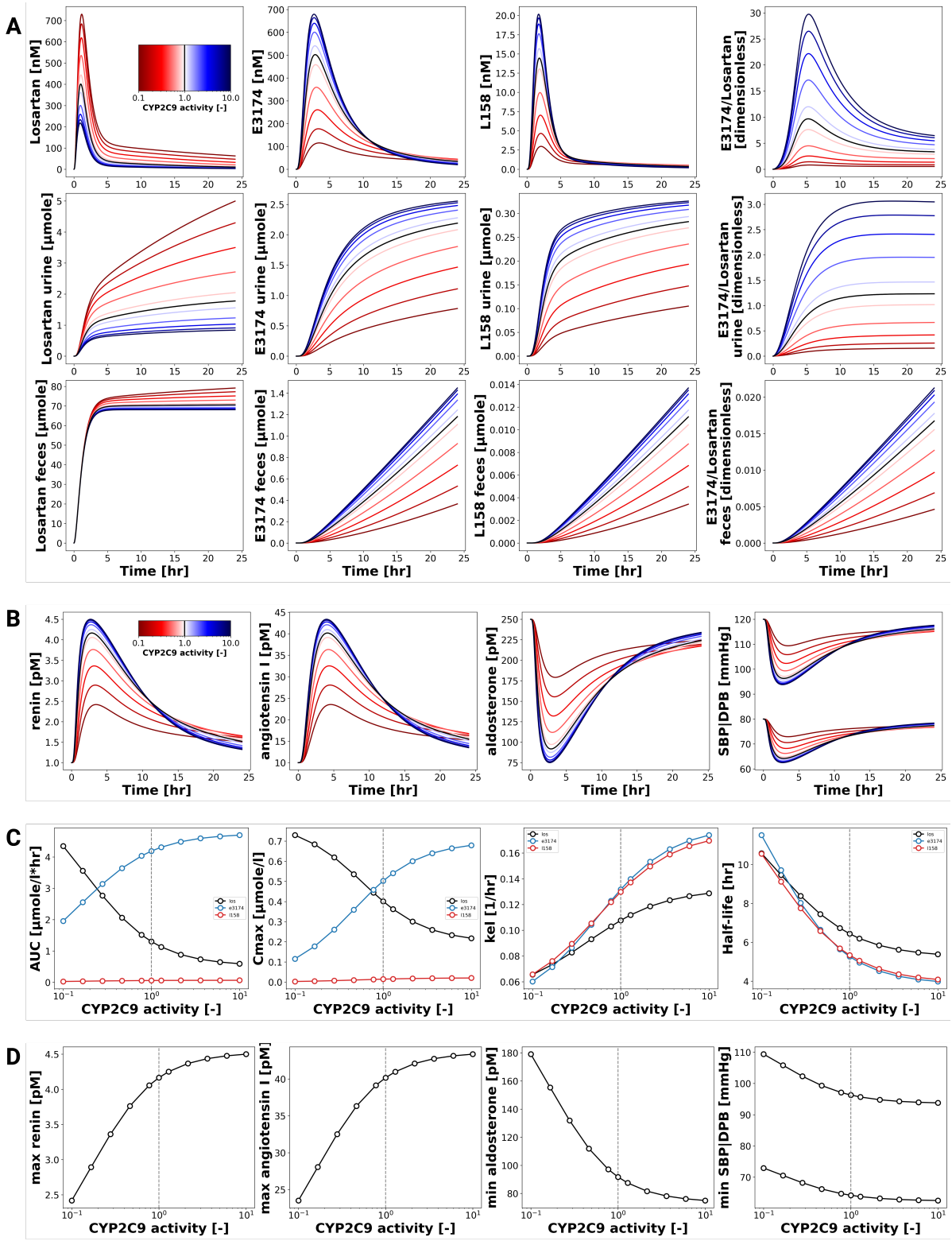

Figure 23: **Pharmacokinetics of losartan and its metabolites across varying CYP2C9 activity levels (A)** Pharmacokinetic concentration time-courses for losartan, metabolites and metabolite to parent ratio under varying CYP2C9 activity. **(B)** Pharmacodynamic concentration time-courses for key RAAS biomarkers under varying CYP2C9 activity. **(C)** Pharmacokinetic parameters: AUC, Cmax, kel and half-life under varying CYP2C9 activity. **(D)** Pharmacodynamic parameters: maximum renin and angiotensin I and minimum aldosterone and blood pressure (SBP, DBP) under varying CYP2C9 activity.

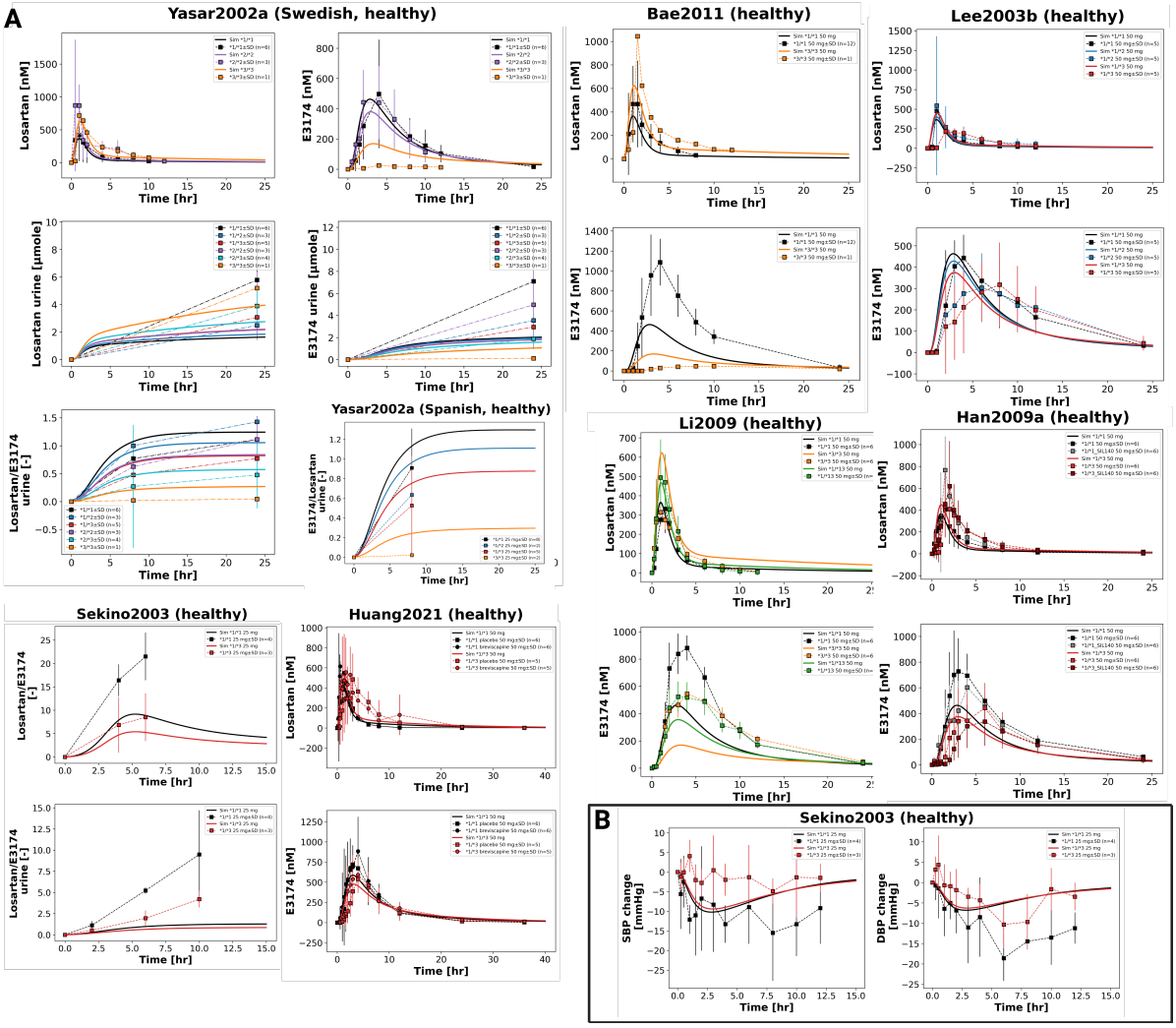

Figure 24: **Model performance of clinical data simulation across CYP2C9 avctivity levels. (A)** Simulated versus observed losartan pharmacokinetics. Data from [92, 5, 50, 51, 30, 71, 35] **(B)** Simulated versus observed losartan pharmacodynamics. Data from [71] Figures from individual studies can also be viewed in supplements.

3.5 Summary

The developed PBPK/PD model of losartan successfully characterized its pharmacokinetics and pharmacodynamics across diverse physiological, pathological, and genetic scenarios. Simulations incorporated dose escalation, hepatic and renal impairment, and functional variability in the ABCB1 and CYP2C9 genes, based on data from multiple curated clinical studies. Key findings include: non-linear dose dependency with relative saturation of E3174 formation at higher doses; hepatic impairment markedly increasing losartan exposure due to reduced biotransformation capacity; renal dysfunction to some degree elevating metabolite levels and enhancing antihypertensive effects; reduced ABCB1 activity increasing systemic drug and metabolite exposure with minimal impact on pharmacodynamics; and decreased CYP2C9 activity lowering metabolite formation and attenuating pharmacodynamic responses. Model predictions provide mechanistic insights into inter-individual variability in response to losartan and a foundation for individualized antihypertensive therapy.

4 Discussion

4.1 Data quality and limitations

The quality and availability of pharmacokinetic and pharmacodynamic (PK/PD) data were key determinants in the development and validation of the PBPK/PD model of losartan and its active metabolite E3174. Although losartan's pharmacokinetics are well-characterized in the literature, data on certain physiological processes remain scarce, especially the dynamics of RAAS components. For instance, the model does not account for circadian variation in plasma renin activity, angiotensin II, or aldosterone concentrations, despite their well-established diurnal patterns. Consequently, simulations may not accurately reflect time-of-day–dependent fluctuations in hormone levels or blood pressure regulation. Additionally, the pharmacodynamic contribution of the parent compound was not accounted for in the model, which may have introduced minor deviations between the simulated and observed data.
Moreover, the pharmacodynamic data underlying RAAS responses are heterogeneous, with high inter-study variability likely attributable to differences in analytical methods, patient populations, and experimental protocols. RAAS regulation is inherently complex and influenced by factors such as sodium intake, fluid balance, sympathetic tone, and hormonal feedback, many of which were outside the scope of this model. The absence of mechanistic modules for vasodilation/constriction, sodium and water retention, and autonomic feedback further limits the model's physiological resolution.
Excretion data were also limited—particularly regarding fecal elimination and the kinetics of the secondary metabolite L158, which are only described in the FDA review [14]. Furthermore, available pharmacodynamic datasets were insufficient for robust validation of RAAS responses across all physiological and genetic conditions.
Taken together, these limitations restrict the model's predictive accuracy under complex or individualized conditions. Nevertheless, the framework successfully reproduces general system-level dynamics and provides insight into key relationships between dose, drug exposure, and RAAS-mediated blood pressure responses.

4.2 Computational model development

The PBPK/PD model for losartan integrates distinct organ submodels intestine, liver and kidney into a unified framework capable of simulating both pharmacokinetic processes under varying physiological and genetic conditions. By incorporating mechanistic representations of intestinal absorption, hepatic metabolism via CYP2C9, and renal excretion, the model enables comprehensive evaluation of losartan and E3174 pharmacokinetics across different clinical scenarios. In addition to pharmacokinetics, the model links systemic exposure of the active metabolite E3174 to its pharmacodynamic effects via a simplified RAAS submodel. This PD submodel captures the core hormonal cascade from renin to aldosterone and enables simulation of blood pressure regulation as a downstream effect of AT1 receptor blockade. Although simplified, this structure allows quantitative assessment of the relationship between E3174 plasma levels and RAAS-mediated changes in blood pressure. More precicely, blood pressure changes were modeled as linearly proportional to aldosterone deviations from baseline. Intermediate processes, were not explicitly included, such as sodium retention or plasma volume expansion. The model also lacks feedback regulation and circadian rhythmicity, two critical components of RAAS physiology. As a result, it can simulate initial pharmacodynamic responses but not long-term homeostatic adaptations.
Parameter estimation showed successful convergence for most parameters, and key values related to absorption, metabolism, and excretion aligned well with reported literature values for losartan. Assumptions regarding transporter-mediated intestinal absorption and phase I hepatic

metabolism enabled physiologically plausible predictions under baseline and perturbed conditions.
The model offers a mechanistically grounded and clinically relevant representation of losartan pharmacology, despite certain simplifications, such as the absence of circadian regulation or hormonal feedback. It serves as a platform for exploring genotype effects, optimizing dosing strategies, and evaluating drug responses in impaired physiological states. Therefore it provides a valuable addition to clinical trials, in which such comparisons are often constrained by ethical, logistical, or statistical limitations.

4.3 Physiological variability and functional impairment

Dose dependency The PBPK/PD model successfully confirmed known effects in losartan pharmacokinetic and pharmacodynamic response. With increasing dosing, the plasma, urine and feces concentrations of losartan, E3174 and L158 increased too. Notably, the metabolite-to-parent ratio (E3174/losartan) declined with increasing dose. At higher doses, CYP2C9 approaches saturation, so the fraction of losartan converted to E3174 decreases, even if absolute formation continues to increase. Higher doses also produced more pronounced and sustained suppression of aldosterone and blood pressure, along with compensatory increases in renin and angiotensin I due to disrupted feedback regulation. These effects reflect disruption of the RAAS by AT1 receptor blockade and are consistent with the known pharmacodynamics of losartan. Small deviations between model and clinical data are presumably because of high inter-study variability, especially in study design for pharmacodynamic research. Together, the results indicate that the model adequately captures both nonlinear PK behavior and dose-dependent regulatory responses of the RAAS.

Hepatic impairment The PBPK/PD model simulations predict an increase in losartan plasma and urine concentration with increasing cirrhosis degree, which is in good agreement with clinical data [8, 75]. As indicated by the decrease of kel, clearance is reduced in patients with cirrhosis, possibly due to reduced hepatic blood flow and CYP2C9 function. Model simulations suggested reduced formation of E3174 and predicts corresponding attenuation of pharmacodynamic effects. While these pharmacokinetic results are mostly qualitatively consistent with the limited clinical data available, discrepancies occur especially in E3174 concentration. The active compound increases 1.5-2 due to altered pharmacokinetics according to McIntyre et al. [55]. The model does not properly reflect this accumulation of E3174, but indicates this trend by the prolonged elevated E3174 plasma levels in patients with a higher degree of cirrhosis. The initial low E3174 levels are likely caused by high losartan plasma levels and underestimated levels of excretion. Further limiting are the lack of control groups and sparse pharmacodynamic endpoints. Notably, the model underestimated the reported 4- to 5-fold increase in losartan plasma levels [75], suggesting that additional mechanisms may play a role. Despite these limitations, the model confirms the importance of dose adjustments in hepatic dysfunction to a lower starting dose. This is especially relevant in conditions like heart failure, where liver impairment is common and RAAS inhibition has heightened clinical relevance [92, 71]. On the contrary, hypertension with co-existing liver disease is less common [55].

Renal impairment Simulations of renal impairment reveal a clear effect: reduced losartan and E3174 clearance lead to prolonged systemic exposure, despite unaffected formation of the active metabolite. This mirrors the compound's known renal elimination route and aligns with available PK data [74]. AUC and Cmax remain relatively stable for losartan, in line with the data from Sica et al. [74]. However less fitting, the model predicts E3174 plasma concentration, AUC and Cmax to increase with worsening of renal function. Contrary to that, according to Sica et al [74] and Pedro et al. [63] AUC and Cmax are stable for E3174. This sugests, an alteration

of losartan absorption, biotransformation and/or hepatic clearance of E317 [75], which is not accounted for in this PBPK/PD model.

Although direct pharmacodynamic data in renally impaired populations are lacking, the model predicted slightly stronger blood pressure suppression, paralleling the dose-dependent effects observed at higher plasma concentrations. This highlights the model's utility in extending pharmacodynamic predictions beyond available clinical endpoints. However, the model forecasts enhanced pharmacodynamic responses (e.g., blood pressure reduction), which may slightly overestimate clinical effects. This discrepancy likely reflects missing compensatory mechanisms—such as altered hepatic clearance [19, 71, 17].

ABCB1 genotypes The PBPK/PD model simulations across a range of ABCB1 (P-gp) activity levels indicate visible effects on losartan pharmacokinetics. Low ABCB1 activity, as associated with GT/CT or TT/TT diplotype results in increased losartan and metabolite plasma concentrations as well as excretion. Only fecal excretion is lowered for decreased ABCB1 acticity, likely because of less intestinal efflux. The ratio of E3174/losartan in plasma and urine is slightly decreased for low ABCB1 activity. AUC of losartan increased only merely with decreased ABCB1 activity. These trends align with clinical observations from Shin et al. [72]. The model could predict increased hypotensive effects at lower transporter activity levels, despite the scarce availability of pharmacodynamic data. Though, the difference in blood pressure between observed ABCB1 genotypes was not big, suggesting minimal need for clinical dose adjustment based on ABCB1 genotype alone. Nevertheless, more studies with larger populations, especially concerning pharmacodynamic effects of ABCB1 genotypes could improve the predictive capability of the model. In humans, P-gp is also expressed proximal renal tubular system, contributing to renal clearance [72], posing a further possibility for model improvement.

CYP2C9 genotypes The PBPK/PD model demonstrated a pronounced impact of CYP2C9 genetic variability on the pharmacokinetics of losartan and its active metabolite E3174. Reduced-function alleles, particularly *2 and *3, were associated with progressively decreased metabolic conversion to E3174, resulting in reduced systemic exposure to the active metabolite and impaired blood pressure lowering effect via lowered aldosterone. Simulated individuals with low CYP2C9 activity exhibited markedly lower E3174 concentrations and diminished blood pressure reduction. These results are consistent with clinical findings reporting 1.6- to 3-fold increases in losartan AUC and significantly decreased E-3174 levels among carriers of reduced-function alleles [92, 71, 19]. Although the limited availability of patient-level kinetic data for rare CYP2C9 genotypes restricts direct validation, the model robustly reproduced the expected trends. The use of a continuous CYP2C9 activity scale allowed simulation of a wide range of genotypic variability and captured the nonlinear relationship between enzyme activity and metabolite formation. However, as with other drugs metabolized by polymorphic enzymes, genotype alone is unlikely to fully explain inter-individual differences in losartan response. Factors such as age, comorbidities etc. may further influence both pharmacokinetics and pharmacodynamics. Future model extensions could incorporate these interacting variables to improve predictions in diverse patient populations. From a clinical perspective, the findings support the potential of genotype-guided dosing to improve therapeutic outcomes in patients carrying low-function CYP2C9 alleles. Nevertheless, the high degree of variability within genotype groups suggests that genetic testing should be targeted toward individuals with inadequate response or increased risk of adverse effects, rather than applied universally.

5 Outlook

The PBPK/PD model of losartan developed in this thesis provides a mechanistic framework for simulating drug behavior across a range of physiological and genetic conditions. It integrates absorption, metabolism, distribution, and elimination processes with a simplified RAAS module to simulate pharmacodynamic responses. Building on this foundation, several opportunities for model refinement and application emerge.

First, enhancing the pharmacodynamic component would improve the physiological fidelity of RAAS regulation. Incorporating feedback mechanisms, such as baroreflex and hormonal compensation, along with circadian rhythms and additional regulatory pathways (e.g., vasopressin, ACTH), would allow for more accurate predictions of blood pressure regulation over time. These additions could also better account for the complex temporal dynamics observed in clinical studies but not captured in the current model.

Second, the inclusion of more detailed mechanistic submodels for aldosterone's effects — such as sodium retention, fluid balance, and vascular resistance — could offer more nuanced predictions of blood pressure response. These extensions would also improve the model's ability to simulate long-term adaptations and homeostatic buffering, which are especially relevant in chronic disease states or prolonged therapy.

Furthermore, the model could be extended to simulate clinically relevant drug–drug interactions. Losartan is frequently co-administered with other cardiovascular agents, such as diuretics, beta-blockers, or calcium channel blockers, which may influence its pharmacokinetics or pharmacodynamics. For instance, CYP2C9 inhibitors could reduce the formation of E-3174, while P-glycoprotein inhibitors might alter losartan's distribution and elimination. Integrating such interactions into the model would allow for prediction of exposure changes and help guide dose adjustments in polypharmacy settings.

The simulation framework also highlights the impact of genetic variability on losartan pharmacokinetics and pharmacodynamics. While this thesis focused on CYP2C9 and ABCB1, future iterations could incorporate additional genes, like other genes that could influence the absorption, distribution, metabolism, and excretion of losartan such as UGT. This would enable a more comprehensive representation of interindividual variability and support pharmacogenetic-guided dosing strategies. However, the high within-genotype variability observed suggests that such models should be complemented by other clinical or demographic factors (e.g., age, comorbidities, polypharmacy).

Lastly, model accuracy could be improved through better data availability. In particular, high-resolution pharmacodynamic datasets, especially in impaired organ function or rare genotypes—would support stronger model validation. Additional clinical studies focusing on PD endpoints like renin, angiotensin II, and aldosterone in response to losartan would enhance calibration and increase translational relevance.

In conclusion, the current PBPK/PD model serves as a solid foundation for mechanistic simulations of losartan behavior. With continued refinement, it offers strong potential for use in personalized medicine, risk stratification, and the design of genotype- or disease-specific dosing strategies.

6 Supplements

Study simulations

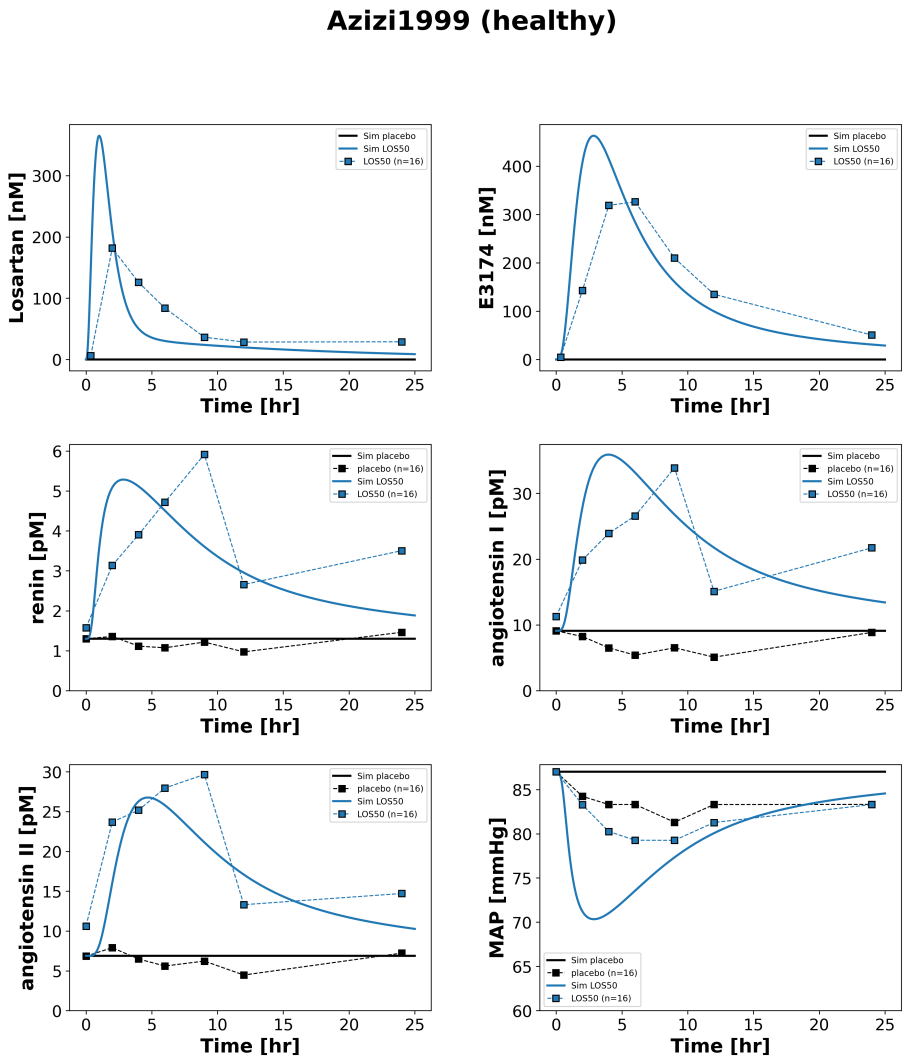

Figure 25: **Simulation Azizi1999** [4]. Simulated and observed plasma concentrations of losartan, E3174, renin, angiotensin I amd angiotensin II, as well as mean arterial blood pressure (MAP) after a single oral 50 mg dose in healthy volunteers (n=16).

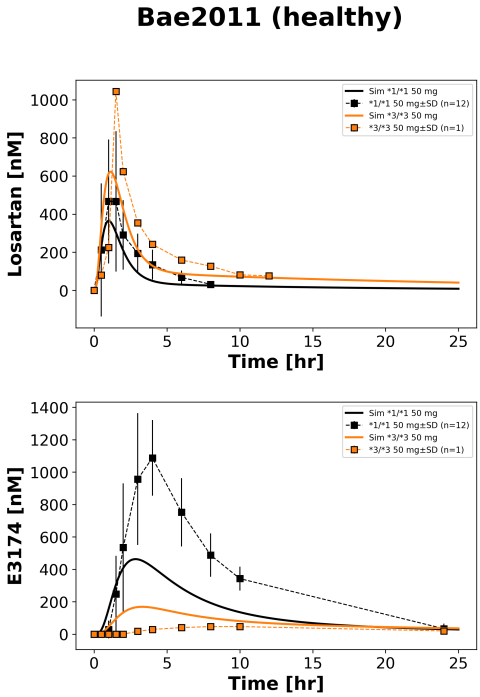

Figure 26: **Simulation Bae2011** [5]. Simulated and observed plasma concentrations of losartan and E3174 after a single 50 mg oral dose in healthy volunteers with CYP2C9 *1/*1 (n=12) or *3/*3 (n=1) genotype; mean ± SD displayed.

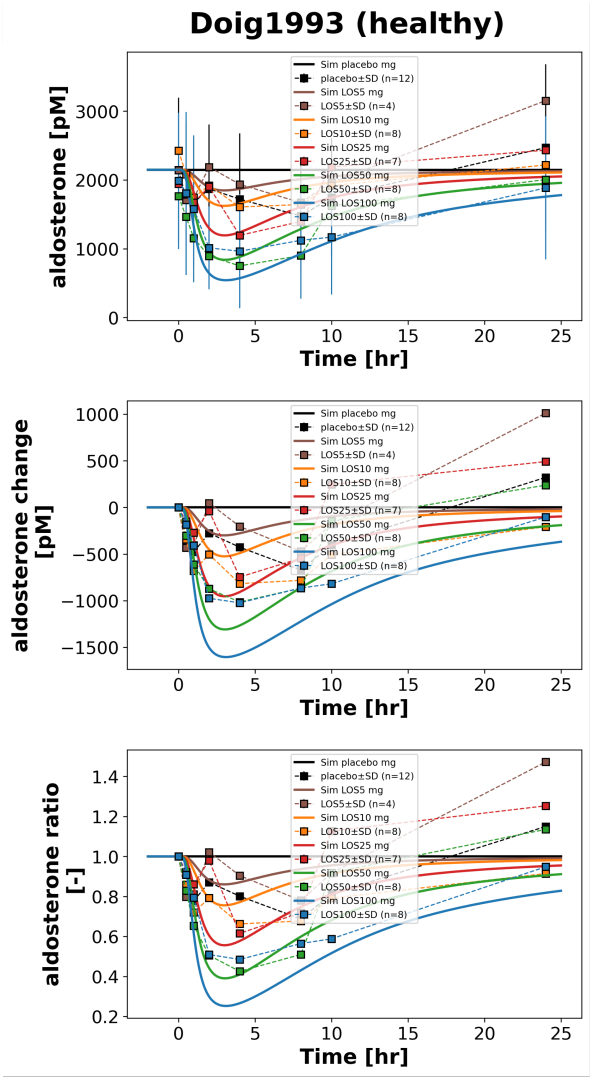

Figure 27: **Simulation Doig1993** [12]. Simulated and observed plasma concentrations, concentration change and ratio (post/pre dose) of aldosterone after oral administration of placebo (n=12), 5 (n=4), 10 (n=8), 25 (n=7), 50 (n=8)or 100 (n=8) mg losartan in healthy subjects; mean ± SD displayed.

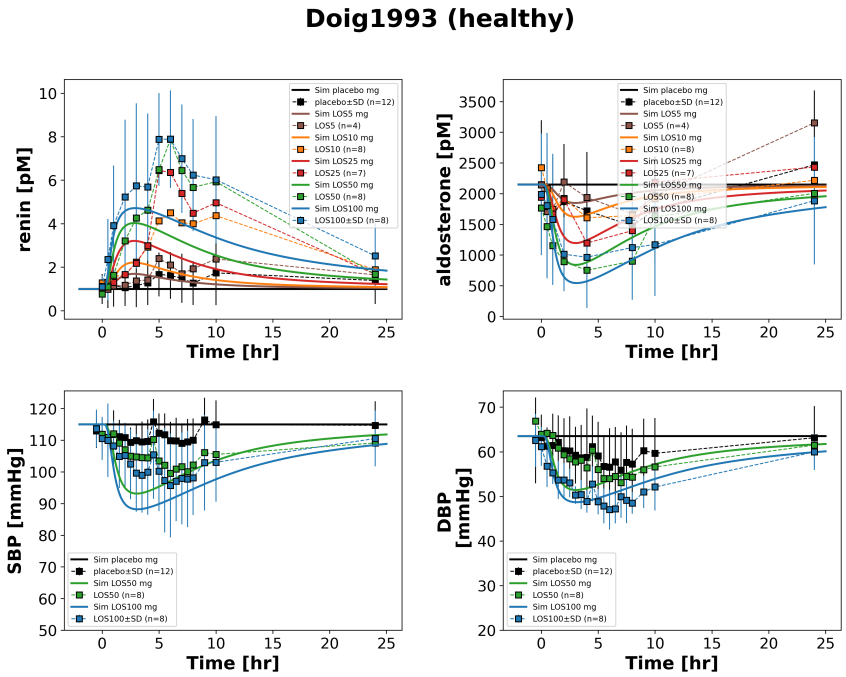

Figure 28: **Simulation Doig1993** [12]. Simulated and observed plasma concentrations of renin and aldosterone, as well as SBP and DBP after oral administration of placebo (n=12) or 5 (n=4), 10 (n=8), 25 (n=7), 50 (n=8)or 100 (n=8) mg losartan in healthy subjects; mean ± SD displayed.

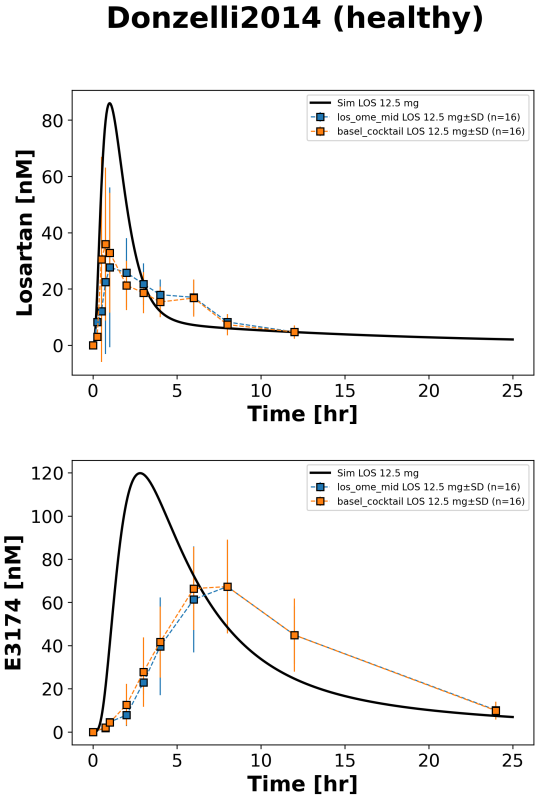

Figure 29: **Simulation Donzelli2014** [13]. Simulated and observed plasma concentrations of losartan and E3174 after single 12.5 mg losartan oral dose in healthy volunteers (n=16); combination with omeprazolam and midazolam (blue) or basel cocktail (orange); mean ± SD displayed.

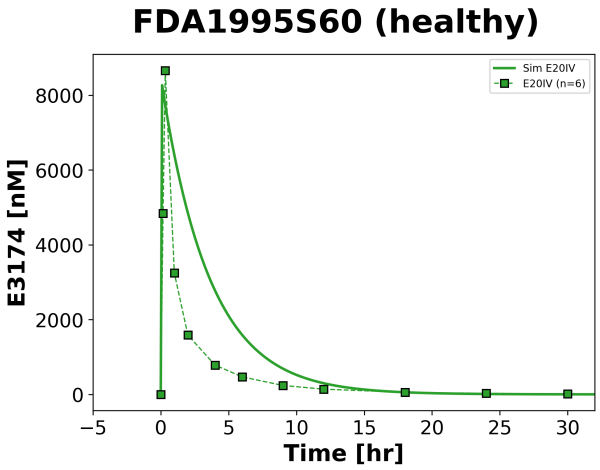

Figure 30: **Simulation FDA1995S60** [16]. Simulated and observed plasma concentration of E3174 after a 20 mg IV losartan dose in healthy volunteers (n=6).

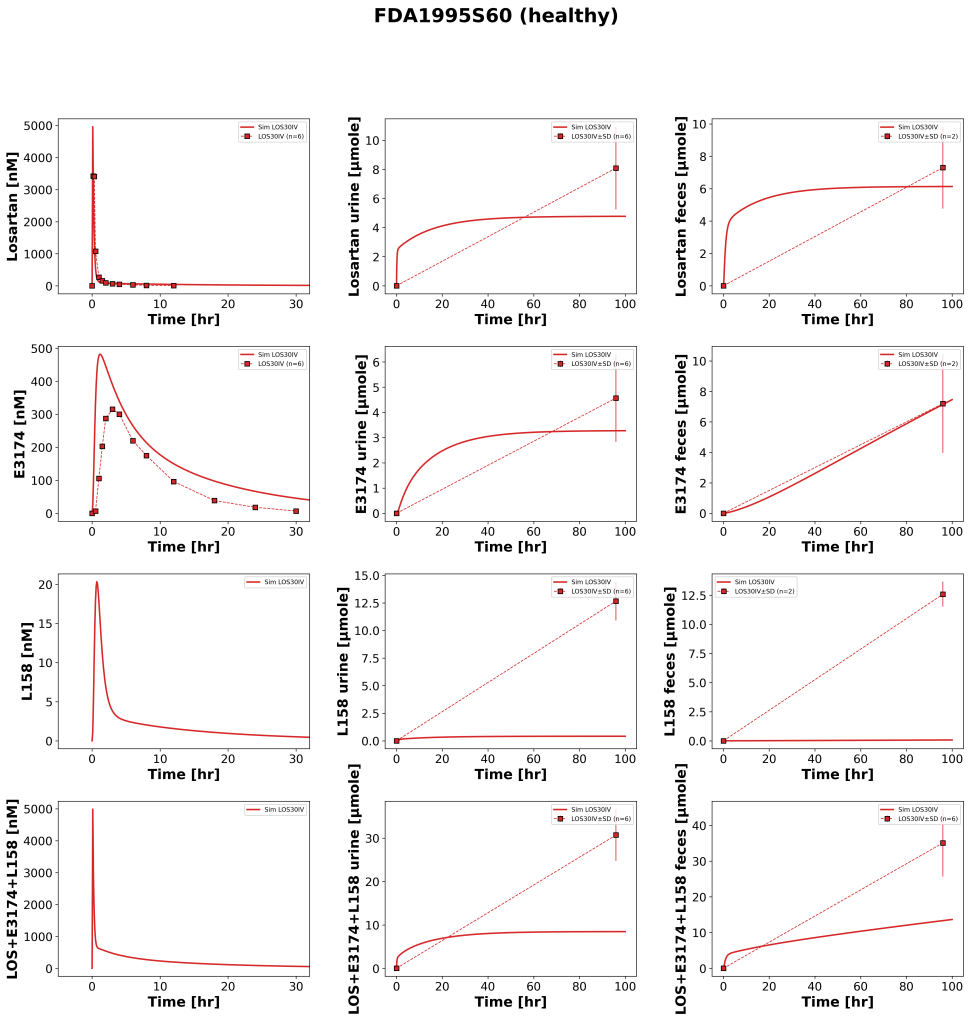

Figure 31: **Simulation FDA1995S60** [16]. Simulated and observed plasma, urine and feces concentrations of losartan, E3174, L158 (no plasma data) and cumulated compounds after a 30 mg IV losartan dose in healthy volunteers (n=6); mean ± SD displayed.

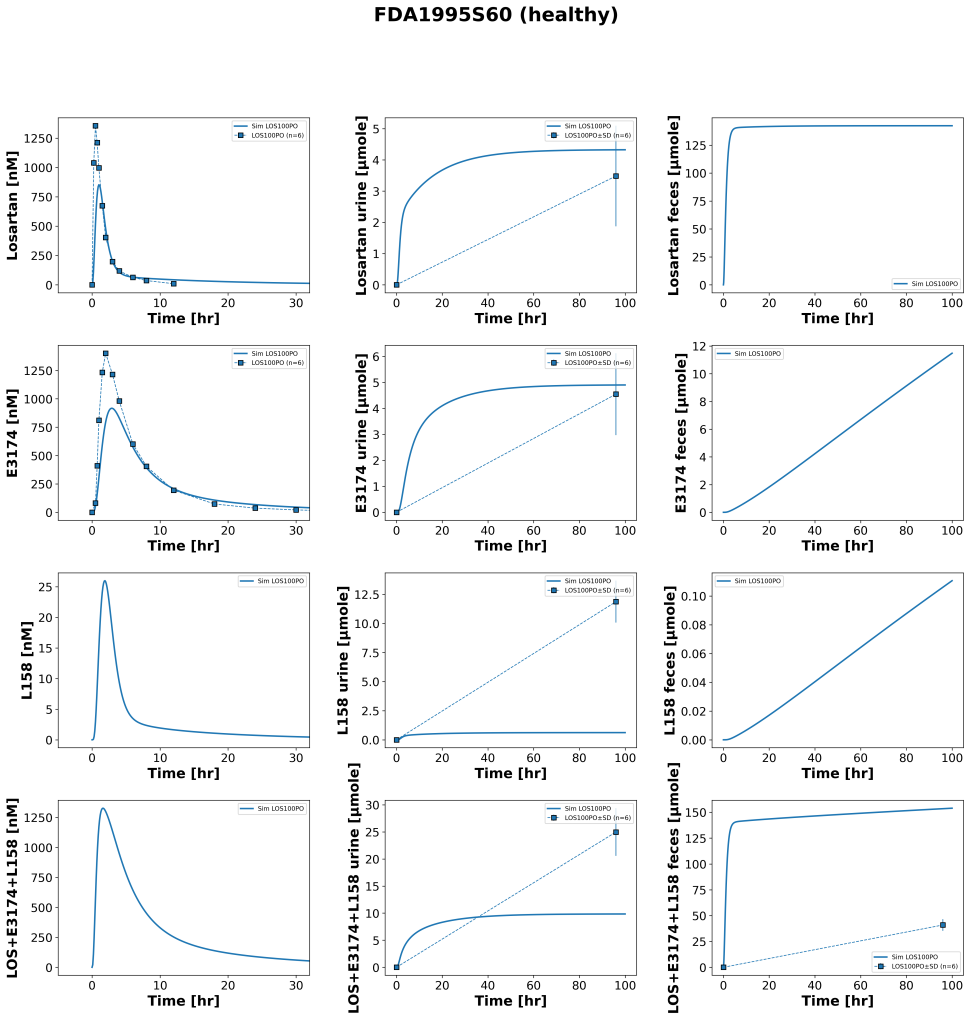

Figure 32: **Simulation FDA1995S60** [16]. Simulated and observed plasma, urine and feces concentrations of losartan (no feces data), E3174 (no feces data), L158 (no plasma or feces data) and cumulated compounds after a 100 mg oral losartan dose in healthy volunteers (n=6); mean ± SD displayed.

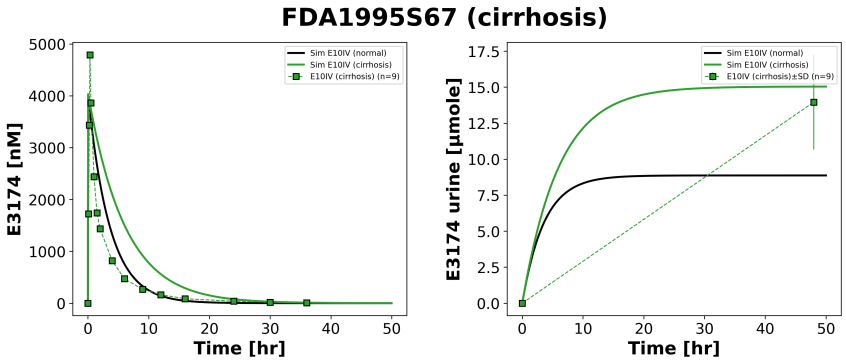

Figure 33: **Simulation FDA1995S67** [17]. Simulated and observed plasma and urine concentration of E3174 after a 10 mg IV E3174 dose in volunteers (n=9) with mild to moderate stage cirrhosis (CTP=5-9); mean ± SD displayed.

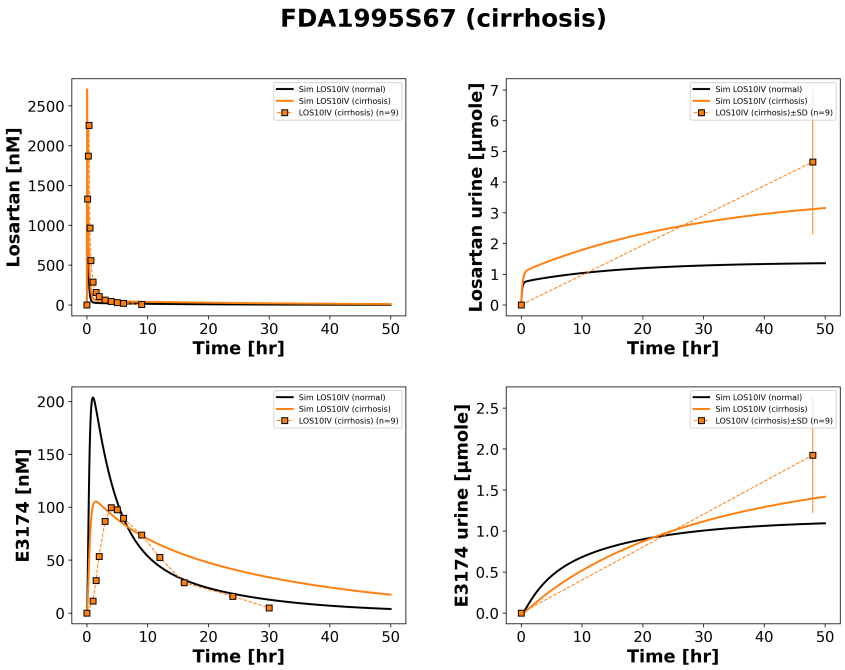

Figure 34: **Simulation FDA1995S67** [17]. Simulated and observed plasma and urine concentrations of losratan and E3174 after a 10 mg IV losartan dose in volunteers (n=9) with mild to moderate stage cirrhosis (CTP=5-9); mean ± SD displayed.

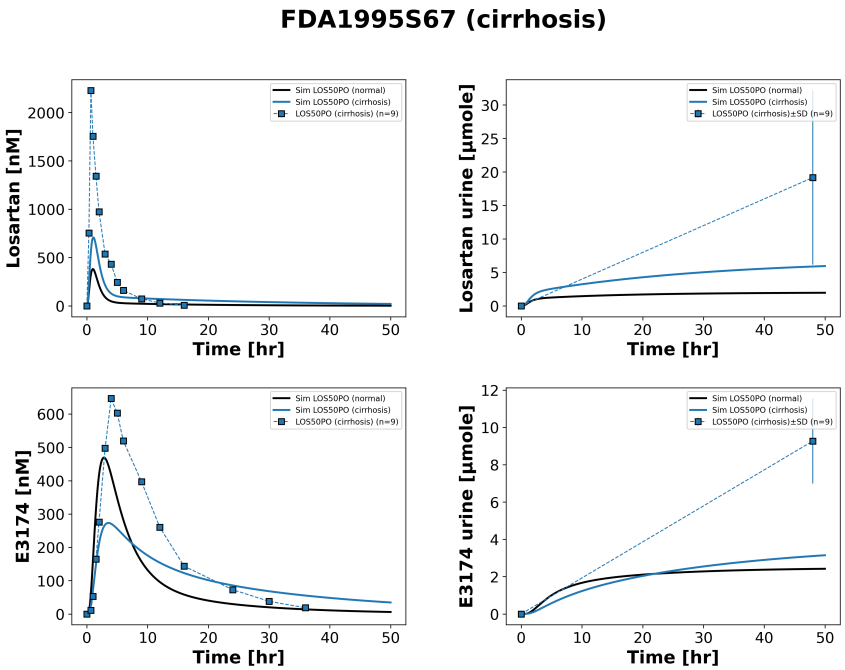

Figure 35: **Simulation FDA1995S67** [17]. Simulated and observed plasma and urine concentrations of losratan and E3174 after a 50 mg oral losartan dose in volunteers (n=9) with mild to moderate stage cirrhosis (CTP=5-9); mean ± SD displayed.

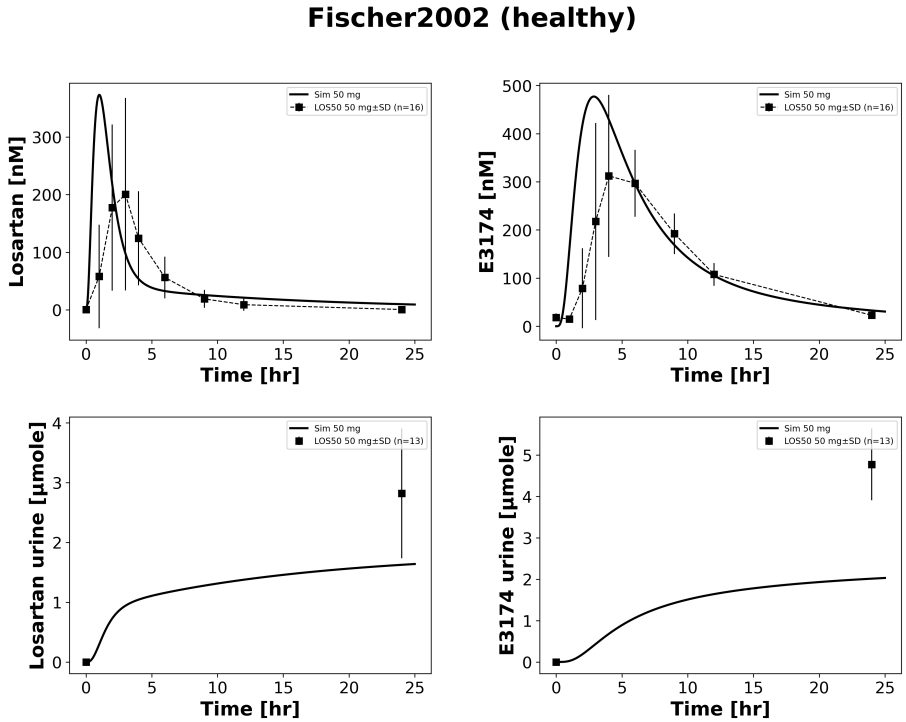

Figure 36: **Simulation Fischer2002** [19]. Simulated and observed plasma and urine concentrations of losartan and E3174 after a 50 mg losartan oral dose in healthy volunteers (n=16); mean ± SD displayed.

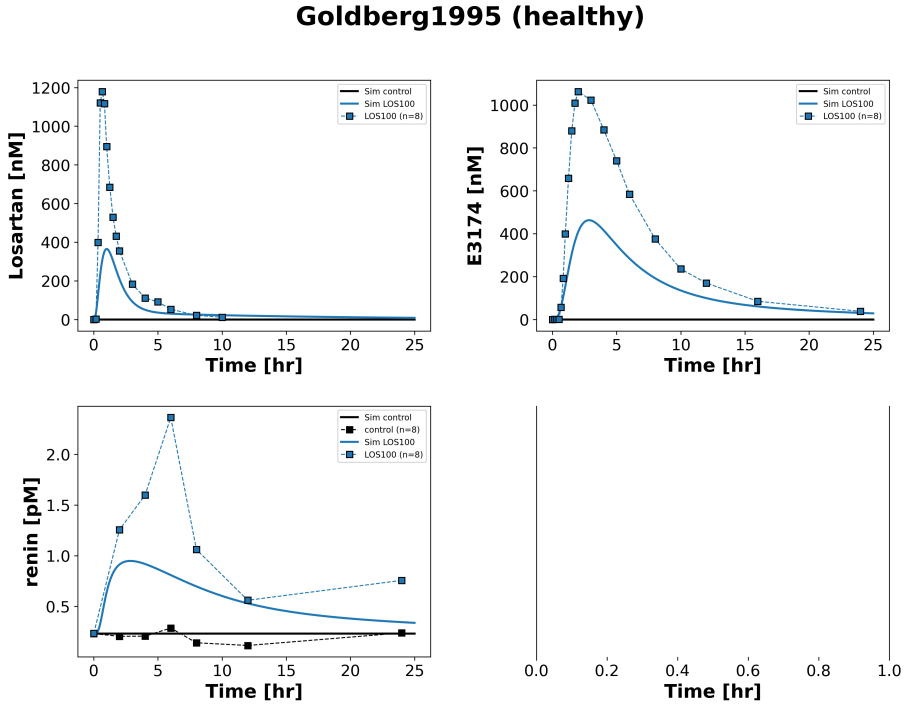

Figure 37: **Simulation Goldberg1995** [27]. Simulated and observed plasma concentrations of losartan, E3174 and renin after a 100 mg oral losartan dose in healthy volunteers (n=8).

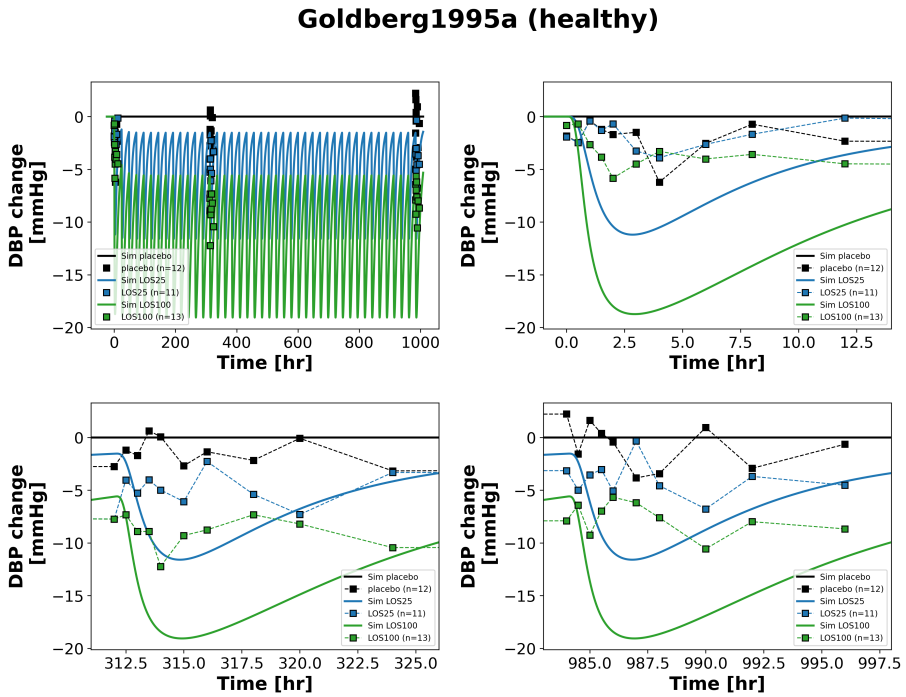

Figure 38: **Simulation Goldberg1995a** [26]. Simulated and observed changes in DBP after multiple placebo (n=12), 25 (n=11) or 100 (n=13) mg losartan oral dose in healthy volunteers.

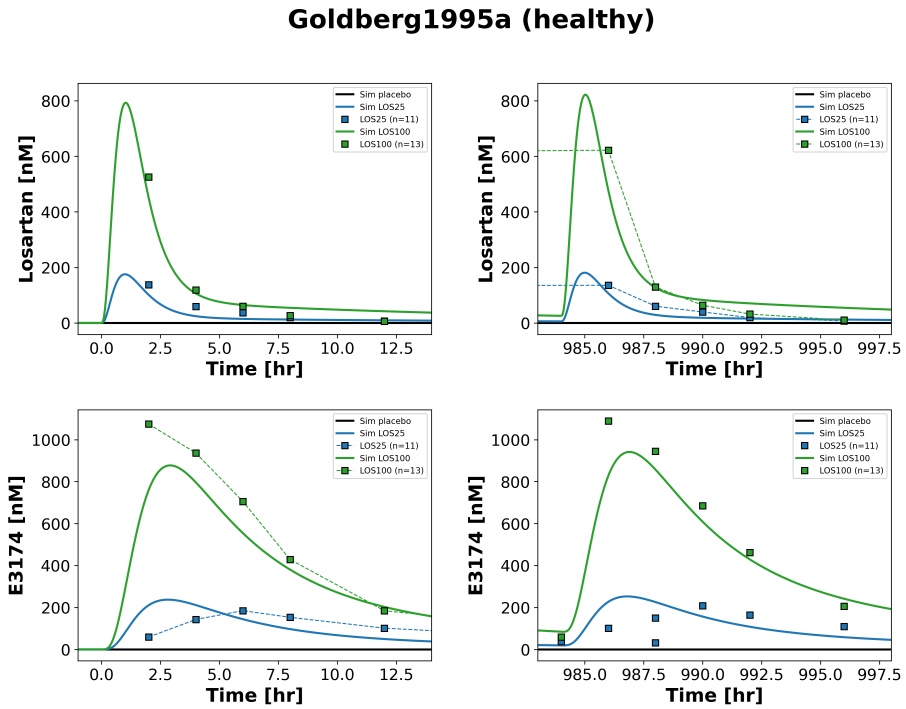

Figure 39: **Simulation Goldberg1995a** [26]. Simulated and observed plasma concentrations of losartan and E3174 after multiple placebo (n=12), 25 (n=11) or 100 (n=13) mg losartan oral dose in healthy volunteers.

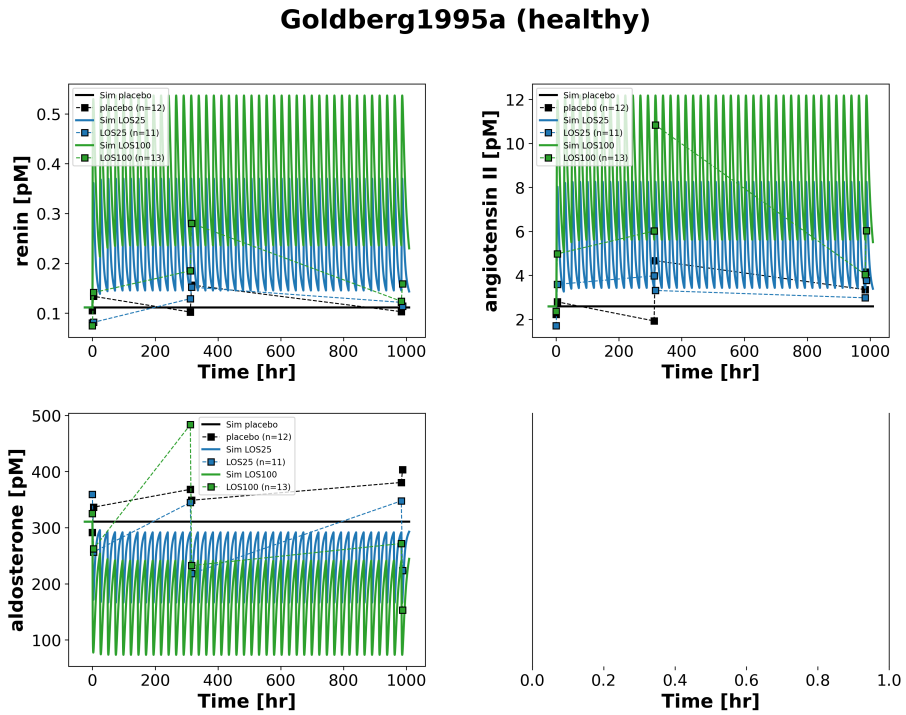

Figure 40: **Simulation Goldberg1995a** [26]. Simulated and observed plasma concentrations of renin, angiotensin II and aldosterone after multiple placebo (n=12), 25 (n=11) or 100 (n=13) mg losartan oral dose in healthy volunteers.

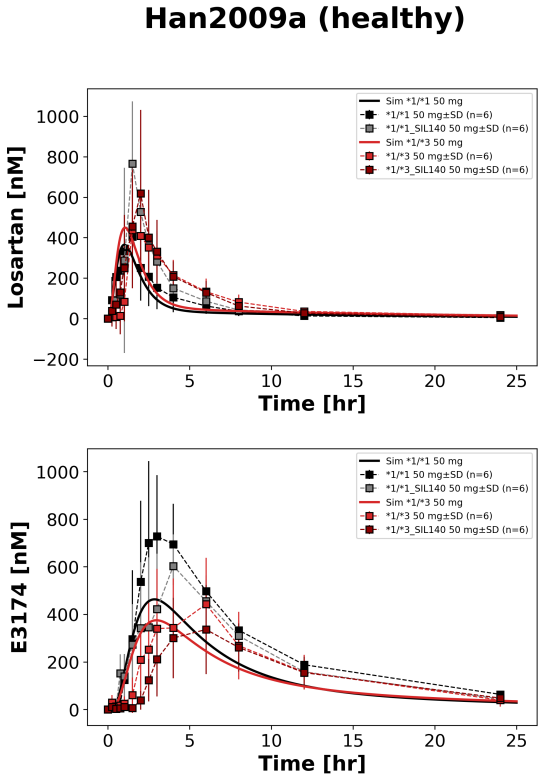

Figure 41: **Simulation Han2009a** [30]. Simulated and observed plasma concentrations of losartan and E3174 after 50 mg losartan oral dose (with and without silymarin) in healthy volunteers with CYP2C9 *1/*1 (n=6) or *1/*3 (n=6) genotype; mean ±SD displayed.

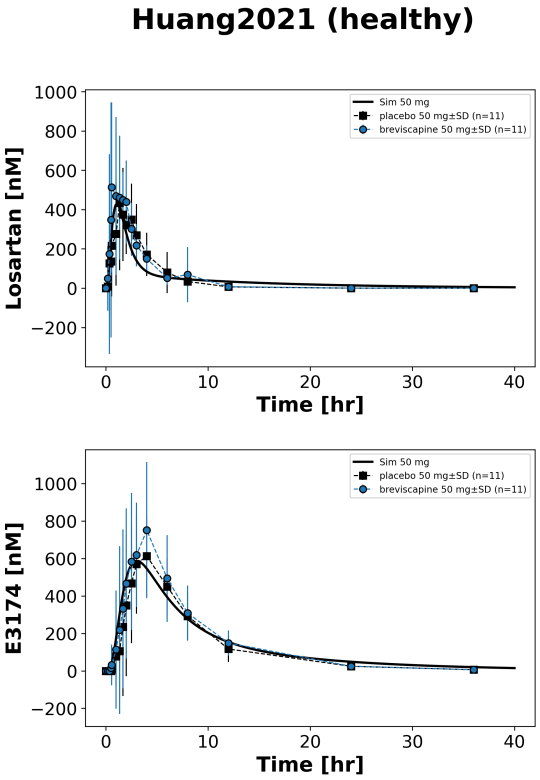

Figure 42: **Simulation Huang2021** [35]. Simulated and observed plasma concentrations of losartan and E3174 after 50 mg losartan oral dose without (black) or with breviscapine (blue) in healthy volunteers (n=11); mean ±SD displayed.

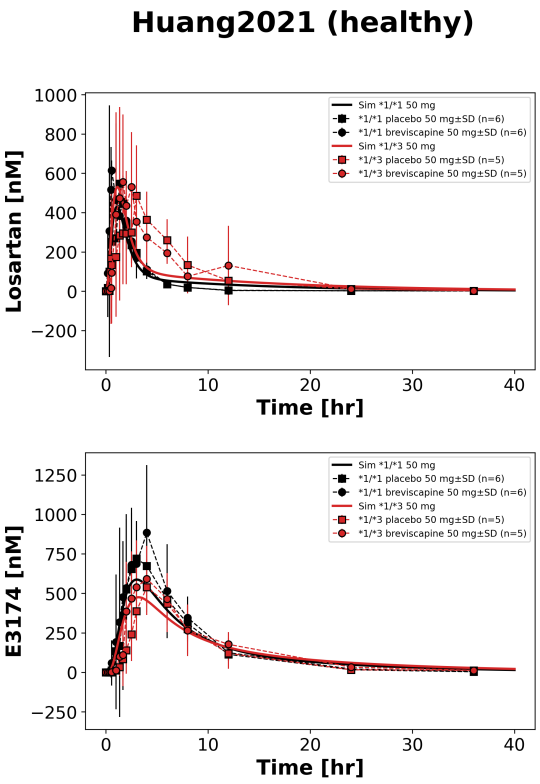

Figure 43: **Simulation Huang2021** [35]. Simulated and observed plasma concentrations of losartan and E3174 after 50 mg losartan oral dose without (black) or with breviscapine (blue) in healthy volunteers with CYP2C9 *1/*1 (n=6) or *1/*3 (n=5) genotype; mean ±SD displayed.

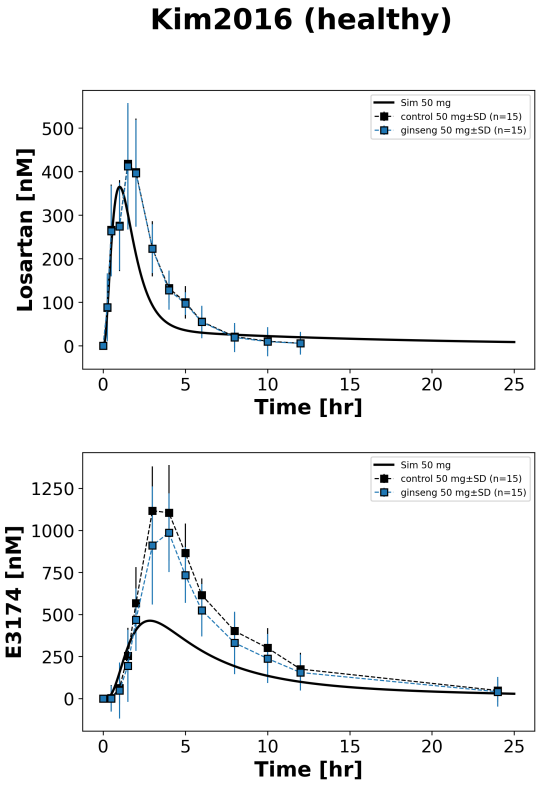

Figure 44: **Simulation Kim2016** [41]. Simulated and observed plasma concentrations of losartan and E3174 after 50 mg losartan oral dose without (black) or with ginseng (blue) in healthy volunteers (n=15); mean ±SD displayed.

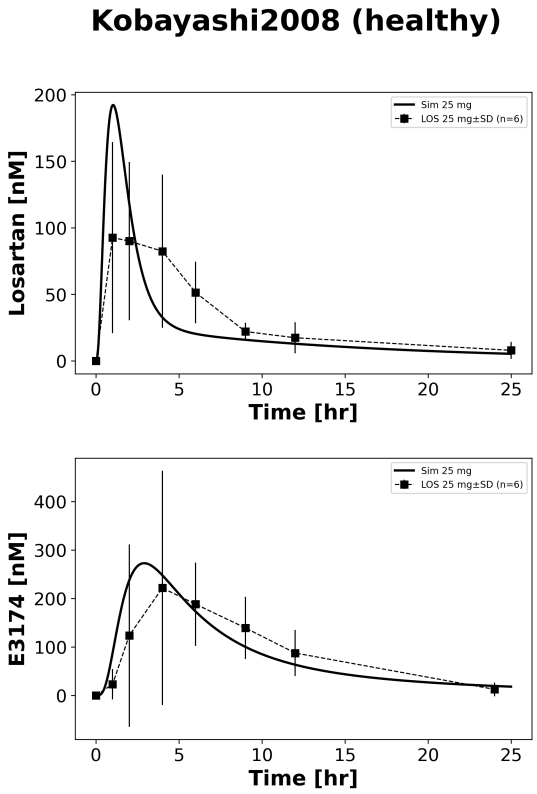

Figure 45: **Simulation Kobayashi2008** [42]. Simulated and observed plasma concentrations of losartan and E3174 after 25 mg losartan oral dose in healthy volunteers (n=6); mean ±SD displayed.

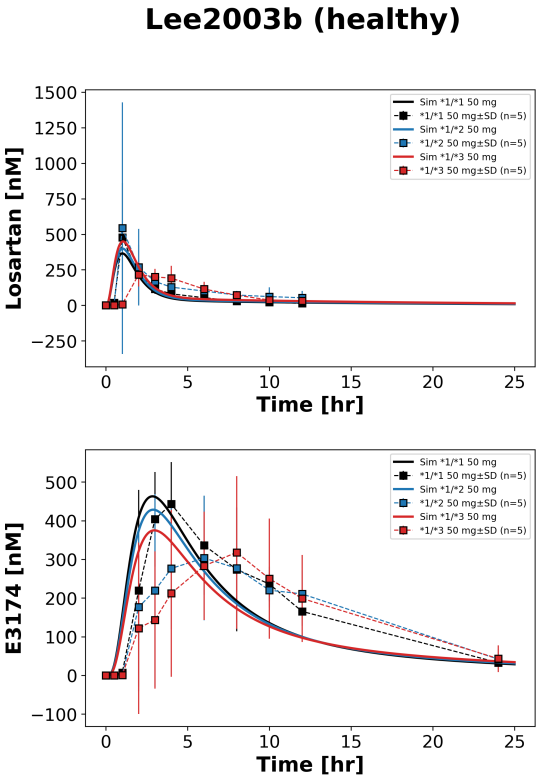

Figure 46: **Simulation Lee2003b** [50]. Simulated and observed plasma concentrations of losartan and E3174 after 50 mg losartan oral dose in healthy volunteers with CYP2C9 *1/*1 (n=5), *1/*2 (n=5) or *1/*3 (n=5) genotype; mean ±SD displayed.

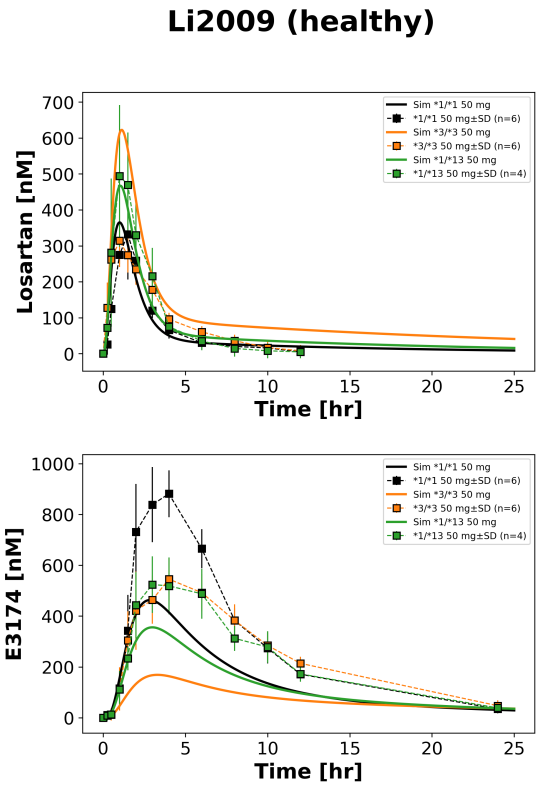

Figure 47: **Simulation Li2009** [51]. Simulated and observed plasma concentrations of losartan and E3174 after 50 mg losartan oral dose in healthy volunteers with CYP2C9 *1/*1 (n=6), *3/*3 (n=6) or *1/*13 (n=4) genotype; mean ±SD displayed.

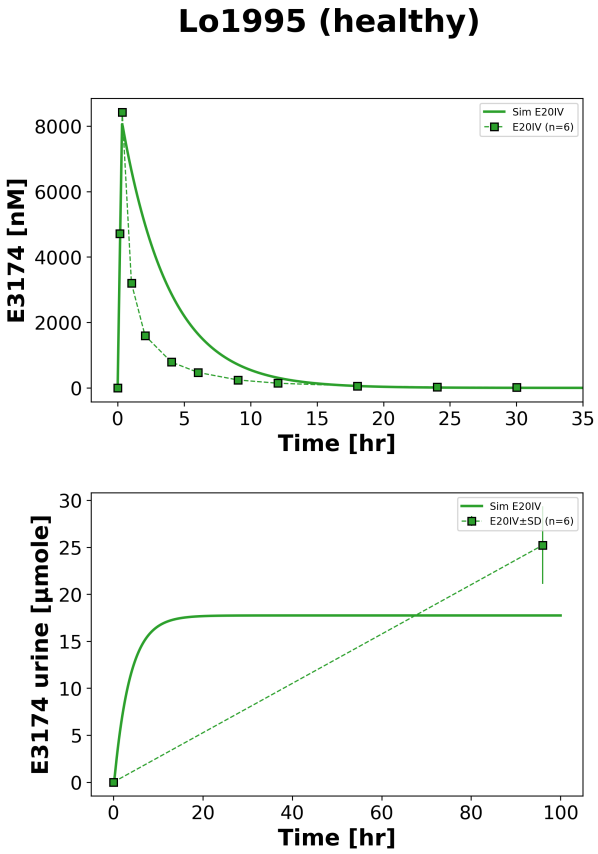

Figure 48: **Simulation Lo1995** [52]. Simulated and observed plasma and urine concentration of E3174 after 20 mg E3174 IV dose in healthy volunteers (n=6); mean ±SD displayed.

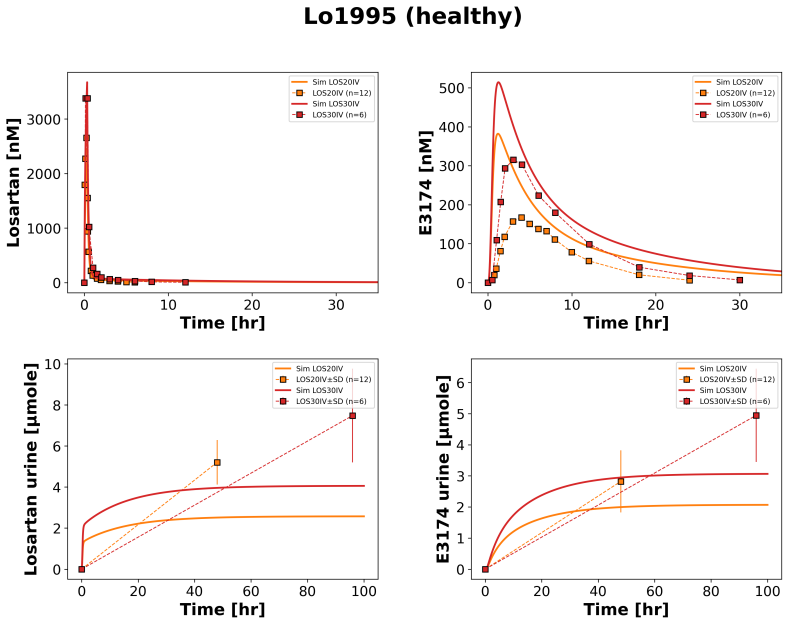

Figure 49: **Simulation Lo1995** [52]. Simulated and observed plasma and urine concentrations of losartan and E3174 after 20 (n=12) or 30 (n=6) mg losartan IV dose in healthy volunteers; mean ±SD displayed.

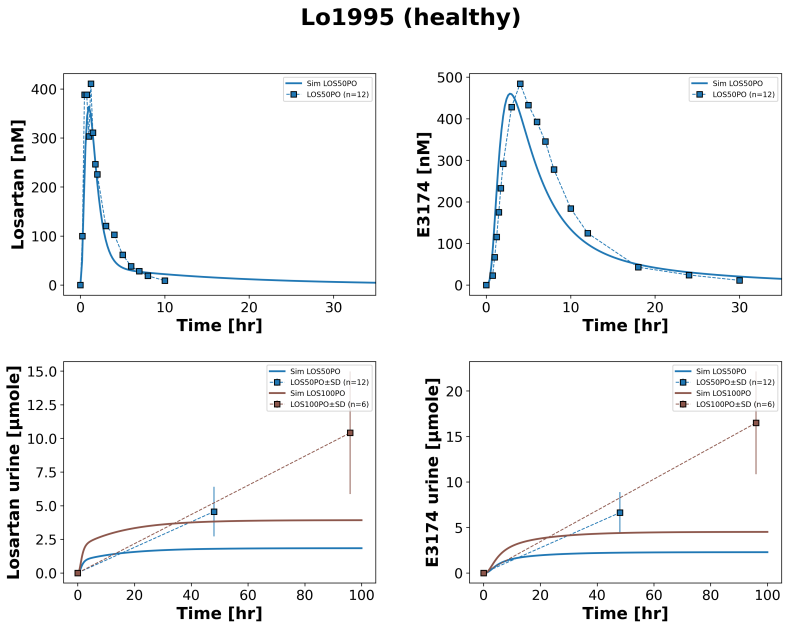

Figure 50: **Simulation Lo1995** [52]. Simulated and observed plasma and urine concentrations of losartan and E3174 after 50 (n=12) or 100 (n=6) mg losartan oral dose in healthy volunteers; mean ±SD displayed.

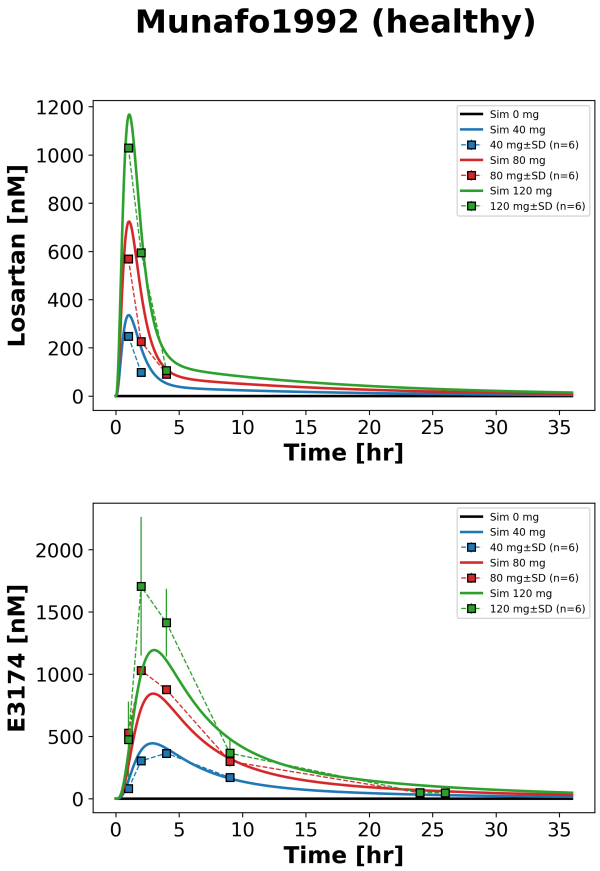

Figure 51: **Simulation Munafo1992** [57]. Simulated and observed plasma concentrations of losartan and E3174 after 40 (n=6), 80 (n=6) or 120 (n=6) mg losartan oral dose in healthy volunteers; mean ±SD displayed.

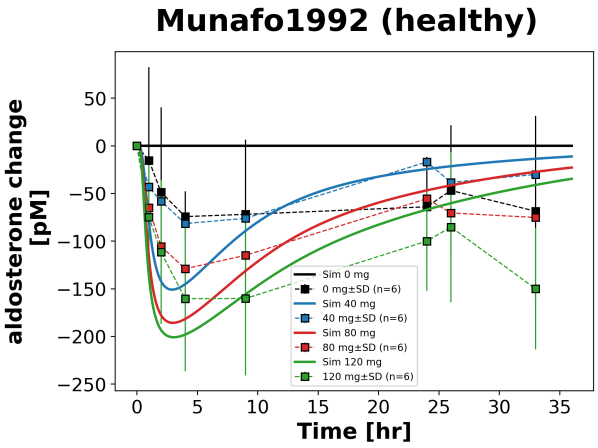

Figure 52: **Simulation Munafo1992** [57]. Simulated and observed aldosterone change after 0 (n=6), 40 (n=6), 80 (n=6) or 120 (n=6) mg losartan oral dose in healthy volunteers; mean ±SD displayed.

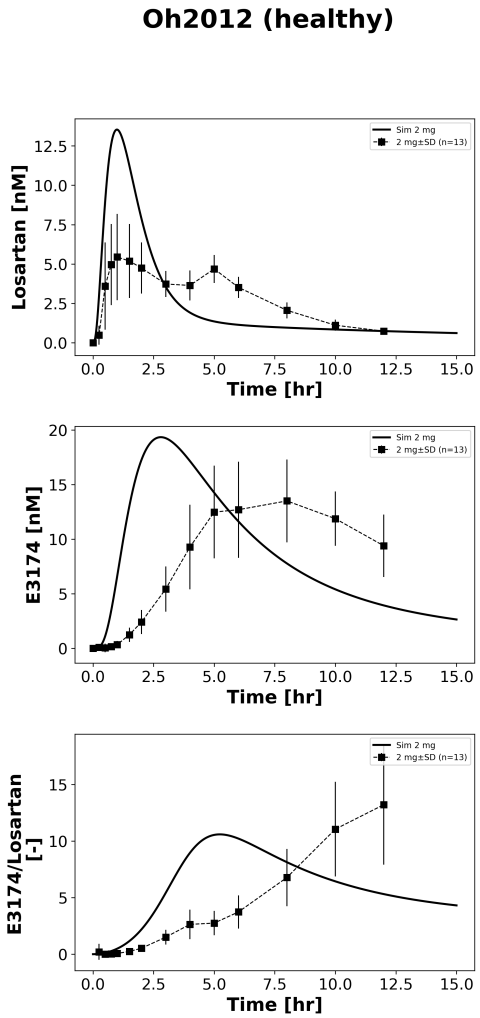

Figure 53: **Simulation Oh2012** [61]. Simulated and observed plasma concentrations of losartan and E3174, as well as E3174/losartan ratio after 2 mg losartan oral dose in healthy volunteers (n=13); mean ±SD displayed.

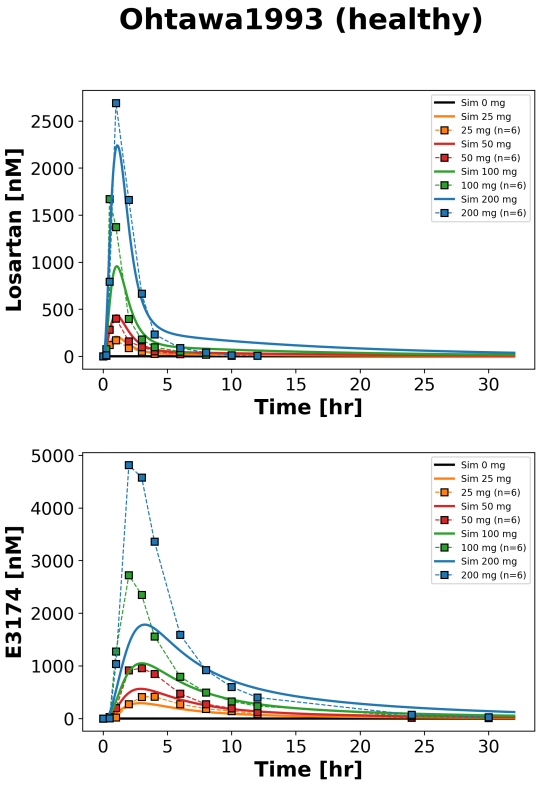

Figure 54: **Simulation Ohtawa1993** [62]. Simulated and observed plasma concentrations of losartan and E3174 after 25, 50, 100 or 200 mg losartan oral dose in healthy volunteers (each n=6).

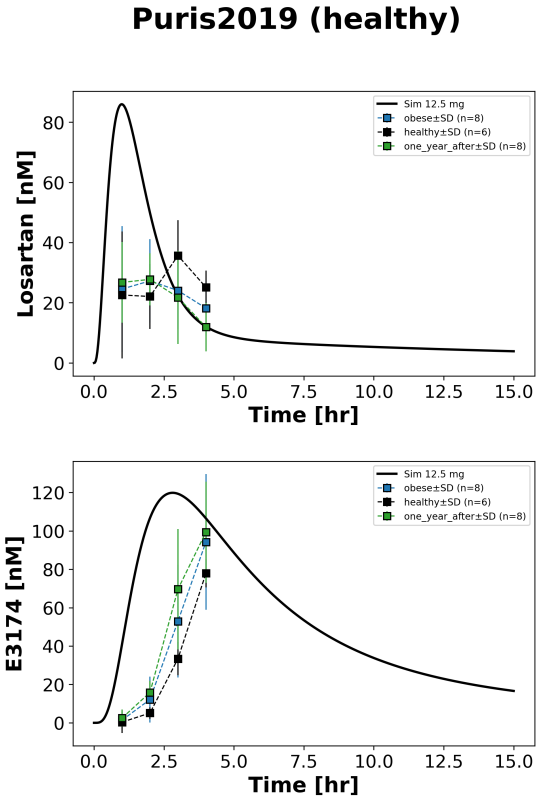

Figure 55: **Simulation Puris2019** [65]. Simulated and observed plasma concentrations of losartan and E3174 after 12.5 mg losartan oral dose in healthy (n=6), obese (n=8) or 1 year post operation (n=8) volunteers; mean ± SD displayed.

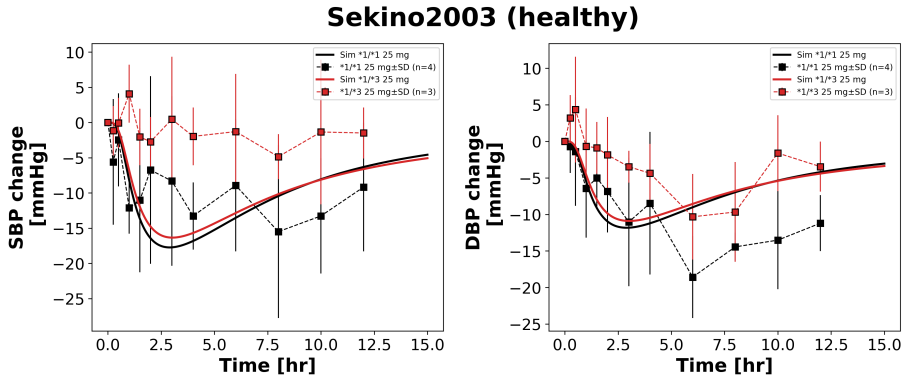

Figure 56: **Simulation Sekino2003 [71]**. Simulated and observed changes in SBP and DBP after 25 mg losartan oral dose in healthy volunteers with CYP2C9 *1/*1 (n=4) or *1/*3 (n=3) genotype; mean ± SD displayed.

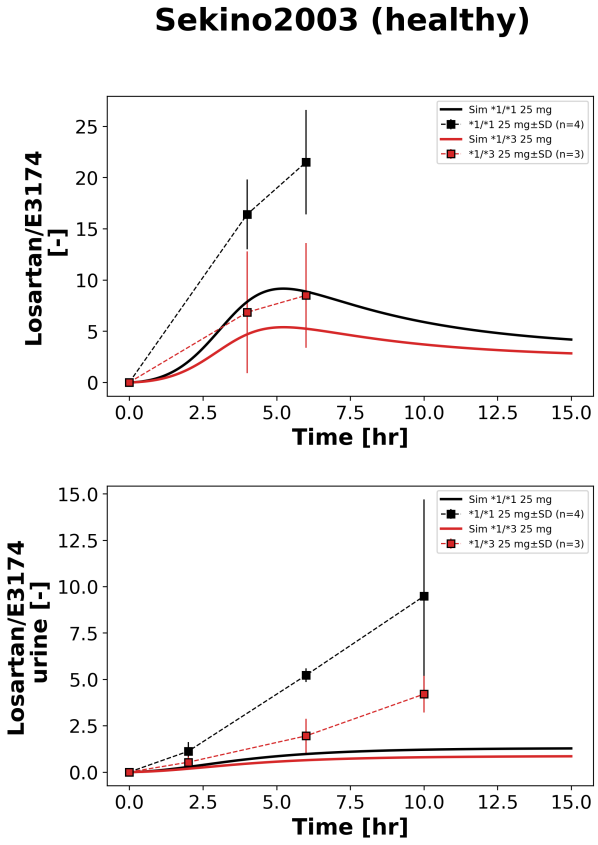

Figure 57: **Simulation Sekino2003 [71]**. Simulated and observed plasma and urine losartan/E3174 ratio after 25 mg losartan oral dose in healthy volunteers with CYP2C9 *1/*1 (n=4) or *1/*3 (n=3) genotype; mean ± SD displayed.

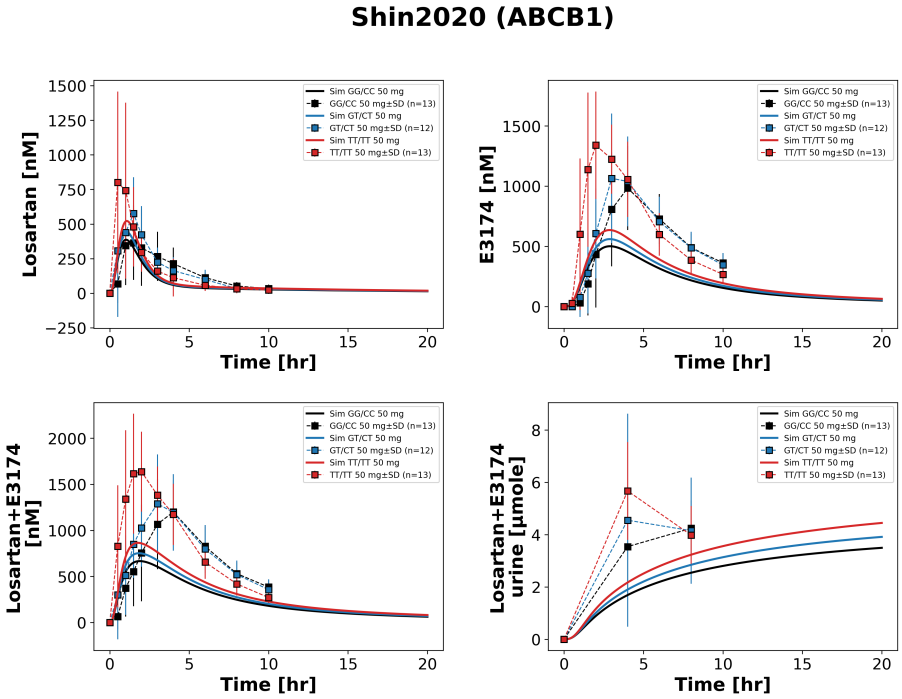

Figure 58: **Simulation Shin2020** [72]. Simulated and observed plasma concentrations of losartan, E3174 and losartanE3174, as well as losartanE3174 in urine after 50 mg losartan oral dose in healthy volunteers with ABCB1 GG/CC (n=13), GT/CT (n=12) or TT/TT (n=13) genotype; mean ± SD displayed.

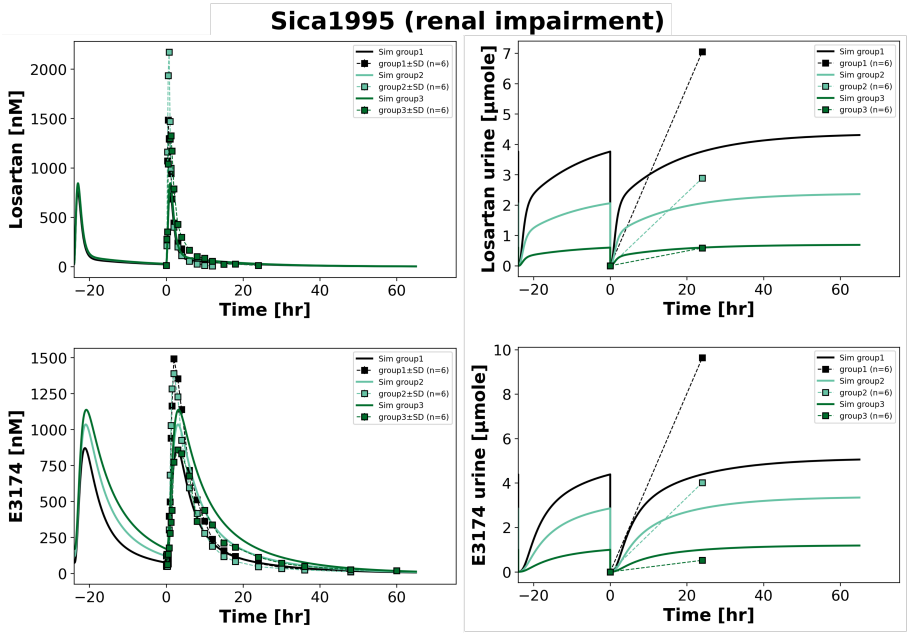

Figure 59: **Simulation Sica1995** [74]. Simulated and observed plasma and urine concentrations of losartan and E3174 after 50 mg losartan oral dose in volunteers with no (1), mild (2) or severe (3) renal impairment (each n=6).

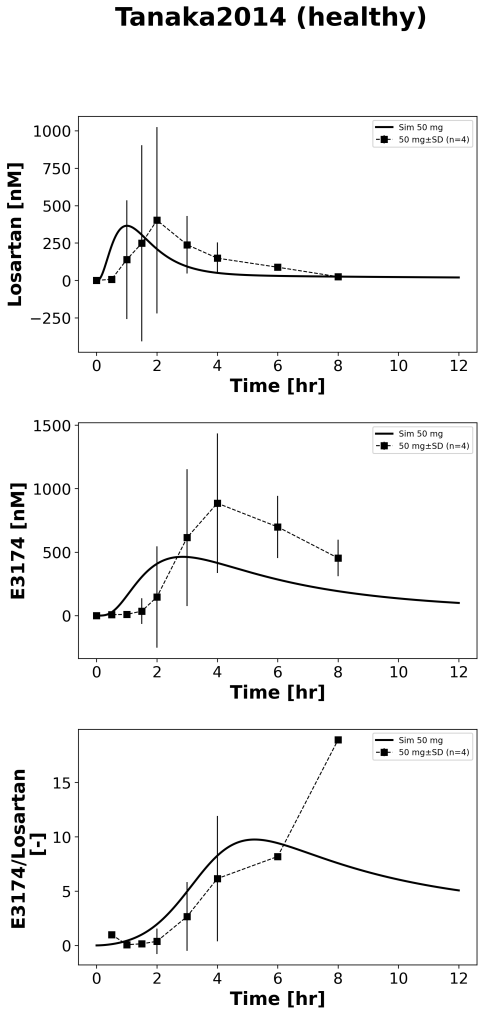

Figure 60: Simulation (Tanaka2014) [82]. Simulated and observed plasma concentration of E3174 and E3174/losartan ratio after 50 mg losartan oral dose in healthy volunteers (n=4); mean ± SD displayed.

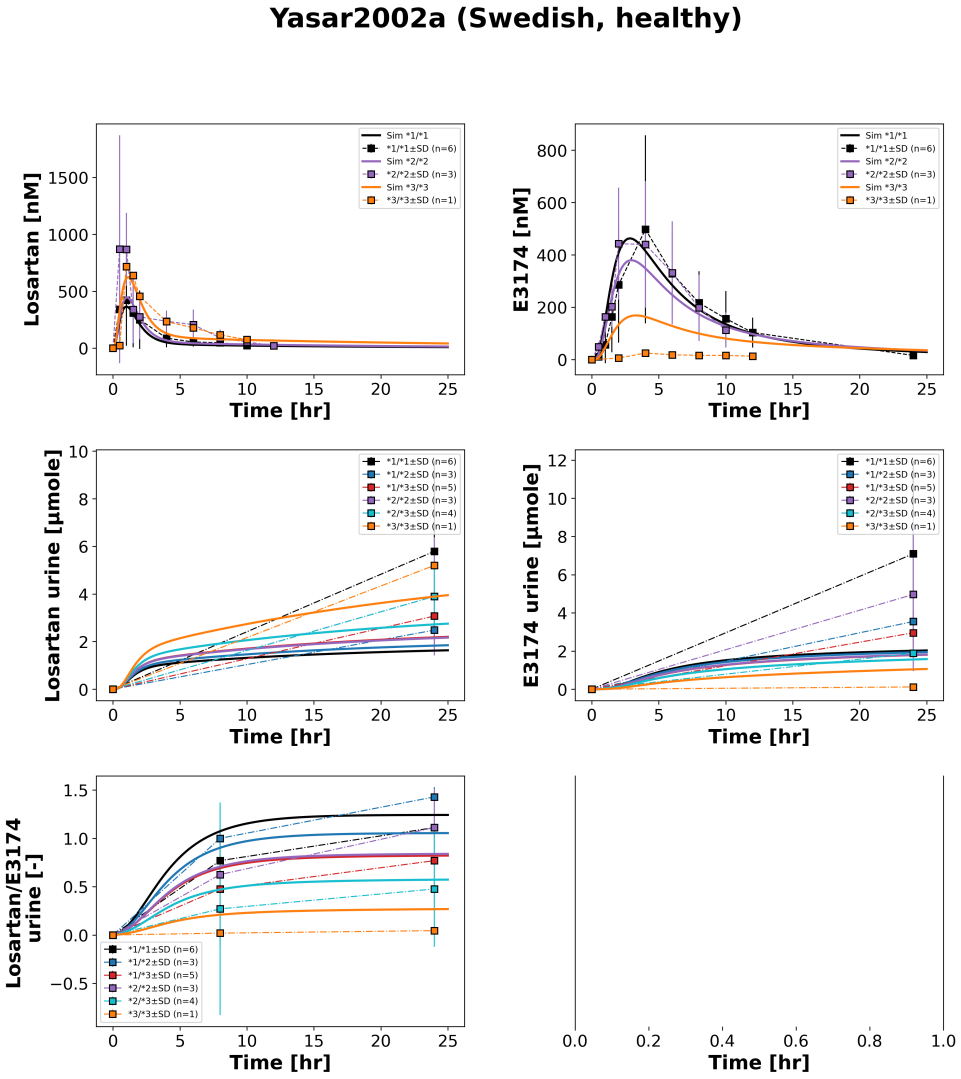

Figure 61: **Simulation Yasar2002a [92]**. Simulated and observed plasma and urine concentrations of losartan and E3174, as well as losartan/E3174 ratio in urine after 50 mg losartan oral dose in healthy volunteers with CYP2C9 *1/*1 (n=6), *1/*2 (n=3), *1/*3 (n=5), *2/*2 (n=3), *2/*3 (n=4) or *3/*3 (n=1) genotype; mean ± SD displayed.

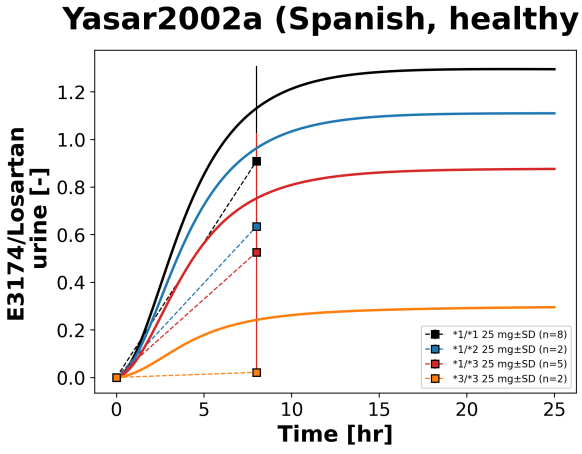

Figure 62: **Simulation Yasar2002a [92]**. Simulated and observed urine E3174/losartan ratio after 25 mg losartan oral dose in healthy volunteers with CYP2C9 *1/*1 (n=8), *1/*2 (n=2), *1/*3 (n=5) or *3/*3 (n=2) genotype; mean ± SD displayed.

Model simulations

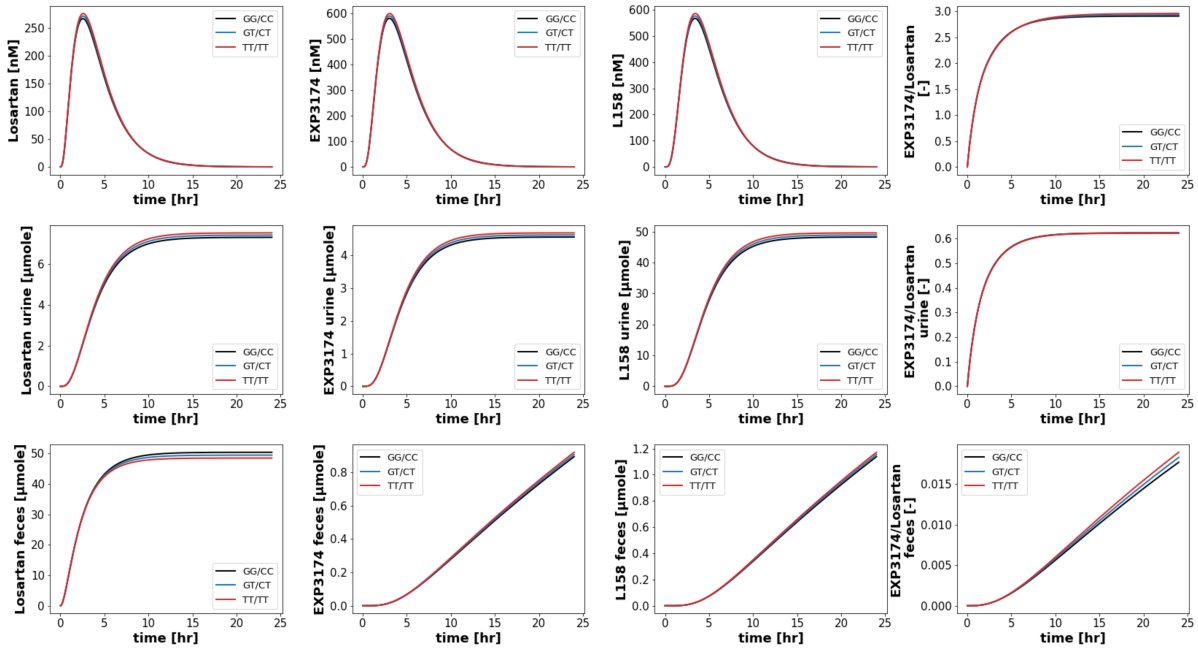

Figure 63: **ABCB1 genotype-specific simulations for losartan pharmacokinetics.** Simulated losartan, E3174 and L158 concentrations as well the E3174/losartan ratio in plasma, urine and feces for the diplotypes GG/CC (wild type), GT/CT and TT/TT.

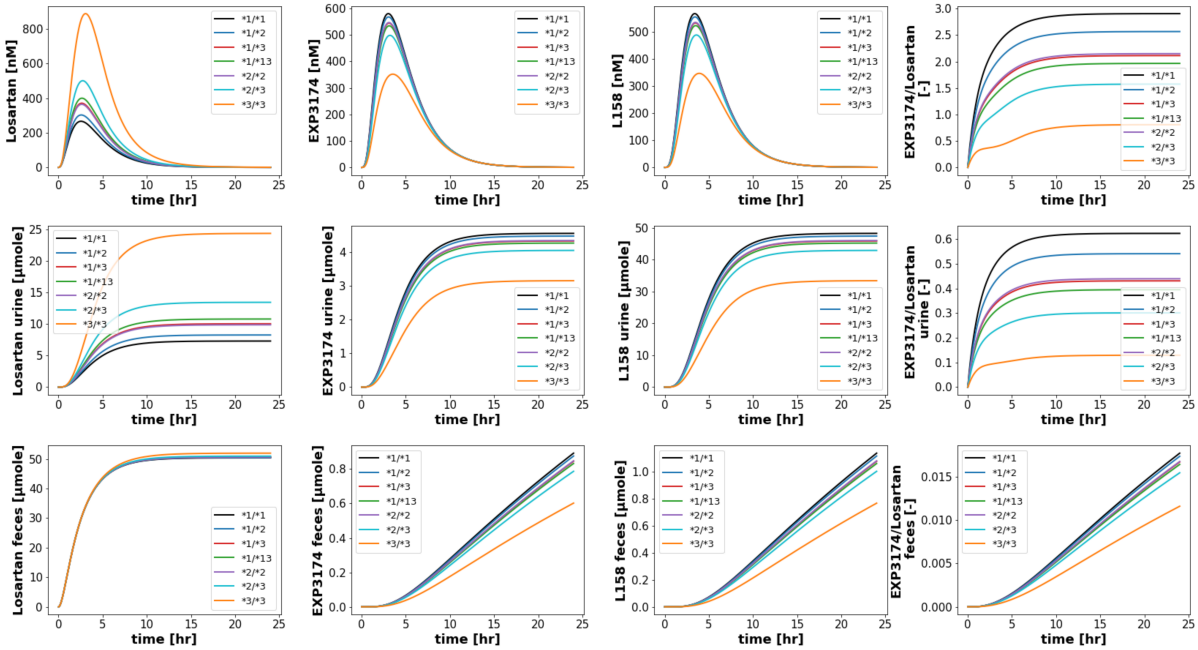

Figure 64: **CYP2C9 genotype-specific simulations for losartan pharmacokinetics.** Simulated losartan, E3174 and L158 concentrations as well the E3174/losartan ratio in plasma, urine and feces for the genotypes *1/*1 (wild type), *1/*2, *1/*3, *1/*13, *2/*2, *2/*3 and *3/*3.

References

[1] World Health Organisation (WHO). *Hypertension*. URL: https://www.who.int/news-room/fact-sheets/detail/hypertension (visited on 01/23/2025).

[2] Anna Alonen, Moshe Finel, and Risto Kostiainen. "The Human UDP-glucuronosyltransferase UGT1A3 Is Highly Selective towards N2 in the Tetrazole Ring of Losartan, Candesartan, and Zolarsartan." In: *Biochemical pharmacology* 76.6 (Sept. 15, 2008), pp. 763–772. DOI: 10.1016/j.bcp.2008.07.006. PMID: 18674515.

[3] Steven A. Atlas. "The Renin-Angiotensin Aldosterone System: Pathophysiological Role and Pharmacologic Inhibition". In: *Journal of Managed Care Pharmacy* 13 (8 Supp B Oct. 2007), pp. 9–20. DOI: 10.18553/jmcp.2007.13.s8-b.9. URL: https://www.jmcp.org/doi/10.18553/jmcp.2007.13.s8-b.9 (visited on 03/04/2025).

[4] M. Azizi, G. Chatellier, T. T. Guyene, and J. Ménard. "Pharmacokinetic-Pharmacodynamic Interactions of Candesartan Cilexetil and Losartan." In: *Journal of hypertension* 17.4 (Apr. 1999), pp. 561–568. DOI: 10.1097/00004872-199917040-00015. PMID: 10404959.

[5] Jung-woo Bae, Chang-ik Choi, Mi-jeong Kim, Da-hee Oh, Seul-ki Keum, Jung-in Park, Bo-hye Kim, Hye-kyoung Bang, Sung-gon Oh, Byung-sung Kang, Hyun-joo Park, Hae-deun Kim, Ji-hey Ha, Hee-jung Shin, Young-hoon Kim, Han-sung Na, Myeon-woo Chung, Choon-gon Jang, and Seok-yong Lee. "Frequency of CYP2C9 Alleles in Koreans and Their Effects on Losartan Pharmacokinetics." In: *Acta pharmacologica Sinica* 32.10 (Oct. 2011), pp. 1303–1308. DOI: 10.1038/aps.2011.100. PMID: 21841812.

[6] R. Bell and R. Mandalia. "Diuretics and the Kidney". In: *BJA education* 22.6 (June 2022), pp. 216–223. DOI: 10.1016/j.bjae.2022.02.003. PMID: 35614905.

[7] U. Brinkmann and M. Eichelbaum. "Polymorphisms in the ABC Drug Transporter Gene MDR1". In: *The Pharmacogenomics Journal* 1.1 (2001), pp. 59–64. DOI: 10.1038/sj.tpj.6500001. PMID: 11913728.

[8] Michel Burnier and Grégoire Wuerzner. "Pharmacokinetic Evaluation of Losartan." In: *Expert opinion on drug metabolism & toxicology* 7.5 (May 2011), pp. 643–649. DOI: 10.1517/17425255.2011.570333. PMID: 21417956.

[9] C. G. Child and J. G. Turcotte. "Surgery and Portal Hypertension". In: *Major Problems in Clinical Surgery* 1 (1964), pp. 1–85. PMID: 4950264.

[10] Balram Chowbay, Shufeng Zhou, and Edmund J. D. Lee. "An Interethnic Comparison of Polymorphisms of the Genes Encoding Drug-Metabolizing Enzymes and Drug Transporters: Experience in Singapore". In: *Drug Metabolism Reviews* 37.2 (2005), pp. 327–378. DOI: 10.1081/dmr-28805. PMID: 15931768.

[11] D. D. Christ. "Human Plasma Protein Binding of the Angiotensin II Receptor Antagonist Losartan Potassium (DuP 753/MK 954) and Its Pharmacologically Active Metabolite EXP3174." In: *Journal of clinical pharmacology* 35.5 (May 1995), pp. 515–520. DOI: 10.1002/j.1552-4604.1995.tb04097.x. PMID: 7657853.

[12] J. K. Doig, R. J. MacFadyen, C. S. Sweet, K. R. Lees, and J. L. Reid. "Dose-Ranging Study of the Angiotensin Type I Receptor Antagonist Losartan (DuP753/MK954), in Salt-Deplete Normal Man". In: *Journal of Cardiovascular Pharmacology* 21.5 (May 1993), pp. 732–738. DOI: 10.1097/00005344-199305000-00007. PMID: 7685442.

[13] Massimiliano Donzelli, Adrian Derungs, Maria-Giovanna Serratore, Christoph Noppen, Lana Nezic, Stephan Krähenbühl, and Manuel Haschke. "The Basel Cocktail for Simultaneous Phenotyping of Human Cytochrome P450 Isoforms in Plasma, Saliva and Dried Blood Spots." In: *Clinical pharmacokinetics* 53.3 (Mar. 2014), pp. 271–282. DOI: 10.1007/s40262-013-0115-0. PMID: 24218006.

[14] FDA. *020386Orig1s000rev*. Apr. 14, 1995.

[15] FDA. *Cozaar Laebling-Package Insert*. Oct. 15, 2021. URL: https://www.accessdata.fda.gov/drugsatfda_docs/label/2021/020386s064lbl.pdf (visited on 01/10/2021).

[16] FDA. *FDA1995S60, Review for NDA020386*. Apr. 14, 1995.

[17] FDA. *FDA1995S67, FDA Review 04/14/1995*. Apr. 14, 1995.

[18] Roberto Ferrari. "RAAS Inhibition and Mortality in Hypertension". In: *Global Cardiology Science and Practice* 2013.3 (Sept. 2013), p. 34. DOI: 10.5339/gcsp.2013.34. URL: http://www.qscience.com/doi/abs/10.5339/gcsp.2013.34 (visited on 01/23/2025).

[19] Tracy L. Fischer, John A. Pieper, Donald W. Graff, Jo E. Rodgers, Jeffrey D. Fischer, Kimberly J. Parnell, Joyce A. Goldstein, Robert Greenwood, and J. Herbert Patterson. "Evaluation of Potential Losartan-Phenytoin Drug Interactions in Healthy Volunteers." In: *Clinical pharmacology and therapeutics* 72.3 (Sept. 2002), pp. 238–246. DOI: 10.1067/mcp.2002.127945. PMID: 12235444.

[20] Colleen Ann Flynn, Bruno A. Hagenbuch, and Gregory A. Reed. "Losartan Is a Substrate of Organic Anion Transporting Polypeptide 2B1". In: *The FASEB Journal* 24.S1 (Apr. 2010). DOI: 10.1096/fasebj.24.1_supplement.758.2. URL: https://faseb.onlinelibrary.wiley.com/doi/10.1096/fasebj.24.1_supplement.758.2 (visited on 10/31/2024).

[21] John H. Fountain, Jasleen Kaur, and Sarah L. Lappin. "Physiology, Renin Angiotensin System". In: *StatPearls*. Treasure Island (FL): StatPearls Publishing, 2024. PMID: 29261862. URL: http://www.ncbi.nlm.nih.gov/books/NBK470410/ (visited on 01/02/2025).

[22] Flávio D. Fuchs and Paul K. Whelton. "High Blood Pressure and Cardiovascular Disease". In: *Hypertension (Dallas, Tex.: 1979)* 75.2 (Feb. 2020), pp. 285–292. DOI: 10.1161/HYPERTENSIONAHA.119.14240. PMID: 31865786.

[23] *Gene-Specific Information Tables for CYP2C9*. PharmGKB. URL: https://www.pharmgkb.org/page/cyp2c9RefMaterials (visited on 06/18/2025).

[24] K. L. Goa and A. J. Wagstaff. "Losartan Potassium: A Review of Its Pharmacology, Clinical Efficacy and Tolerability in the Management of Hypertension." In: *Drugs* 51.5 (May 1996), pp. 820–845. DOI: 10.2165/00003495-199651050-00008. PMID: 8861549.

[25] M. T. Göktaş, F. Pepedil, Ö Karaca, S. Kalkışım, L. Cevik, E. Gumus, G. S. Guven, M. O. Babaoglu, A. Bozkurt, and U. Yasar. "Relationship between Genetic Polymorphisms of Drug Efflux Transporter MDR1 (ABCB1) and Response to Losartan in Hypertension Patients". In: *European Review for Medical and Pharmacological Sciences* 20.11 (June 2016), pp. 2460–2467. PMID: 27338075.

[26] M. R. Goldberg, T. E. Bradstreet, E. J. McWilliams, W. K. Tanaka, S. Lipert, T. D. Bjornsson, S. A. Waldman, B. Osborne, L. Pivadori, and G. Lewis. "Biochemical Effects of Losartan, a Nonpeptide Angiotensin II Receptor Antagonist, on the Renin-Angiotensin-Aldosterone System in Hypertensive Patients". In: *Hypertension (Dallas, Tex.: 1979)* 25.1 (Jan. 1995), pp. 37–46. DOI: 10.1161/01.hyp.25.1.37. PMID: 7843751.

[27] M. R. Goldberg, M. W. Lo, T. E. Bradstreet, M. A. Ritter, and P. Höglund. "Effects of Cimetidine on Pharmacokinetics and Pharmacodynamics of Losartan, an AT1-selective Non-Peptide Angiotensin II Receptor Antagonist." In: *European journal of clinical pharmacology* 49.1–2 (1995), pp. 115–119. DOI: 10.1007/BF00192369. PMID: 8751032.

[28] Ferran Gonzalez Hernandez, Simon J Carter, Juha Iso-Sipilä, Paul Goldsmith, Ahmed A. Almousa, Silke Gastine, Watjana Lilaonitkul, Frank Kloprogge, and Joseph F Standing. "An Automated Approach to Identify Scientific Publications Reporting Pharmacokinetic Parameters". In: *Wellcome Open Research* 6 (Apr. 21, 2021), p. 88. DOI: 10.12688/wellcomeopenres.16718.1. URL: https://wellcomeopenresearch.org/articles/6-88/v1 (visited on 04/24/2024).

[29] Jan Grzegorzewski, Janosch Brandhorst, Kathleen Green, Dimitra Eleftheriadou, Yannick Duport, Florian Barthorscht, Adrian Köller, Danny Yu Jia Ke, Sara De Angelis, and Matthias König. "PK-DB: Pharmacokinetics Database for Individualized and Stratified Computational Modeling". In: *Nucleic Acids Research* 49.D1 (Jan. 8, 2021), pp. D1358–D1364. DOI: 10.1093/nar/gkaa990. PMID: 33151297.

[30] Yang Han, Dong Guo, Yao Chen, Yu Chen, Zhi-Rong Tan, and Hong-Hao Zhou. "Effect of Silymarin on the Pharmacokinetics of Losartan and Its Active Metabolite E-3174 in Healthy Chinese Volunteers." In: *European journal of clinical pharmacology* 65.6 (June 2009), pp. 585–591. DOI: 10.1007/s00228-009-0624-9. PMID: 19221727.

[31] Vincent Haufroid. "Genetic Polymorphisms of ATP-binding Cassette Transporters ABCB1 and ABCC2 and Their Impact on Drug Disposition". In: *Current Drug Targets* 12.5 (May 2011), pp. 631–646. DOI: 10.2174/138945011795378487. PMID: 21039333.

[32] Timothy F. Herman and Cynthia Santos. "First-Pass Effect". In: *StatPearls*. Treasure Island (FL): StatPearls Publishing, 2025. PMID: 31869143. URL: http://www.ncbi.nlm.nih.gov/books/NBK551679/ (visited on 01/09/2025).

[33] Laura M. Hodges, Svetlana M. Markova, Leslie W. Chinn, Jason M. Gow, Deanna L. Kroetz, Teri E. Klein, and Russ B. Altman. "Very Important Pharmacogene Summary: ABCB1 (MDR1, P-glycoprotein)". In: *Pharmacogenetics and Genomics* 21.3 (Mar. 2011), pp. 152–161. DOI: 10.1097/FPC.0b013e3283385a1c. PMID: 20216335.

[34] S. Hoffmeyer, O. Burk, O. von Richter, H. P. Arnold, J. Brockmöller, A. Johne, I. Cascorbi, T. Gerloff, I. Roots, M. Eichelbaum, and U. Brinkmann. "Functional Polymorphisms of the Human Multidrug-Resistance Gene: Multiple Sequence Variations and Correlation of One Allele with P-glycoprotein Expression and Activity in Vivo". In: *Proceedings of the National Academy of Sciences of the United States of America* 97.7 (Mar. 28, 2000), pp. 3473–3478. DOI: 10.1073/pnas.97.7.3473. PMID: 10716719.

[35] Hang-Xing Huang, He Wu, Yingying Zhao, Tao Zhou, Xin Ai, Yu Dong, Yan Zhang, and Yong Lai. "Effect of CYP2C9 Genetic Polymorphism and Breviscapine on Losartan Pharmacokinetics in Healthy Subjects." In: *Xenobiotica; the fate of foreign compounds in biological systems* 51.5 (May 2021), pp. 616–623. DOI: 10.1080/00498254.2021.1880670. PMID: 33509019.

[36] Michael Hucka, Frank T. Bergmann, Claudine Chaouiya, Andreas Dräger, Stefan Hoops, Sarah M. Keating, Matthias König, Nicolas Le Novère, Chris J. Myers, Brett G. Olivier, Sven Sahle, James C. Schaff, Rahuman Sheriff, Lucian P. Smith, Dagmar Waltemath, Darren J. Wilkinson, and Fengkai Zhang. "The Systems Biology Markup Language (SBML): Language Specification for Level 3 Version 2 Core Release 2". In: *Journal of Integrative Bioinformatics* 16.2 (June 20, 2019). DOI: 10.1515/jib-2019-0021. URL: https://www.degruyter.com/document/doi/10.1515/jib-2019-0021/html (visited on 04/19/2024).

[37] Saadettin Hülagü, Omer Sentürk, Aysun Erdem, Orhan Ozgür, Altay Celebi, A. Turgut Karakaya, Mualla Seyhogullari, and Ali Demirci. "Effects of Losartan, Somatostatin and Losartan plus Somatostatin on Portal Hemodynamics and Renal Functions in Cirrhosis". In: *Hepato-Gastroenterology* 49.45 (2002), pp. 783–787. PMID: 12063990.

[38] Kamryn E. Jones, Shaun L. Hayden, Hannah R. Meyer, Jillian L. Sandoz, William H. Arata, Kylie Dufrene, Corrado Ballaera, Yair Lopez Torres, Patricia Griffin, Adam M. Kaye, Sahar Shekoohi, and Alan D. Kaye. "The Evolving Role of Calcium Channel Blockers in Hypertension Management: Pharmacological and Clinical Considerations". In: *Current Issues in Molecular Biology* 46.7 (June 22, 2024), pp. 6315–6327. DOI: 10.3390/cimb46070377. PMID: 39057019.

[39] Martin C. Kammerl, Wolfgang Richthammer, Armin Kurtz, and Bernhard K. Krämer. "Angiotensin II Feedback Is a Regulator of Renocortical Renin, COX-2, and nNOS Expression". In: *American Journal of Physiology-Regulatory, Integrative and Comparative Physiology* 282.6 (June 1, 2002), R1613–R1617. DOI: 10.1152/ajpregu.00464.2001. URL: https://www.physiology.org/doi/10.1152/ajpregu.00464.2001 (visited on 03/14/2025).

[40] Sarah M. Keating, Dagmar Waltemath, Matthias König, Fengkai Zhang, Andreas Dräger, Claudine Chaouiya, Frank T. Bergmann, Andrew Finney, Colin S. Gillespie, Tomáš Helikar, Stefan Hoops, Rahuman S. Malik-Sheriff, Stuart L. Moodie, Ion I. Moraru, Chris J. Myers, Aurélien Naldi, Brett G. Olivier, Sven Sahle, James C. Schaff, Lucian P. Smith, Maciej J. Swat, Denis Thieffry, Leandro Watanabe, Darren J. Wilkinson, Michael L. Blinov, Kimberly Begley, James R. Faeder, Harold F. Gómez, Thomas M. Hamm, Yuichiro Inagaki, Wolfram Liebermeister, Allyson L. Lister, Daniel Lucio, Eric Mjolsness, Carole J. Proctor, Karthik Raman, Nicolas Rodriguez, Clifford A. Shaffer, Bruce E. Shapiro, Joerg Stelling, Neil Swainston, Naoki Tanimura, John Wagner, Martin Meier-Schellersheim, Herbert M. Sauro, Bernhard Palsson, Hamid Bolouri, Hiroaki Kitano, Akira Funahashi, Henning Hermjakob, John C. Doyle, Michael Hucka, and SBML Level 3 Community members. "SBML Level 3: An Extensible Format for the Exchange and Reuse of Biological Models". In: *Molecular Systems Biology* 16.8 (Aug. 2020), e9110. DOI: 10.15252/msb.20199110. PMID: 32845085.

[41] Min-Gul Kim, Yunjeong Kim, Ji-Young Jeon, and Dal-Sik Kim. "Effect of Fermented Red Ginseng on Cytochrome P450 and P-glycoprotein Activity in Healthy Subjects, as Evaluated Using the Cocktail Approach." In: *British journal of clinical pharmacology* 82.6 (Dec. 2016), pp. 1580–1590. DOI: 10.1111/bcp.13080. PMID: 27495955.

[42] Mariko Kobayashi, Miho Takagi, Kyoko Fukumoto, Ryuji Kato, Kazuhiko Tanaka, and Kazuyuki Ueno. "The Effect of Bucolome, a CYP2C9 Inhibitor, on the Pharmacokinetics of Losartan." In: *Drug metabolism and pharmacokinetics* 23.2 (2008), pp. 115–119. DOI: 10.2133/dmpk.23.115. PMID: 18445991.

[43] Adrian Köller, Jan Grzegorzewski, and Matthias König. "Physiologically Based Modeling of the Effect of Physiological and Anthropometric Variability on Indocyanine Green Based Liver Function Tests". In: *Frontiers in Physiology* 12 (Nov. 22, 2021), p. 757293. DOI: 10.3389/fphys.2021.757293. URL: https://www.frontiersin.org/articles/10.3389/fphys.2021.757293/full (visited on 04/22/2024).

[44] Adrian Köller, Jan Grzegorzewski, Hans-Michael Tautenhahn, and Matthias König. "Prediction of Survival After Partial Hepatectomy Using a Physiologically Based Pharmacokinetic Model of Indocyanine Green Liver Function Tests". In: *Frontiers in Physiology* 12 (Nov. 22, 2021), p. 730418. DOI: 10.3389/fphys.2021.730418. URL: https://www.frontiersin.org/articles/10.3389/fphys.2021.730418/full (visited on 04/22/2024).

[45] Matthias König. *Sbmlsim: SBML Simulation Made Easy*. Version 0.2.2. [object Object], Sept. 27, 2021. DOI: 10.5281/ZENODO.5531088. URL: https://zenodo.org/record/5531088 (visited on 04/19/2024).

[46] Matthias König. *Sbmlutils: Python Utilities for SBML*. Version 0.9.0. Zenodo, Aug. 15, 2024. DOI: 10.5281/ZENODO.13325770. URL: https://zenodo.org/doi/10.5281/zenodo.13325770 (visited on 09/13/2024).

[47] Matthias König, Andreas Dräger, and Hermann-Georg Holzhütter. "CySBML: A Cytoscape Plugin for SBML". In: *Bioinformatics* 28.18 (Sept. 15, 2012), pp. 2402–2403. DOI: 10.1093/bioinformatics/bts432. URL: https://academic.oup.com/bioinformatics/article/28/18/2402/251682 (visited on 04/19/2024).

[48] Dipak Kotecha, Marcus D. Flather, Douglas G. Altman, Jane Holmes, Giuseppe Rosano, John Wikstrand, Milton Packer, Andrew J. S. Coats, Luis Manzano, Michael Böhm, Dirk J. van Veldhuisen, Bert Andersson, Hans Wedel, Thomas G. von Lueder, Alan S. Rigby, Åke Hjalmarson, John Kjekshus, John G. F. Cleland, and Beta-Blockers in Heart Failure Collaborative Group. "Heart Rate and Rhythm and the Benefit of Beta-Blockers in Patients With Heart Failure". In: *Journal of the American College of Cardiology* 69.24 (June 20, 2017), pp. 2885–2896. DOI: 10.1016/j.jacc.2017.04.001. PMID: 28467883.

[49] Makiko Kusama, Kazuya Maeda, Koji Chiba, Akinori Aoyama, and Yuichi Sugiyama. "Prediction of the Effects of Genetic Polymorphism on the Pharmacokinetics of CYP2C9 Substrates from in Vitro Data." In: *Pharmaceutical research* 26.4 (Apr. 2009), pp. 822–835. DOI: 10.1007/s11095-008-9781-2. PMID: 19082874.

[50] Craig R. Lee, John A. Pieper, Alan L. Hinderliter, Joyce A. Blaisdell, and Joyce A. Goldstein. "Losartan and E3174 Pharmacokinetics in Cytochrome P450 2C9*1/*1, *1/*2, and *1/*3 Individuals." In: *Pharmacotherapy* 23.6 (June 2003), pp. 720–725. DOI: 10.1592/phco.23.6.720.32187. PMID: 12820813.

[51] Z. Li, G. Wang, L.-S. Wang, W. Zhang, Z.-R. Tan, L. Fan, B.-L. Chen, Q. Li, J. Liu, J.-H. Tu, D.-L. Hu, Z.-Q. Liu, and H.-H. Zhou. "Effects of the CYP2C9*13 Allele on the Pharmacokinetics of Losartan in Healthy Male Subjects." In: *Xenobiotica; the fate of foreign compounds in biological systems* 39.10 (Oct. 2009), pp. 788–793. DOI: 10.1080/00498250903134435. PMID: 19604036.

[52] M. W. Lo, M. R. Goldberg, J. B. McCrea, H. Lu, C. I. Furtek, and T. D. Bjornsson. "Pharmacokinetics of Losartan, an Angiotensin II Receptor Antagonist, and Its Active Metabolite EXP3174 in Humans." In: *Clinical pharmacology and therapeutics* 58.6 (Dec. 1995), pp. 641–649. DOI: 10.1016/0009-9236(95)90020-9. PMID: 8529329.

[53] Keiko Maekawa, Noriko Harakawa, Emiko Sugiyama, Masahiro Tohkin, Su-Ryang Kim, Nahoko Kaniwa, Noriko Katori, Ryuichi Hasegawa, Kazuki Yasuda, Kei Kamide, Toshiyuki Miyata, Yoshiro Saito, and Jun-ichi Sawada. "Substrate-Dependent Functional Alterations of Seven CYP2C9 Variants Found in Japanese Subjects". In: *Drug Metabolism and Disposition: The Biological Fate of Chemicals* 37.9 (Sept. 2009), pp. 1895–1903. DOI: 10.1124/dmd.109.027003. PMID: 19541829.

[54] Beatrice Stemmer Mallol, Jan Grzegorzewski, Hans-Michael Tautenhahn, and Matthias König. *Insights into Intestinal P-glycoprotein Function Using Talinolol: A PBPK Modeling Approach*. Nov. 22, 2023. DOI: 10.1101/2023.11.21.568168. URL: http://biorxiv.org/lookup/doi/10.1101/2023.11.21.568168 (visited on 05/05/2024). Pre-published.

[55] M. McIntyre, S. E. Caffe, R. A. Michalak, and J. L. Reid. "Losartan, an Orally Active Angiotensin (AT1) Receptor Antagonist: A Review of Its Efficacy and Safety in Essential Hypertension." In: *Pharmacology & therapeutics* 74.2 (1997), pp. 181–194. DOI: 10.1016/s0163-7258(97)82002-5. PMID: 9336021.

[56] John O. Miners and Donald J. Birkett. "Cytochrome P4502C9: An Enzyme of Major Importance in Human Drug Metabolism". In: *British Journal of Clinical Pharmacology* 45.6 (June 1998), pp. 525–538. DOI: 10.1046/j.1365-2125.1998.00721.x. URL: https://bpspubs.onlinelibrary.wiley.com/doi/10.1046/j.1365-2125.1998.00721.x (visited on 01/04/2025).

[57] A. Munafo, Y. Christen, J. Nussberger, L. Y. Shum, R. M. Borland, R. J. Lee, B. Waeber, J. Biollaz, and H. R. Brunner. "Drug Concentration Response Relationships in Normal Volunteers after Oral Administration of Losartan, an Angiotensin II Receptor Antagonist." In: *Clinical pharmacology and therapeutics* 51.5 (May 1992), pp. 513–521. DOI: 10.1038/clpt.1992.56. PMID: 1587065.

[58] Pablo Nakagawa and Curt D. Sigmund. "Under Pressure: A Baroreceptor Mechanism in the Renal Renin Cell Controlling Renin". In: *Circulation Research* 129.2 (July 9, 2021), pp. 277–279. DOI: 10.1161/CIRCRESAHA.121.319559. PMID: 34236885.

[59] NCD Risk Factor Collaboration (NCD-RisC). "Worldwide Trends in Hypertension Prevalence and Progress in Treatment and Control from 1990 to 2019: A Pooled Analysis of 1201 Population-Representative Studies with 104 Million Participants". In: *Lancet (London, England)* 398.10304 (Sept. 11, 2021), pp. 957–980. DOI: 10.1016/S0140-6736(21)01330-1. PMID: 34450083.

[60] Bjoern Neubauer, Julia Schrankl, Dominik Steppan, Katharina Neubauer, Maria Luisa Sequeira-Lopez, Li Pan, R. Ariel Gomez, Thomas M. Coffman, Kenneth W. Gross, Armin Kurtz, and Charlotte Wagner. "Angiotensin II Short-Loop Feedback: Is There a Role of Ang II for the Regulation of the Renin System In Vivo?" In: *Hypertension (Dallas, Tex.: 1979)* 71.6 (June 2018), pp. 1075–1082. DOI: 10.1161/HYPERTENSIONAHA.117.10357. PMID: 29661841.

[61] Kyung-Suk Oh, Su-Jin Park, Dhananjay D. Shinde, Jae-Gook Shin, and Dong-Hyun Kim. "High-Sensitivity Liquid Chromatography-Tandem Mass Spectrometry for the Simultaneous Determination of Five Drugs and Their Cytochrome P450-specific Probe Metabolites in Human Plasma." In: *Journal of chromatography. B, Analytical technologies in the biomedical and life sciences* 895–896 (May 1, 2012), pp. 56–64. DOI: 10.1016/j.jchromb.2012.03.014. PMID: 22483397.

[62] M. Ohtawa, F. Takayama, K. Saitoh, T. Yoshinaga, and M. Nakashima. "Pharmacokinetics and Biochemical Efficacy after Single and Multiple Oral Administration of Losartan, an Orally Active Nonpeptide Angiotensin II Receptor Antagonist, in Humans." In: *British journal of clinical pharmacology* 35.3 (Mar. 1993), pp. 290–297. DOI: 10.1111/j.1365-2125.1993.tb05696.x. PMID: 8471405.

[63] A. A. Pedro, T. W. Gehr, D. F. Brophy, and D. A. Sica. "The Pharmacokinetics and Pharmacodynamics of Losartan in Continuous Ambulatory Peritoneal Dialysis." In: *Journal of clinical pharmacology* 40.4 (Apr. 2000), pp. 389–395. DOI: 10.1177/00912700022009099. PMID: 10761166.

[64] R. N. Pugh, I. M. Murray-Lyon, J. L. Dawson, M. C. Pietroni, and R. Williams. "Transection of the Oesophagus for Bleeding Oesophageal Varices". In: *The British Journal of Surgery* 60.8 (Aug. 1973), pp. 646–649. DOI: 10.1002/bjs.1800600817. PMID: 4541913.

[65] Elena Puris, Markku Pasanen, Veli-Pekka Ranta, Mikko Gynther, Aleksanteri Petsalo, Pirjo Käkelä, Ville Männistö, and Jussi Pihlajamäki. "Laparoscopic Roux-en-Y Gastric Bypass Surgery Influenced Pharmacokinetics of Several Drugs given as a Cocktail with the Highest Impact Observed for CYP1A2, CYP2C8 and CYP2E1 Substrates." In: *Basic & clinical pharmacology & toxicology* 125.2 (Aug. 2019), pp. 123–132. DOI: 10.1111/bcpt.13234. PMID: 30916845.

[66] Senthilkumar B. Rajamohan, Gayatri Raghuraman, Nanduri R. Prabhakar, and Ganesh K. Kumar. "NADPH Oxidase-Derived H(2)O(2) Contributes to Angiotensin II-induced Aldosterone Synthesis in Human and Rat Adrenal Cortical Cells". In: *Antioxidants & Redox Signaling* 17.3 (Aug. 1, 2012), pp. 445–459. DOI: 10.1089/ars.2011.4176. PMID: 22214405.

[67] A. E. Rettie, L. C. Wienkers, F. J. Gonzalez, W. F. Trager, and K. R. Korzekwa. "Impaired (S)-Warfarin Metabolism Catalysed by the R144C Allelic Variant of CYP2C9". In: *Pharmacogenetics* 4.1 (Feb. 1994), pp. 39–42. DOI: 10.1097/00008571-199402000-00005. PMID: 8004131.

[68] Ankit Rohatgi. *WebPlotDigitizer*. Version 4.7. 2024. URL: https://automeris.io/WebPlotDigitizer.html.

[69] M. Romkes, M. B. Faletto, J. A. Blaisdell, J. L. Raucy, and J. A. Goldstein. "Cloning and Expression of Complementary DNAs for Multiple Members of the Human Cytochrome P450IIC Subfamily". In: *Biochemistry* 30.13 (Apr. 2, 1991), pp. 3247–3255. DOI: 10.1021/bi00227a012. PMID: 2009263.

[70] Gian Paolo Rossi, Livia Lenzini, Brasilina Caroccia, Giacomo Rossitto, and Teresa Maria Seccia. "Angiotensin Peptides in the Regulation of Adrenal Cortical Function". In: *Exploration of Medicine* 2.3 (June 30, 2021), pp. 294–304. DOI: 10.37349/emed.2021.00047. URL: https://www.explorationpub.com/Journals/em/Article/100147 (visited on 03/12/2025).

[71] Kazuishi Sekino, Takahiro Kubota, Yuko Okada, Yasuhiko Yamada, Koujirou Yamamoto, Ryuya Horiuchi, Kenjirou Kimura, and Tatsuji Iga. "Effect of the Single CYP2C9*3 Allele on Pharmacokinetics and Pharmacodynamics of Losartan in Healthy Japanese Subjects." In: *European journal of clinical pharmacology* 59.8–9 (Nov. 2003), pp. 589–592. DOI: 10.1007/s00228-003-0664-5. PMID: 14504849.

[72] Hyo-Bin Shin, Eui Hyun Jung, Pureum Kang, Chang Woo Lim, Kyung-Yul Oh, Chang-Keun Cho, Yun Jeong Lee, Chang-Ik Choi, Choon-Gon Jang, Seok-Yong Lee, and Jung-Woo Bae. "ABCB1 c.2677G>T/c.3435C>T Diplotype Increases the Early-Phase Oral Absorption of Losartan." In: *Archives of pharmacal research* 43.11 (Nov. 2020), pp. 1187–1196. DOI: 10.1007/s12272-020-01294-3. PMID: 33249530.

[73] D. A. Sica, C. E. Halstenson, T. W. Gehr, and W. F. Keane. "Pharmacokinetics and Blood Pressure Response of Losartan in End-Stage Renal Disease." In: *Clinical pharmacokinetics* 38.6 (June 2000), pp. 519–526. DOI: 10.2165/00003088-200038060-00005. PMID: 10885588.

[74] D. A. Sica, M. W. Lo, W. C. Shaw, W. F. Keane, T. W. Gehr, C. E. Halstenson, K. Lipschutz, C. I. Furtek, M. A. Ritter, and S. Shahinfar. "The Pharmacokinetics of Losartan in Renal Insufficiency." In: *Journal of hypertension. Supplement : official journal of the International Society of Hypertension* 13.1 (July 1995), S49–52. DOI: 10.1097/00004872-199507001-00007. PMID: 18800456.

[75] Domenic A. Sica, Todd W. B. Gehr, and Siddhartha Ghosh. "Clinical Pharmacokinetics of Losartan." In: *Clinical pharmacokinetics* 44.8 (2005), pp. 797–814. DOI: 10.2165/00003088-200544080-00003. PMID: 16029066.

[76] Werner Siegmund, Karen Ludwig, Thomas Giessmann, Peter Dazert, Eike Schroeder, Bernhard Sperker, Rolf Warzok, Heyo K. Kroemer, and Ingolf Cascorbi. "The Effects of the Human MDR1 Genotype on the Expression of Duodenal P-glycoprotein and Disposition of the Probe Drug Talinolol". In: *Clinical Pharmacology and Therapeutics* 72.5 (Nov. 2002), pp. 572–583. DOI: 10.1067/mcp.2002.127739. PMID: 12426521.

[77] K. L. Simpson and K. J. McClellan. "Losartan: A Review of Its Use, with Special Focus on Elderly Patients." In: *Drugs & aging* 16.3 (Mar. 2000), pp. 227–250. DOI: 10.2165/00002512-200016030-00006. PMID: 10803861.

[78] Endre T. Somogyi, Jean-Marie Bouteiller, James A. Glazier, Matthias König, J. Kyle Medley, Maciej H. Swat, and Herbert M. Sauro. "libRoadRunner: A High Performance SBML Simulation and Analysis Library". In: *Bioinformatics* 31.20 (Oct. 15, 2015), pp. 3315–3321. DOI: 10.1093/bioinformatics/btv363. URL: https://academic.oup.com/bioinformatics/article/31/20/3315/195758 (visited on 04/19/2024).

[79] R. A. Stearns, P. K. Chakravarty, R. Chen, and S. H. Chiu. "Biotransformation of Losartan to Its Active Carboxylic Acid Metabolite in Human Liver Microsomes. Role of Cytochrome P4502C and 3A Subfamily Members." In: *Drug metabolism and disposition: the biological fate of chemicals* 23.2 (Feb. 1995), pp. 207–215. PMID: 7736913.

[80] R. A. Stearns, R. R. Miller, G. A. Doss, P. K. Chakravarty, A. Rosegay, G. J. Gatto, and S. H. Chiu. "The Metabolism of DuP 753, a Nonpeptide Angiotensin II Receptor Antagonist, by Rat, Monkey, and Human Liver Slices." In: *Drug metabolism and disposition: the biological fate of chemicals* 20.2 (Mar. 1992), pp. 281–287. PMID: 1352222.

[81] Paul E. Stevens, Sofia B. Ahmed, Juan Jesus Carrero, Bethany Foster, Anna Francis, Rasheeda K. Hall, Will G. Herrington, Guy Hill, Lesley A. Inker, Rümeyza Kazancıoğlu, Edmund Lamb, Peter Lin, Magdalena Madero, Natasha McIntyre, Kelly Morrow, Glenda Roberts, Dharshana Sabanayagam, Elke Schaeffner, Michael Shlipak, Rukshana Shroff, Navdeep Tangri, Teerawat Thanachayanont, Ifeoma Ulasi, Germaine Wong, Chih-Wei Yang, Luxia Zhang, and Adeera Levin. "KDIGO 2024 Clinical Practice Guideline for the Evaluation and Management of Chronic Kidney Disease". In: *Kidney International* 105.4 (Apr. 2024), S117–S314. DOI: 10.1016/j.kint.2023.10.018. URL: https://linkinghub.elsevier.com/retrieve/pii/S0085253823007664 (visited on 04/22/2024).

[82] Shimako Tanaka, Shinya Uchida, Naoki Inui, Kazuhiko Takeuchi, Hiroshi Watanabe, and Noriyuki Namiki. "Simultaneous LC-MS/MS Analysis of the Plasma Concentrations of a Cocktail of 5 Cytochrome P450 Substrate Drugs and Their Metabolites." In: *Biological & pharmaceutical bulletin* 37.1 (2014), pp. 18–25. DOI: 10.1248/bpb.b13-00401. PMID: 24389476.

[83] J. Taube, D. Halsall, and T. Baglin. "Influence of Cytochrome P-450 CYP2C9 Polymorphisms on Warfarin Sensitivity and Risk of over-Anticoagulation in Patients on Long-Term Treatment". In: *Blood* 96.5 (Sept. 1, 2000), pp. 1816–1819. PMID: 10961881.

[84] Ennie Tensil and Matthias König. *Physiologically Based Pharmacokinetic/ Pharmacodynamic (PBPK/PD) Model of Losartan*. Version 0.7.0. Zenodo, July 2025. DOI: 10.5281/zenodo.15866672. URL: https://doi.org/10.5281/zenodo.15866672.

[85] Yu-Han Wang, Pei-Pei Pan, Da-Peng Dai, Shuang-Hu Wang, Pei-Wu Geng, Jian-Ping Cai, and Guo-Xin Hu. "Effect of 36 CYP2C9 Variants Found in the Chinese Population on Losartan Metabolism in Vitro." In: *Xenobiotica; the fate of foreign compounds in biological systems* 44.3 (Mar. 2014), pp. 270–275. DOI: 10.3109/00498254.2013.820007. PMID: 23844998.

[86] Ciaran Welsh, Jin Xu, Lucian Smith, Matthias König, Kiri Choi, and Herbert M Sauro. "libRoadRunner 2.0: A High Performance SBML Simulation and Analysis Library". In: *Bioinformatics* 39.1 (Jan. 1, 2023). Ed. by Pier Luigi Martelli, btac770. DOI: 10.1093/bioinformatics/btac770. URL: https://academic.oup.com/bioinformatics/article/doi/10.1093/bioinformatics/btac770/6883908 (visited on 04/19/2024).

[87] Gordon H. Williams. "Aldosterone Biosynthesis, Regulation, and Classical Mechanism of Action". In: *Heart Failure Reviews* 10.1 (Jan. 2005), pp. 7–13. DOI: 10.1007/s10741-005-2343-3. PMID: 15947886.

[88] Ying-Ying Yang, Han-Chieh Lin, Wui-Chiang Lee, Ming-Chih Hou, Fa-Yauh Lee, Full-Young Chang, and Shou-Dong Lee. "One-Week Losartan Administration Increases Sodium Excretion in Cirrhotic Patients with and without Ascites". In: *Journal of Gastroenterology* 37.3 (Mar. 2002), pp. 194–199. DOI: 10.1007/s005350200020. URL: http://link.springer.com/10.1007/s005350200020 (visited on 01/10/2025).

[89] U Yasar, G. Tybring, M. Hidestrand, M. Oscarson, M. Ingelman-Sundberg, M. L. Dahl, and E. Eliasson. "Role of CYP2C9 Polymorphism in Losartan Oxidation." In: *Drug metabolism and disposition: the biological fate of chemicals* 29.7 (July 2001), pp. 1051–1056. PMID: 11408373.

[90] U. Yasar, E. Eliasson, C. Forslund-Bergengren, G. Tybring, M. Gadd, F. Sjöqvist, and M. L. Dahl. "The Role of CYP2C9 Genotype in the Metabolism of Diclofenac in Vivo and in Vitro." In: *European journal of clinical pharmacology* 57.10 (Dec. 2001), pp. 729–735. DOI: 10.1007/s00228-001-0376-7. PMID: 11829203.

[91] Umit Yasar, Melih O. Babaoglu, and Atila Bozkurt. "Disposition of a CYP2C9 Phenotyping Agent, Losartan, Is Not Influenced by the Common 3435C > T Variation of the Drug Transporter Gene ABCB1 (MDR1)." In: *Basic & clinical pharmacology & toxicology* 103.2 (Aug. 2008), pp. 176–179. DOI: 10.1111/j.1742-7843.2008.00283.x. PMID: 18816302.

[92] Umit Yasar, Cecilia Forslund-Bergengren, Gunnel Tybring, Pedro Dorado, Adrián Llerena, Folke Sjöqvist, Erik Eliasson, and Marja-Liisa Dahl. "Pharmacokinetics of Losartan and Its Metabolite E-3174 in Relation to the CYP2C9 Genotype." In: *Clinical pharmacology and therapeutics* 71.1 (Jan. 2002), pp. 89–98. DOI: 10.1067/mcp.2002.121216. PMID: 11823761.

[93] Takashi Yoshitani, Hitoshi Yagi, Nobuo Inotsume, and Masato Yasuhara. "Effect of Experimental Renal Failure on the Pharmacokinetics of Losartan in Rats." In: *Biological & pharmaceutical bulletin* 25.8 (Aug. 2002), pp. 1077–1083. DOI: 10.1248/bpb.25.1077. PMID: 12186413.

[94] C. H. Yun, H. S. Lee, H. Lee, J. K. Rho, H. G. Jeong, and F. P. Guengerich. "Oxidation of the Angiotensin II Receptor Antagonist Losartan (DuP 753) in Human Liver Microsomes. Role of Cytochrome P4503A(4) in Formation of the Active Metabolite EXP3174." In: *Drug metabolism and disposition: the biological fate of chemicals* 23.2 (Feb. 1995), pp. 285–289. PMID: 7736926.

[95] Shu-Feng Zhou, Jun-Ping Liu, and Balram Chowbay. "Polymorphism of Human Cytochrome P450 Enzymes and Its Clinical Impact". In: *Drug Metabolism Reviews* 41.2 (2009), pp. 89–295. DOI: 10.1080/03602530902843483. PMID: 19514967.

Acknowledgements

I would like to thank Dr. Matthias König, who supervised this project.
I would also like to acknowledge the utilization of BioRender (https://biorender.com) for the creation of the illustrations incorporated within this thesis.
This work was supervised by Matthias König (MK) https://livermetabolism.com. MK was supported by the BMBF within ATLAS by grant number 031L0304B and the German Research Foundation (DFG) within the Research Unit Program FOR 5151 QuaLiPerF by grant number 436883643 and by grant number 465194077 (Priority Programme SPP 2311, Subproject SimLivA). This work was supported by the BMBF-funded de.NBI Cloud within the German Network for Bioinformatics Infrastructure (de.NBI) (031A537B, 031A533A, 031A538A, 031A533B, 031A535A, 031A537C, 031A534A, 031A532B).

HUMBOLDT-UNIVERSITÄT ZU BERLIN

Lebenswissenschaftliche Fakultät
Institut für Biologie
Institut für Psychologie
Albrecht Daniel Thaer-Institut für Agrar- und Gartenbauwissenschaften

Vorlage für die Eigenständigkeitserklärung (auch Selbständigkeitserklärung) für die Abschlussarbeit

Hiermit erkläre ich, dass ich die vorliegende Arbeit selbständig verfasst habe und sämtliche Quellen, einschließlich Internetquellen, die unverändert oder abgewandelt wiedergegeben werden, insbesondere Quellen für Texte, Grafiken, Tabellen und Bilder, als solche kenntlich gemacht habe.

Ich versichere, dass ich die vorliegende Abschlussarbeit noch nicht für andere Prüfungen eingereicht habe.

Mir ist bekannt, dass bei Verstößen gegen diese Grundsätze ein Verfahren wegen Täuschungsversuchs bzw. Täuschung gemäß der fachspezifischen Prüfungsordnung und/oder der Fächerübergreifenden Satzung zur Regelung von Zulassung, Studium und Prüfung der Humboldt-Universität zu Berlin (ZSP-HU) eingeleitet wird.

Ort, Datum, Unterschrift